Master Thesis

Future energy systems and the protection of the electrical grid

R. Braat

Technische Universiteit Delft

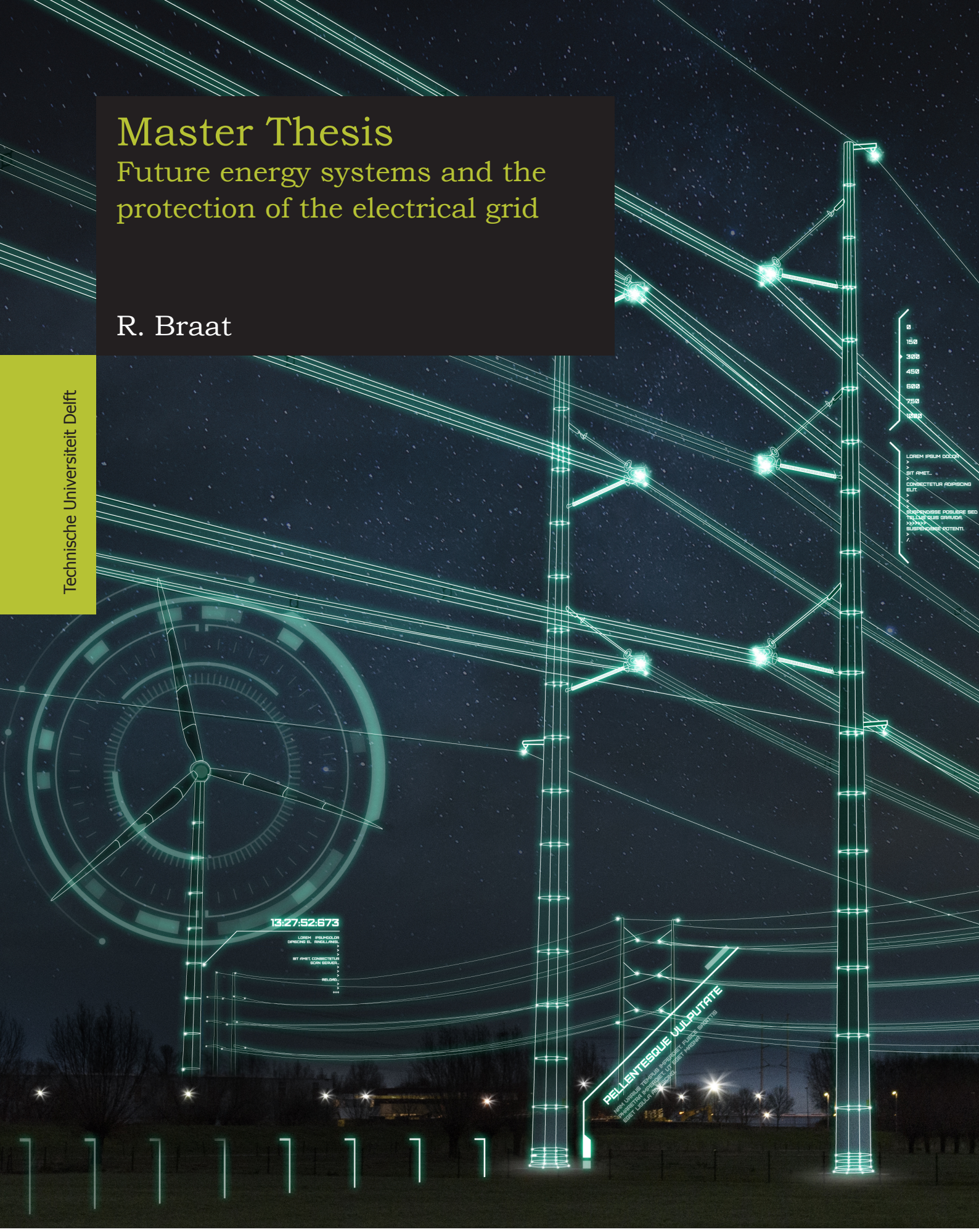

TU Delft Delft University of Technology

Challenge the future

Master Thesis

Future energy systems and the protection of the electrical grid

by

R. Braat

in partial fulfillment of the requirements for the degree of

Master of Science
in Electrical Power Engineering

at the Delft University of Technology,
to be defended publicly on Tuesday 7 July, 2015 at 14:00.

Student number:	4215176	
Project duration:	Monday 4 August, 2014 – Wednesday 27 May, 2015	
Supervisor:	Dr. ir. M. Popov	
Thesis committee:	Prof. dr. M. van der Meijden,	TU Delft
	Dr. ir. M. Popov,	TU Delft
	Dr. J. Popovic,	TU Delft
	H. Folkersma,	Joulz Energy Solutions

version 1.2
29-6-2015

TU Delft Delft University of Technology

Joulz onderdeel van Eneco

Voor mijn moeder
Mijn inspiratie
Josephina Maria Catharina Braat - de Vries

27 May 1955 - 14 June 2010†

Preface

This work was carried out at the department of engineering and consultancy at the company Joulz Energy Solutions (part of the Eneco Group) Netherlands, located in Rotterdam, in the period between August 2014 and May 2015. Joulz is a leading technical service provider and system integrator for intelligent grid solutions with many years of experience relating to the Dutch electrical grids. Joulz possesses specialized knowledge in the area of both existing and new energy infrastructures, design and engineering, substation automation systems, connections, stations and of managing and maintaining complex grids.

The vision of Joulz Energy Solutions towards the core of a future-proof and sustainable energy supply is providing Smart Grid services to their costumers. Smart Grid services is defined by Joulz as applying automation and ICT to further improve quality of energy distribution, e.g., substation automation systems, real-time detailed monitoring of the utilization of the grid components and proactive fault detection to prevent unplanned downtime.

The engineering and consultancy department is currently a system integrator and is specialized in substation automation systems, together with the latest communication protocol IEC61850, into the energy distribution systems. These systems are protecting assets equipped inside the distribution system against large overcurrents to guarantee safety and continuity of the energy supply. The main interest of the engineering and consultancy department is towards Smart Grids technologies and how these technologies can be implemented within the electrical distribution systems in the coming years to our benefit.

It is expected that the distribution system will have to be more flexible in the coming years regarding the implementation of renewable energy sources and changes in the energy demand. To provide this flexibility the correct protection needs to be implemented by applying substation automation systems. This is the main motivation for the start of this project.

Abstract

In the coming years more flexibility of the distribution system will be required due to the implementation of decentralized generation of energy by renewable energy sources (wind and solar) and the change in energy consumption with the introduction of the electric car and heat pumps. These technologies will increase the demand in transport capacity of the electrical infrastructure inside the distribution system which, in the current philosophy applied by the distribution network operators, will probably lead to the installation of additional feeders. The question arises if it is always necessary and even feasible to install these feeders, due to the impact that these installation of these feeders will have on the surrounding area and built environment, without taking into consideration the nearby installed infrastructure already available inside the system.

The present infrastructure and protection schemes are designed for a distribution system with a radial topology. This radial topology is realized by incorporating net openings inside the electrical infrastructure, which ultimately means that transport capacity will be lost. The main reason for applying this radial topology is to reduce the down time of energy delivery after the occurrence of a fault inside the system by re-routing the energy delivery and to create a selective protection scheme which is considered to be one of the most important characteristics of an accurate operating protection scheme. The goal is to increase the transport capacity of the infrastructure by closing most of the net openings, thus operating the distribution system from a radial to a meshed topology, without the loss of selectivity. These results will not be maintained when the current protection strategies are applied inside the protection schemes, which use current- and time-grading for providing the selective behavior.

In the present system it is desirable to apply numerical protection relays. These relays allow the use of multiple protection functions inside only one single device. Moreover the present numerical relays are applied with substation automation functionality and the latest standardized communication protocol. This protocol replaces traditional wiring schemes between devices by an ethernet based communication network and allows fast communication of tripping signals between server and client over a fibre-optic cable.

In this research it is shown how with the conventional protection technique of the directional relay (which have to discriminate in both the forward and reverse current direction), a fast communication network and a logic diagrams the desirable characteristics for the protection scheme are obtained without the need of applying a complex algorithm. When additional feeders still have to be installed the logic diagram and pick-up currents of the directional relays need to be slightly altered to incorporate this extra feeder inside the protection scheme. This allows flexibility in the case of an extension of the infrastructure without the loss of selectivity inside the protection scheme. With an additional function next to the protective functionality it would be even possible to realise a self healing grid for maintaining high availability of transport capacity inside the distribution system, to guarantee energy delivery to the end-users of the system.

The proposed protection scheme mentioned above is applied to the distribution system of Goeree-Overflakkee (island found south-west of the Netherlands) and tested inside the simulation environment of Digsilent PowerFactory. This study shows that indeed the transport capacity of the infrastructure applied on this island will be enhanced by changing the topology from radial to meshed, where the right protective coordination is maintained by the proposed protection scheme. This is especially beneficial in the coming years because Goeree-Overflakkee has the ambition to become energy neutral in the year 2030 with the application of extra decentralized generation units on the island. The main disadvantage of a meshed topology is that some of the feeders will be loaded to a higher rated short-time withstand current compared to a radially operated system. For Goeree-Overflakkee this will be true for a limited amount of feeders. This problem could be resolved be replacing these underground feeder by thicker feeders or by investigating if the protective coordination of the proposed protection scheme is fast enough to stay within the borders of the rated short-time withstand current.

Acknowledgement

I would like to thank Joulz Energy Solutions for the opportunity they gave me to realise this research at the department of engineering and consultancy. For this I would like to thank A. Vijselaar, M. Roelofs and H. de Raaf. During the research period I received great technical guidance and support of H. Folkersma. Thank you for your support and patience during this process. I wish to express my sincere thanks to Dr. Ir. M. Popov for the technical advice and guidance I received during the research and writing of my thesis. Also great thanks to the colleagues of the engineering and consultancy department for the support and many laughs.

At last I would like to thank my partner (F. Koreman), father (T. Braat), brother (K. Braat) and especially my mother (J. Braat - de Vries). You are and will always be my greatest inspiration.

R. Braat
E-mail: ruud.braat@gmail.com
Telephone: +31 (0)613714613
Rotterdam, Wednesday 27 May 2015

Contents

List of Figures xiii

List of Tables xv

1 Introduction 1
- 1.1 Objectives of this thesis . . . 1
- 1.2 Outline of this thesis . . . 2

2 Smart Grid 3
- 2.1 The current energy system . . . 4
  - 2.1.1 Transport network . . . 5
  - 2.1.2 Distribution network . . . 5
  - 2.1.3 Energy mix . . . 7
- 2.2 Smart Grid . . . 9
  - 2.2.1 Distribution network . . . 10
  - 2.2.2 Low voltage network . . . 11

3 Power System Protection 13
- 3.1 Fault types . . . 14
  - 3.1.1 Short-circuit transient . . . 14
  - 3.1.2 Symmetrical components . . . 15
  - 3.1.3 Symmetrical fault . . . 16
- 3.2 Protective relays . . . 18
  - 3.2.1 Overcurrent relay . . . 18
  - 3.2.2 Directional overcurrent relay . . . 21
  - 3.2.3 Differential relay . . . 22
  - 3.2.4 Distance relay . . . 23
- 3.3 Protection Problems with the implementation of DG . . . 24
  - 3.3.1 Short-circuit contribution of DG . . . 24
  - 3.3.2 False Tripping . . . 26
  - 3.3.3 Protection blinding . . . 27
  - 3.3.4 Instantaneous current protection . . . 28
  - 3.3.5 Directional protection . . . 30
  - 3.3.6 Islanding . . . 30

4 Protection Schemes for Meshed Operated Distribution Systems 31
- 4.1 Current protection scheme . . . 32
- 4.2 Numerical relay ABB REF630 . . . 33
- 4.3 IEC 61850 . . . 35
- 4.4 Smart Grid protection scheme . . . 36
  - 4.4.1 Version 1 . . . 36
  - 4.4.2 Version 2 . . . 40
- 4.5 Connecting with multiple zones . . . 42
- 4.6 Back-up protection . . . 43
  - 4.6.1 Maintenance of feeder/circuit-breaker . . . 43
  - 4.6.2 Loss of communication . . . 44
  - 4.6.3 Malfunction of circuit-breaker . . . 44
- 4.7 Research towards Smart Grid protection . . . 44

5 Modelling and Simulation Results **45**
5.1 Case study 1 . . . 45
5.1.1 Distribution system . . . 45
5.1.2 Relay model . . . 47
5.1.3 Loadability . . . 48
5.1.4 Emergency operations . . . 49
5.1.5 Rated short-time withstand current . . . 50
5.1.6 Protective coordination . . . 51
5.1.7 Protective coordination problems . . . 54
5.1.8 Undervoltage tripping . . . 54
5.1.9 Self healing principle . . . 56
5.2 Case study 2 . . . 57
5.2.1 Goeree-Overflakkee . . . 57
5.2.2 Distribution system . . . 57
5.2.3 Protection scheme . . . 60
5.2.4 Loadability . . . 64
5.2.5 Rated short-time withstand current . . . 65

6 Conclusion and Recommendation **67**
6.1 Conclusion . . . 67
6.2 Recommendation for future work . . . 68

Bibliography **69**

Abbreviations and symbols **71**

A Wind turbine **73**
A.1 Wind power . . . 73
A.1.1 Performance coefficient . . . 75
A.1.2 Shaft . . . 77
A.1.3 DFIG wind turbine . . . 77

B Model for Digsilent PowerFactory **81**
B.1 Models . . . 81
B.2 RMS vs. EMT simulation . . . 82
B.3 Evenst . . . 83

C MatLab scripts **85**
C.1 Short circuit transient . . . 85
C.2 False Tripping . . . 87
C.3 Protection Blinding . . . 91
C.4 Instantaneous current protection . . . 95

List of Figures

2.1 Present electrical system . . . 3
2.2 The future electrical system . . . 4
2.3 Applied voltage levels in the Netherlands . . . 5
2.4 Electricity network of the Netherlands . . . 6
2.5 Topology distribution network . . . 7
2.6 Energy mix in the Netherlands 2012 total of 3255,76PJ, [1] . . . 7
2.7 Energy flow of the Netherlands during the year 2013, text written in Dutch, source Compendium voor de Leefomgeving . . . 8
2.8 Smart Grid concept, according to ETP [2] . . . 9
2.9 conceptual medium voltage network . . . 10
2.10 conceptual low voltage network . . . 11

3.1 Typical power system protection in a distribution network . . . 13
3.2 Equivalent short-circuit scheme . . . 14
3.3 Short-circuit transient, U_{grid} = 13kV, S_{grid} = 300 MVA, R/X = 0.341 . . . 15
3.4 Symmetrical components . . . 16
3.5 Unbalanced three phase system . . . 16
3.6 Representation of a symmetrical three-phase fault . . . 17
3.7 Sequence network of a three-phase fault . . . 17
3.8 Protection scheme long feeder . . . 18
3.9 Model overcurrent relay . . . 19
3.10 Characteristic definite time over-current relay . . . 19
3.11 Characteristic inverse time over-current relay . . . 20
3.12 Model overcurrent relay with additional directional unit . . . 21
3.13 Directional relay principle for protecting phase 1, feeding the relay I_1 and polarization voltage $U'_{32} = U_{32} + 45°$ . . . 21
3.14 Application overcurrent relays with directional unit . . . 22
3.15 Differential protection . . . 22
3.16 R-X plot distance relay with mho characteristic . . . 23
3.17 Time-distance plot between multiple distance relays . . . 23
3.18 Short circuit contribution DG . . . 24
3.19 Equivalent Thevenin scheme for a three phase sub-transient short circuit calculation . . . 24
3.20 Short-circuit calculation of a distribution network subjected to DG units. From top to bottom: short-circuit calculation over the full length of feeder 2, short-circuit contribution of DG, short-circuit contribution of the grid. . . . 25
3.21 False tripping . . . 26
3.22 Blinding of protection . . . 27
3.23 Example protection blinding . . . 28
3.24 Instantaneous current grading protection . . . 29
3.25 Short-circuit current magnitude seen by the feeder . . . 29
3.26 Short-circuit current contribution of the external grid . . . 29
3.27 Directional current protection . . . 30

4.1 Typical protection scheme with overcurrent protection relays . . . 32
4.2 Numerical directional overcurrent protection with sensitive earth fault detection, ABB REF630 . . . 33
4.3 Programmable environment REF 630 including protection blocks. Top to bottom: directional overcurrent stage (forward), directional overcurrent stage (reverse) and directional instantaneous overcurrent stage (forward or reverse). . . . 34

4.4 Programmable environment REF 630 parameters inside protection blocks 34
4.5 Definition of transfer time by IEC61850 35
4.6 Protection scheme version 1: overcurrent relays with and without directional unit . . . 37
4.7 Protection scheme version 1 with fault in zone 2 37
4.8 Flow chart protection scheme version 1 and 2 38
4.9 Example protective coordination scheme version 1 applied to zone 2 39
4.10 Protection scheme version 2, overcurrent relays with directional unit 40
4.11 Protection scheme version 2 with fault in zone 2 40
4.12 Example protective coordination scheme version 2 applied to zone 2 41
4.13 Protection scheme with connection between more than 2 zones, overcurrent relays with and without directional unit 42
4.14 Logic diagram for relays R12, R13, R24, R23 and R34 43
4.15 Logic diagram adaptation for including maintenance 44

5.1 Distribution system case study 1 46
5.2 Relay model 47
5.3 Protective coordination for a fault in zone 2, with protection scheme version 1 51
5.4 Protective coordination of a phase-to-phase fault on bus 2.2 for protection scheme version 1 52
5.5 Protective coordination of a phase-to-earth fault on bus 2.2 for protection scheme version 1 53
5.6 Concept behind blinding of the directional relays 54
5.7 Voltage magnitude bus 4.1 during a phase-to-phase fault on bus 2.2 for protection scheme version 1 55
5.8 Voltage magnitude bus 4.1 during a phase-to-phase fault on bus 2.2 for protection scheme version 2 55
5.9 Principle behind self healing grid 56
5.10 Self healing grid after a phase-to-phase fault on bus 2.2 56
5.11 Goeree-Overflakkee 57
5.12 Infrastructure connected to main-station Middelharnis 58
5.13 Infrastructure connected to main-station Stellendam 58
5.14 Single line diagram distribution network Stellendam with net openings indicated 59
5.15 Protection scheme version 1 applied to distribution system of Goeree-Overflakkee . . . 61
5.16 Protection scheme version 1 applied to distribution network of Stellendam with interconnected zones indicated 62
5.17 Logic diagram protection scheme version 1 for distribution system Goeree-Overflakkee 63
5.18 Example of an additional input measured from the main feeder for logic diagram zone 2 64
5.19 Critical clearing time calculation radially operated distribution system Stellendam 65
5.20 Critical clearing time calculation meshed operated distribution system Stellendam . . . 65

A.1 Performance coefficient as function of tip speed ratio, with varying pitch angle 75
A.2 Generated energy with varying wind speeds 76
A.3 Two mass mechanical system of a shaft 77
A.4 DFIG wind turbine 78

B.1 Composite frame of a DFIG wind turbine 82

List of Tables

2.1 Generated power and voltage, net code ACM 5

3.1 IEC 60255 constants for defining inverse time relays 20

4.1 Message types and required transfer time according to IEC 61850-5 [3] 35

5.1 Loading of feeders when loads are increased for each step by 10% for radially operated distribution system 48
5.2 Loading of feeders when loads are increased for each step by 10% for meshed operated distribution system 48
5.3 Voltage profile measured for each substaton when loads are increased by 10% for each step, radial topology 49
5.4 Voltage profile measured for each substaton when loads are increased by 10% for each step, meshed topology 49
5.5 Loading of feeders during isolating of one zone from the distribution system 49
5.6 Short-circuit calculation for three phase and phase-to-phase fault with a duration of 1 second 50
5.7 Zone connection 60
5.8 Settings for overcurrent relays with directional unit for protection scheme version 1 . . 63
5.9 Loading main feeders distribution system Stellendam 64

1

Introduction

The present distribution system is evolving towards a Smart Grid. A Smart Grid applies the latest technologies to guarantee a reliable energy system for both the consumers and producers of electrical energy. One of these technologies is the implementation of a communication infrastructure and the generation of energy by renewable energy sources (e.g. solar, wind and biomass). The topic of Smart Grid enjoys much attention with the many stakeholders inside the energy market and is therefore the driving force behind this research.

One of the main research topics during this research will be on what the effect will be on the present protection scheme when distributed generation units are extensively implemented inside the distribution system. The application of distributed generation will have an impact on the present protection scheme. This because the distributed generation units will, besides the external grid, contribute current as well to a faulty component initiated inside the distribution system. Hence the energy flow during a fault will change from radially to meshed perspective. This will ultimately have an impact on the reliability of the protection scheme which will be studied during this research.

Currently one of the main reasons the topology of the distribution system is mostly set radially is due to the implications the present protection scheme will encounter, regarding protective coordination, during a fault inside a meshed operated system. In this research a proposal will be given on how this protection scheme can be enhanced with the help of Smart Grid technologies to still provide the appropriate protective coordination inside a meshed operated distribution system. As mentioned earlier these technologies are the implementation of a communication infrastructure with the latest IEC 61850 communication protocol and the use of substation automation systems (IED - intelligent electronic device).

1.1. Objectives of this thesis

This research is realised under the supervision of Joulz Energy Solutions situated in Rotterdam (Netherlands). Joulz is a leading technical service provider and system integrator for intelligent grid solutions with many years of experience relating to the Dutch electrical grids. Joulz is started this project because it holds many interest regarding the implementation of Smart Grid technologies inside electrical infrastructures. At the start of the thesis the following research questions were formulated by Joulz:

Research question 1: *"Are the current protection techniques inside the distribution system suitable for the coming years?"*

Research question 2: *"How will the future distribution system be protected?"*

1.2. Outline of this thesis

This thesis will consist the following chapters with the following content.

Chapter 2: Smart Grid This chapter will give an overall impression of the present electrical system applied inside the Netherlands. Moreover the definition Smart Grid will be explained, and what actually defines a Smart Grid. As a complement towards this subject a few examples will be given of Smart Grid technologies that can be expected inside this type of electrical infrastructure. Special attention will go towards the distribution system and the low voltage system.

Chapter 3: Power System Protection This chapter describes the protection techniques which are mainly applied inside the present distribution system and how these techniques detect if a fault is situated inside the distribution system with the corresponding algorithm. Furthermore this chapter will give an impression on what the effect will be on the present protection scheme when distributed generation units are extensively implemented inside the distribution system. Calculations will be done with the help of Matlab by substitution a simplified distribution system with a distributed generation unit inside this programmable environment of Matlab to provide the answers to research question 1.

Chapter 4: Protection schemes for meshed operated distribution systems First a brief overview will be given on the current strategy applied towards the protection schemes found in the present distribution systems. Moreover the Smart Grid technologies will be explained which will be utilized in the design of the two proposed protection schemes regarding the protection of meshed operated distribution systems. This will to give a proposal regarding research question 2. Each concept will have its own advantages and drawbacks, which will be described during this chapter.

Chapter 5: Modelling and simulation results The protection concepts in chapter 4 will be firstly applied to a simplified distribution sytem to show the working principle. The simulation for this chapter, including the relay models of the suggested protection scheme, are created inside the programmable environment of DigSilent PowerFactory. This model will be briefly discussed in this chapter. Furthermore a simulation will be given of a distribution system which is derived from the radially operated distribution system of Goeree-Overflakkee (island south-west of the Netherlands). This chapter will show how the performance of this distribution system changes when the radially operated distribution is altered towards a meshed operated distribution system with the help of the protection scheme described in chapter 4. The operating limits regarding loading of the infrastructure and the change in rated short-time withstand current the components will experience will be discussed.

Chapter 6: Conclusion The last chapter will give conclusive answers to the research questions stated in the earlier section. These answers will summarise the results of the studies performed in Chapter 3, 4 and 5.

2

Smart Grid

The electrical power system is regarded as one of the greatest achievements of the 20th century, but also one of the most complex system ever designed. The principal behind the way electrical energy is generated, transported and distributed has not changed since the first application of electrical distribution grids. In the present electrical power system, the generation of energy is done in power plants with electrical generators and is mainly done with non-renewable energy sources like fossil fuels and nuclear energy. This generated energy is transported via a transmission network (lines, cables and transformers) which is controlled and operated by a Transport System Operator (TSO). This transmission network divides the generated energy over several distribution networks, operated by several Distribution Network Operators (DNOs), see figure 2.1. This energy transport from top (power plants) to bottom (end-users) is already changing with the application of large and small wind farms both on land and sea and the implementation of solar farms.

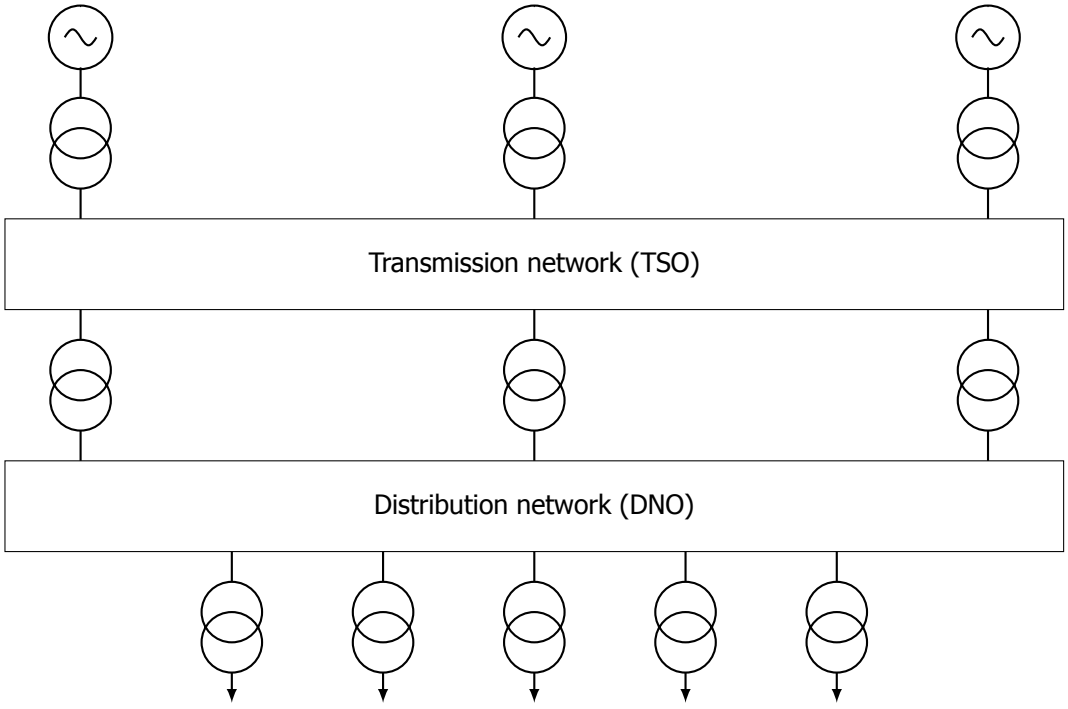

Figure 2.1: Present electrical system

The policy as defined by the Dutch government on the energy agreement is reflected in the renewable energy pact [4]. This pact states that a share of 16% renewable energy must be realized by 2023 and full dependence on renewable energy sources in 2050. This policy corresponds with the energy agreement for 2050, as stated by the European Union. Renewable energy sources in the form of solar, wind, geothermal, water and biomass will be utilized to achieve this agreement.

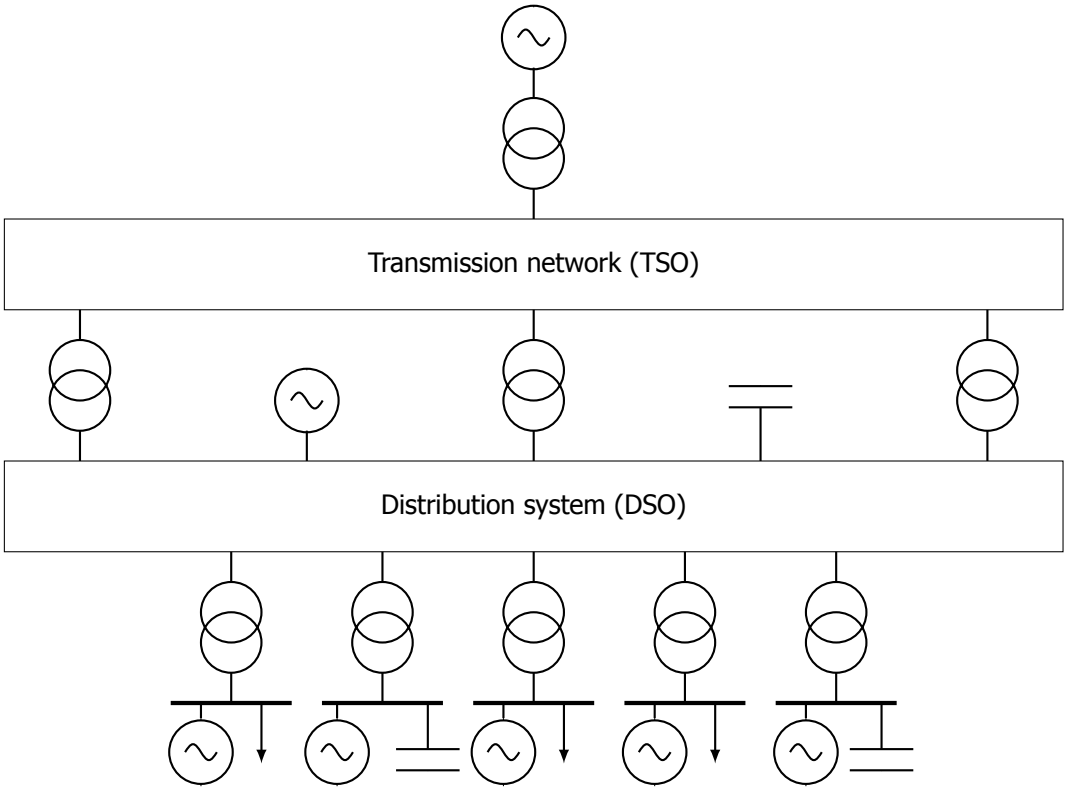

Figure 2.2: The future electrical system

Also communities become more active in being more self sufficient by implementing more DG from renewable energy sources, like the municipal of Goeree-Overflakkee and the inhabitants of Texel. In 2014, the inhabitants of the island Texel (part of the Netherlands) have decided to be self-sufficient with respect to energy generation, and have started a corporation under the name TexelEnergie. A cost/benefit analyses between investing in DG or installing an extra connection to the main land was performed, where the decision was made to implement more DG units on the island [5]. Also the municipal of Goeree-Overflakkee have decided to become energy neutral in the year 2030 with the production of energy realised with the help of wind, solar, biomass and the tides [6].

Implementation of DG from renewable energy sources (e.g. wind and solar) inside the distribution system will create different kind of energy flows over the course of a day. The main reason for this changing energy flow is the unreliability that goes with these renewable energy sources. Not only DG but also the consumption of energy will alter in the future. The trends show that consumption will only increase in the future. Some examples are the rise in popularity of hybrid and/or electric cars usage in comparison with combustion cars of today, and also the use of electrical heating with heat pumps. Not only consumption but also the way we are able to store energy in the future (batteries or the circular motion of a flywheel) will influence the energy flow inside the distribution system.

2.1. The current energy system

The energy system transports electrical energy with the help of different voltage levels which are interconnected via power-transformers. The energy is mainly generated with the help of big centralized energy plants where the energy is transported to the end-user (industry or households) via this described electrical system. Figure 2.3 shows the voltage levels that are currently being applied in the electrical system of the Netherlands [7]. In table 2.1 the voltage levels are given for each production unit with a corresponding generation size [8].

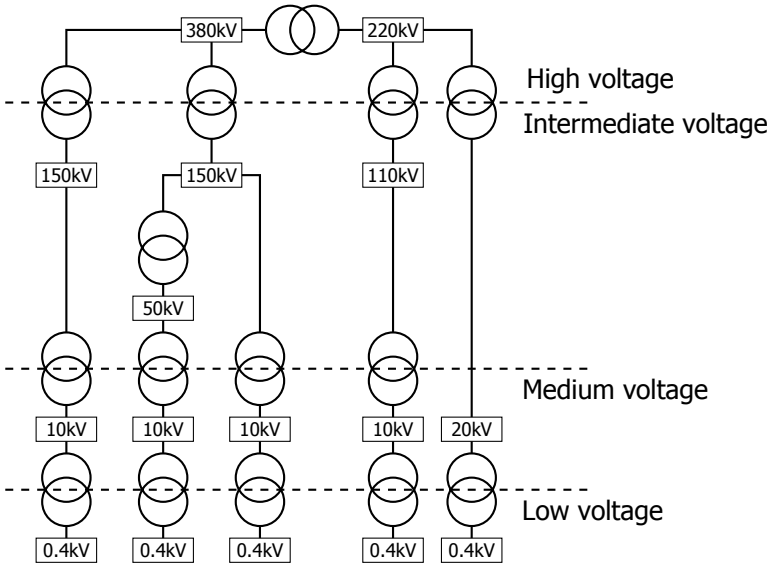

Figure 2.3: Applied voltage levels in the Netherlands

Rated Power	Nominal voltage
< 50 kVA	0.23 kV
50 kVA ≤ 60 kVA	0.4 kV
60 kVA ≤ 0.3 MVA	0.4 kV
0.3 MVA ≤ 3.0 MVA	1 kV < 25kV
3.0 MVA ≤ 100 MVA	25 kV ≤ 50kV
100 MVA<	50 kV <

Table 2.1: Generated power and voltage, net code ACM

1. High voltage, ≥220kV
2. Intermediate voltage, ≥35kV and <220kV
3. Medium voltage, > 1kV and <35kV
4. Low voltage, ≤1kV

2.1.1. Transport network

The high voltage transmission network is used to transport large quantities of generated energy (power plants with generated power levels of 500 MVA and higher) and for the interconnection between neighbouring countries. The ultra high voltage transmission network of the Netherlands is estimated to have around 2750km of transmission lines and 20km of underground cables and is designed to handle critical N-1 situations [9]. This network applies different voltage leves like the 50kV, 110kV and 150kV network with the help of 5250 km of lines and 3800 km of cables. This transport network is controlled and operated by TenneT and is directly connected with Belgium, Germany. This transport nework is also connected with Great-Brittain and Norway but via a high voltage DC (HVDC) connection to decrease the transport losses, see figure 2.4b.

2.1.2. Distribution network

Al the distribution networks in the Netherlands are operated by several DNOs, see figure 2.4a. The rated power levels of the consumers and producers connected to this network are between 0.2 and 35 MVA (for example a wind farm, small gas powered power plants, rail transport, industry, residential area). It is estimated that the distribution network consist of a total of 100.000km of installed underground cable for connecting these consumers and producers.

The distribution network normally is characterized by a loop or multi-loop structure, see figure 2.5. The topology of these loops are altered (with the help of switching devices) to operate the network in a radial structure and thereby simplify the protection scheme. After the occurrence of a fault inside the distribution network, a grid opening can be closed in order to change the configuration of the loop structure and continue the energy delivery to the end-users.

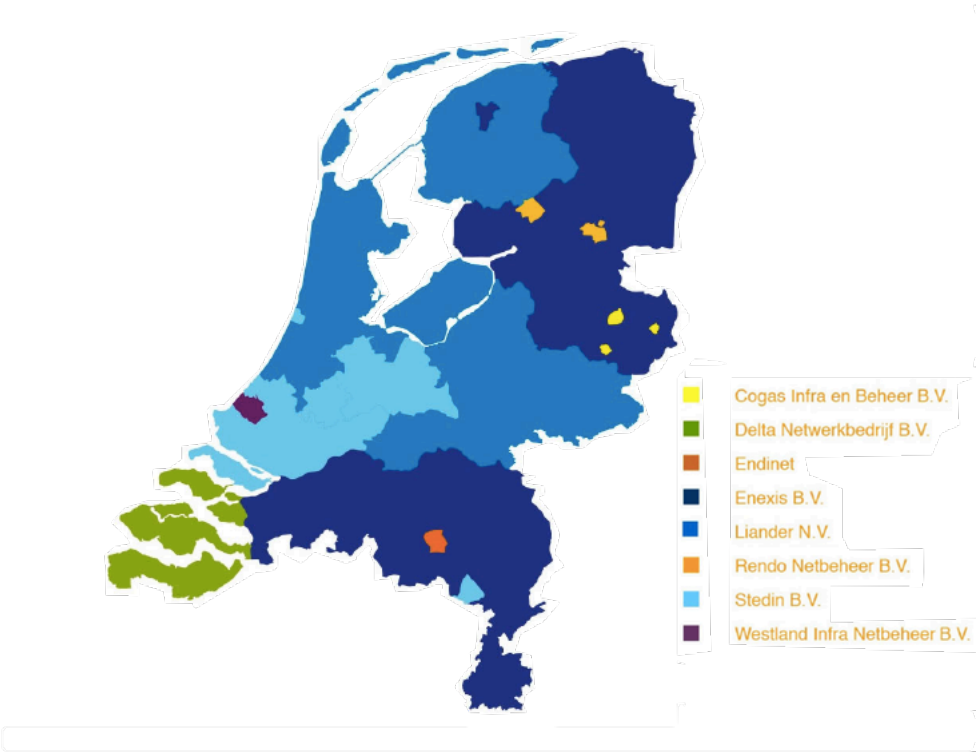

(a) Distribution operators

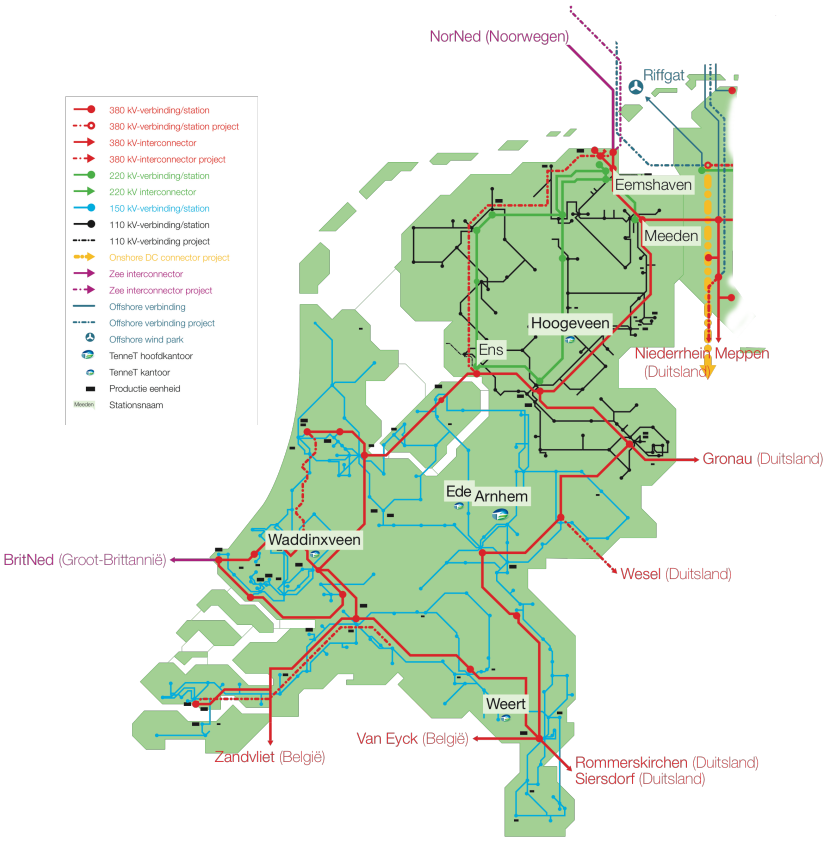

(b) Transmission network, source TenneT

Figure 2.4: Electricity network of the Netherlands

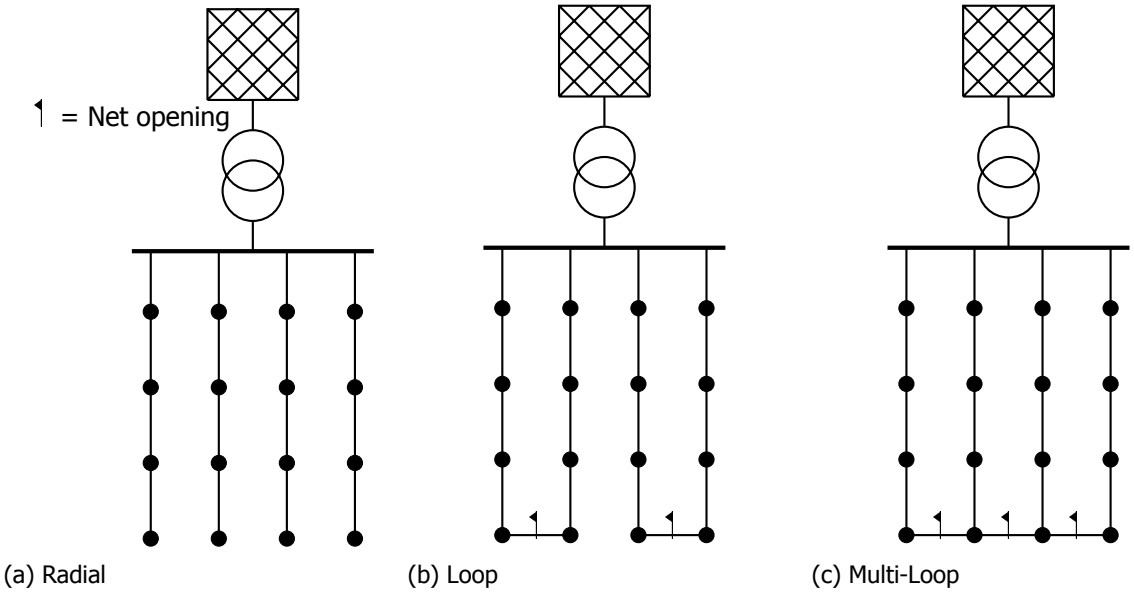

Figure 2.5: Topology distribution network

2.1.3. Energy mix

The Netherlands uses annually around 3.300 PJ (petajoule), see figure 2.6. The generation of energy are mainly realized at a central location, with several primary energy sources which are powered by gas, coal or biomass heated governors. In figure 2.7 an overall representation is given of the energy flow inside the Netherlands during the year 2014. The policy of the Dutch government is a production of 16% of renewable energy sources (RES) by 2020. At the moment RES provides 4%, 130 PJ in total, of the energy mix. This 4% is divided over the following energy sources (source Statistics Netherlands 2013).

- Biomass, 82%
- Wind, 15%
- Solar, 2%
- Geothermal, 0.7%
- Water, 0.3%

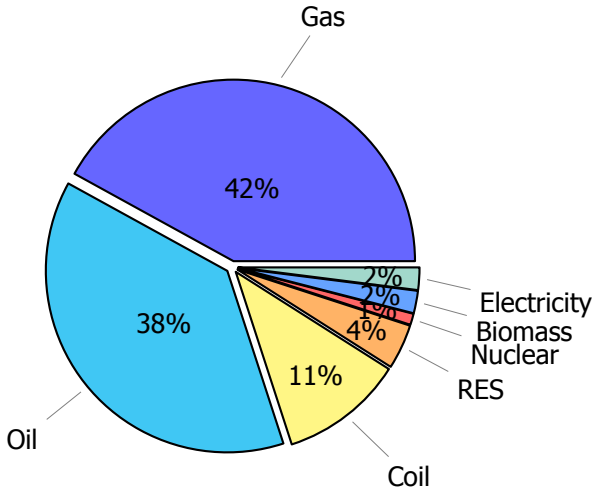

Figure 2.6: Energy mix in the Netherlands 2012 total of 3255,76PJ, [1]

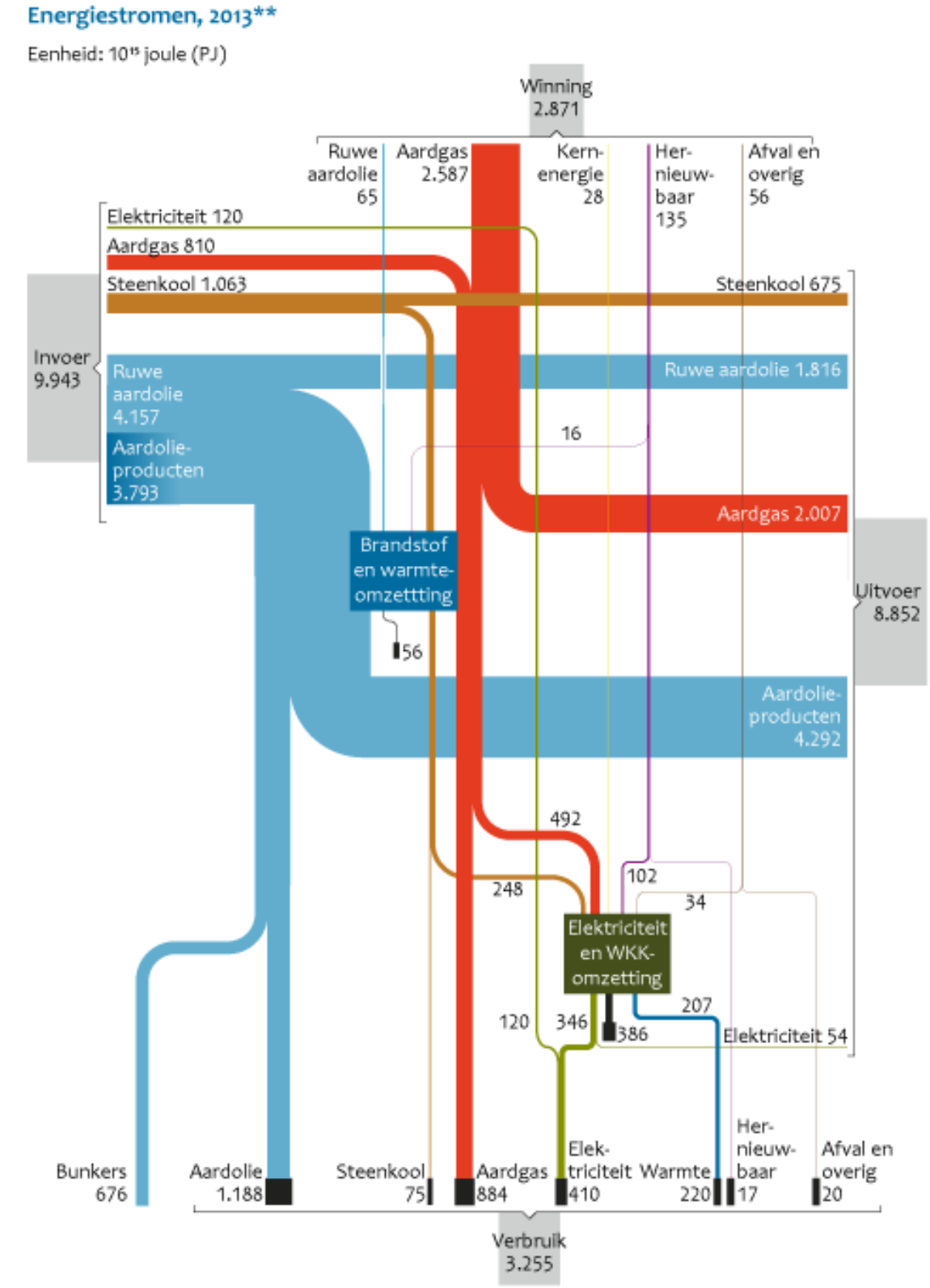

Figure 2.7: Energy flow of the Netherlands during the year 2013, text written in Dutch, source Compendium voor de Leefomgeving

Figure 2.8: Smart Grid concept, according to ETP [2]

2.2. Smart Grid

Europe has a large electric energy system with more than 430 million consumers, 230,000km of transmission lines and 5,000,000km of distribution lines. Secure energy supply has become an important topic of debate in and around Europe, especially when we look at a secure gas supply and the environmental impact of fossil fuels. The European Union has set targets towards energy security and sustainability for 2020 and 2050 [10], under the name SmartGrids. One of the goals is to reduce the greenhouse gas emission by 40% below the 1990 level by 2030. Distributed generation (DG) is described as one of the solutions in order to meet this goal, where DG will use sustainable energy sources like solar, wind, geothermal, water, biomass etc to produce energy. Also the implementation of a large and fast communicating infrastructure between TSOs, DSOs, producers, traders and all the consumers is necessary to avoid disturbances and large scale supply interruptions, by ensuring data is provided in an uniform way. The European Technology Platform (ETP) states that without the use of Smart Grids the security of the future European energy system may not be maintained. Each stake-holder inside the energy system framework applies its own definition for Smart Grids. The ETP defines Smart Grids as follows [2]:

"SmartGrids is a necessary response to the environmental, social and political demands placed on energy supply. SmartGrids will use revolutionary new technologies, products and services to create a strongly user-centric approach for all customers. Where user-centric stand for the increased interest in electricity market opportunities, value added services, flexible demand for energy, lower prices, and micro-generation opportunities." See figure 2.8.

The energy demand in Europe is expected to increase in the future when we look at the demand trend development. This will result in larger power flows inside the transmission and distribution networks. Fast information exchange is crucial when the network is subjected to large DGs, due to the fact that the balance between generations and consumption of electric energy is a crucial factor for a stable electric energy system. Not only the balance, but also the direction of the power will be an important factor to be monitored in future energy transport systems due to the fact that a Smart Grid applies bidirectional power flows depending on the power generated by the DG units. The amount of power will fluctuate over the course of a day when the applied DG units use intermittent renewable energy sources. This intermittent generation will be reinforced with additional bulk generation reserves that can be disconnected from the transport system after enough energy is produced by the DGs.

Not only the generation, but also the loads inside the system will change. One example is the use of the electric cars in comparison with combustion cars, where the end-users will expose the network to

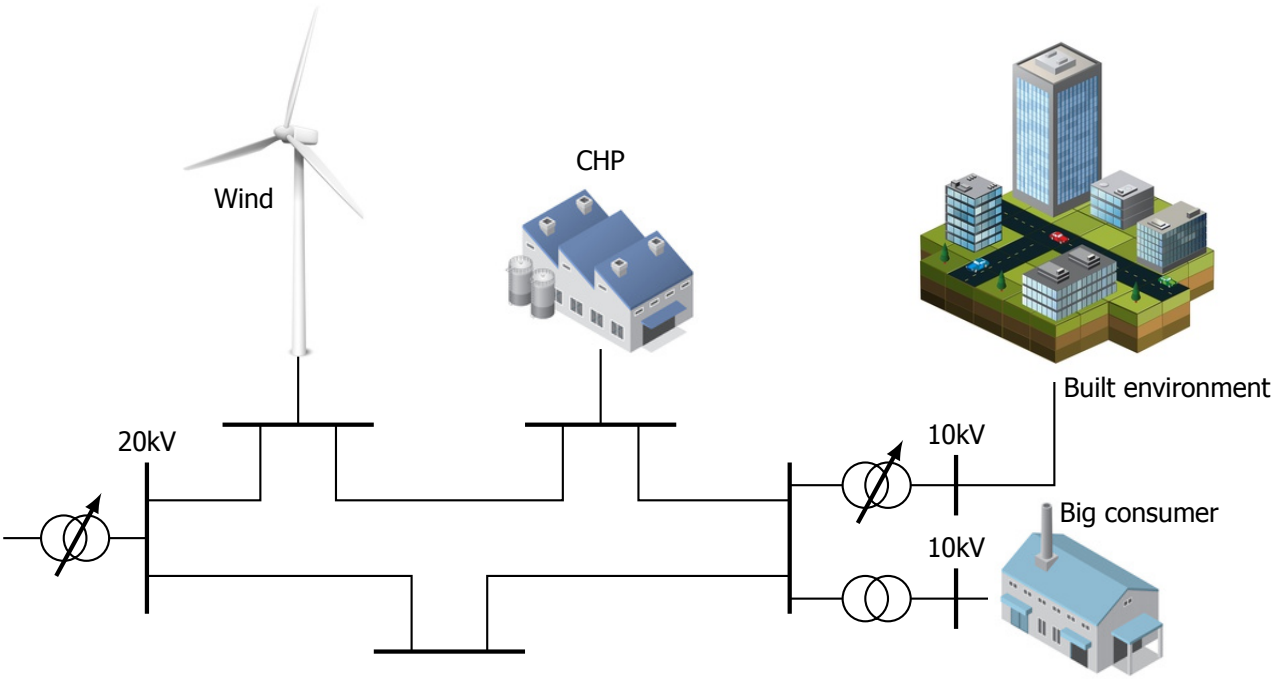

Figure 2.9: conceptual medium voltage network

substantial power flows, if all the electric cars are charged at the same time. Also the implementation of energy storage devices (with the help of battery or flywheel technology) will compensate these loads. The ETP advises the use of a regulatory framework where the market and price signals have to be balanced in the most effective and efficient way.

2.2.1. Distribution network

The current role of the distribution network is mainly to transport an unidirectional power flow from the transport network towards the end-user, via underground feeders. The voltage magnitude during this transport is regulated with the help of transformers. This one-way energy transport is changing in a distribution network of a Smart Grid, because of the DG units (see figure 2.9). Also the use of electric cars, energy storage and smart metering will have an impact on the future role of the DNO. The role of the DNO will change towards the role of a distribution system operator (DSO) with the following operational aspects:

1. Monitoring operational limits of components.
2. Monitoring the power flows inside the network.
3. Monitoring ageing of components.
4. Maintaining reliability of the network.
5. Remote switching and current re-routing.
6. Fault localization.
7. Automatic fault clearing.

Sub-stations inside the distribution network are essential in supplying a steady and reliable power flow towards the LV network. Not only the need for reliability but also the quality of the delivered energy will be an important characteristic that will require monitoring and controlling in the future. DG units inside the distribution network are mostly realised with the help of wind, solar and CHP technologies. The application of dispersed DG will ultimately create different voltage profiles during the course of a day at different locations inside the distribution network. This because the voltage magnitude is

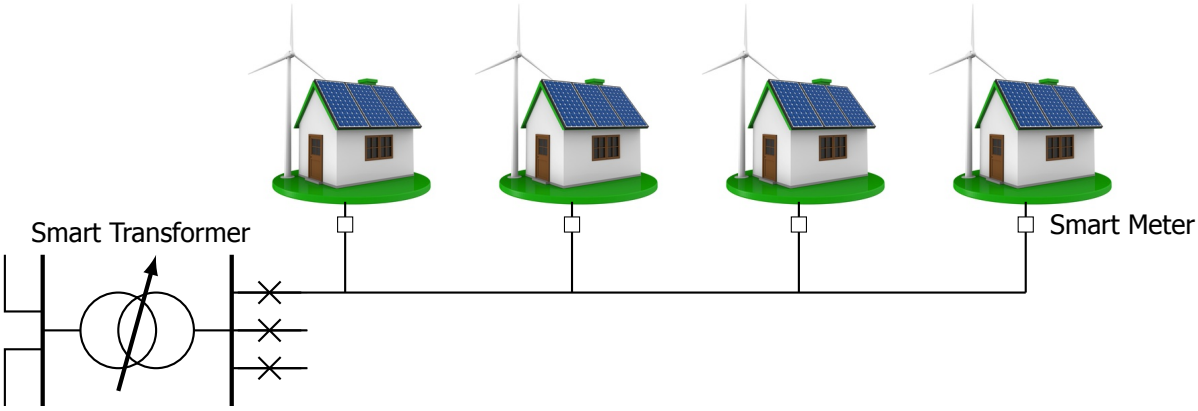

Figure 2.10: conceptual low voltage network

a function of generated power. This situation will create complexity concerning power flow, which is unknown in the current distribution system. To fix this problem, DSOs have an obligation to implement more intelligent monitoring devices concerning on-line voltage control and power flow control, mainly called power quality measurement devices.

The DSO have to guarantee a reliable infrastructure towards the consumers and producers of energy, where the voltage magnitude and frequency have to stay within the set boundaries. Power quality is especially noticeable for the widespread use of sensitive electronics which are vulnerable to large voltage fluctuations (flicker) and harmonics. The measurements towards power quality are currently only available for the transport systems, controlled and monitored by the TSO. Implementation of power quality measuring devices are currently applied inside the distribution network. In the future sub-stations need to get more intelligent regarding data exchange with the operating system of the DSO. Especially when there is a high penetration of DG inside the network. These sub-stations are called intelligent distribution sub-stations (IDS) and are using intelligent measuring systems to compensate voltage dips with the help of smart transformers, power storage to compensate peak loads and reduce the third harmonics inside the distribution network [11]-[12].

The measured data of the voltage, currents, reactive and active power but also the switch position of each circuit breaker or switch gear of each sub-station will be sent, by a wide and fast communication infrastructure, to a centralized controlling system operated by the DSO. This data provides an actual state of the distribution system, where the DSO can take controlling actions when needed, by re-routing energy or disconnect generation units.

2.2.2. Low voltage network

The future low voltage (LV) networks (0.4kV), mainly used for built environment connections, have to guarantee reliable and flexible operations. Most of the distribution networks are designed with a radially topology, where energy is transported in one direction to predictable end-users with an annual load increase of about 2% [13]. Monitoring devices, also called smart meters, are expected to be installed in the coming years at every end-user of the low voltage network. One of the advantages of such kind of meter is in the situation when small DG units are installed over several end-users (like solar or with micro combined heat and power μCHP). Large generation of decentralised energy will create fluctuations in the voltage magnitude that have to be maintained between set boundaries. These digital meters will automatically record consumption and production of energy in hourly intervals and send this information back to the utility for monitoring and billing purposes. These kind of meters allow a two-way communication between the meter and the central system of the utility, which is vital in a Smart Grid. This two-way communication allows the DSO to send signals to the smart meters for activating certain apparatus of end-users (refrigerators, freezers, washing machine, dryers etc.). This action will create an overall smooth loading profile of the distribution network, which leads to more flexibility and reliability. This concept is know as demand response.

The current protection methodology, inside the LV network, is not suited for bidirectional power flows, originated from DGs. A point of connection (POC) can be damaged due to overloading by DGs, when the safety devices inside the distribution sub-station do not notice this inconsistency. This dangerous situation can be resolved by applying power flow estimation, and measurements performed

by the smart meter to monitor each POC for overloading. Moreover fault localization can also be applied with these systems. Not only power flows but also the voltage levels are going to change during the day, because of fluctuating DGs, as stated earlier. This fluctuation can be prevented by using so-called smart transformers in the distribution sub-station, that are equipped with a power electronic tap changer. This tap changer decouples the LV network from the medium voltage (MV), by applying a constant voltage to the MV network.

3

Power System Protection

All the components inside the distribution system need to be protected and monitored to guarantee continuity and safety of the energy supply for both the consumer and the producer of energy. A protective scheme is implemented inside the distribution system to achieve these goals, which utilizes mainly numerical relays, instrumental transformers and circuit-breakers to react on fault events inside the distribution system. One of these fault events can be for example a short-circuit which is initiated by a defective underground connection or a damaged feeder due to excavation works, but also overloading of a component due to surpassing the nominal current it is designed for. The protection scheme applied in this distribution system should fulfill the following characteristics [14]:

1. Reliability: To operate correctly during a fault.
2. Accuracy: To accurately measure the currents and voltages over a wide operating range.
3. Safety: Provide safety for personnel working on the power system.
4. Speed: Minimum operating time is needed, to clear the fault.
5. Selectivity: Only disconnecting the faulted component.
6. Economy: Relays are able to be simple, smaller and cheaper.

The protection schemes are rather simple and straightforward, where each protection relay inside this scheme is protecting one or multiple components (feeders, busbars or transformers) against overcurrents which could ultimately damage the components thermally or mechanically. A reliable protection schemes is easily created because the components are mostly subjected to a unidirectional energy flow which flows from the external grid to the end-users. This unidirectional energy flow is created due the applied topology of the distribution system which is radially operated and connecting only consumers, see figure 3.1. This situation is undergoing a change in the future due to the implementation of large quantities of DG units in the lower parts of the electrical system. Hence, the energy flow is not unidirectional but bidirectional, where the energy vertically and horizontally transported through the electrical system.

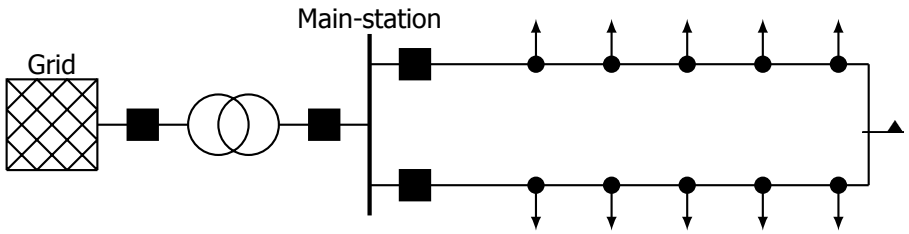

Figure 3.1: Typical power system protection in a distribution network

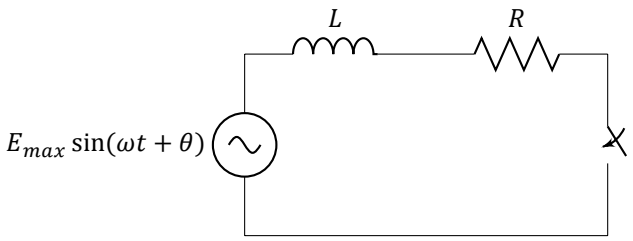

Figure 3.2: Equivalent short-circuit scheme

During this chapter an explanation will be given behind the transient behaviour of the external grid during a short-circuit. Moreover the different types of protective relays that are currently being applied inside the protection schemes will be explained. At last an impression will be given towards the impact large quantity of DG units will have on the overcurrent protection scheme and if this protection strategies is still adequate toward large implementation of DG.

3.1. Fault types

A fault inside the distribution system is defined as any failure that disturbs the normal current flow inside the system. The protection scheme inside the distribution system protects the components against overloading, symmetrical and unsymmetrical faults. This section will mainly concentrate on the symmetrical (three-phase) and unsymmetrical (phase-to-phase, phase-to-ground and phase-phase-to-ground) fault events. The (un)symmetrical fault events are mostly created by defected underground connections (phase-to-earth fault) or excavation work (thee-phase or phase-to-phase fault). The symmetrical three-phase short-circuit has the lowest probability to occur but is the severest faults with the largest currents magnitude. The transient the faulted component experiences during this symmetrical three phase short-circuit will be studied along with the concept behind symmetrical components to calculate unsymmetrical faults.

3.1.1. Short-circuit transient

The current magnitude during a symmetrical three-phase faults depends on the equivalent impedance of the circuit, short-circuit power of the external grid and the moment the short-circuit appears in the circuit. The short-circuit transient can be distinguished in a sub-transient, transient and steady-state current magnitude. Knowledge about this magnitude is important for the selection of circuit breakers and the settings for the protective relays protecting this circuit. The equivalent circuit for a symmetrical three-phase short-circuit (with the capacitance of the cable neglected for this example) can be defined by figure 3.2. The Kirchoff's voltage law for this circuit gives the following nonhomogeneous differential equation, see equation 3.1.

$$E_{max}sin(\omega t+\theta) = Ri + L\frac{di}{dt} \tag{3.1}$$

The solution for the nonhomogeneous differential equation 3.1 is given by equation 3.2, which consist of a steady-state sinusoidal component and a decaying exponential dc component. It has to be noted that this dc component is a function of the equivalent R and L components of the circuit and is better known as the time constant of the circuit. The R and L components for the external grid are better known as the R/X ratio of the connected circuit and need to be included in the equivalent impedance of the circuit to determine the course of the short-circuit transient. This transient can be seen in figure 3.3, where the red line corresponds with the dc component and the blue line with the sum of the dc and sinusoidal component. This transient is separated in a sub-transient, transient and steady-state part.

$$i(t) = e^{-\left(\frac{R}{L}\right)t}\left(\frac{-E_{max}}{\sqrt{R^2+\omega^2L^2}}\sin\left(\theta - tan^{-1}\left(\frac{\omega L}{R}\right)\right)\right) + \frac{E_{max}}{\sqrt{R^2+\omega^2L^2}}\sin\left(\omega t+\theta - tan^{-1}\left(\frac{\omega L}{R}\right)\right) \tag{3.2}$$

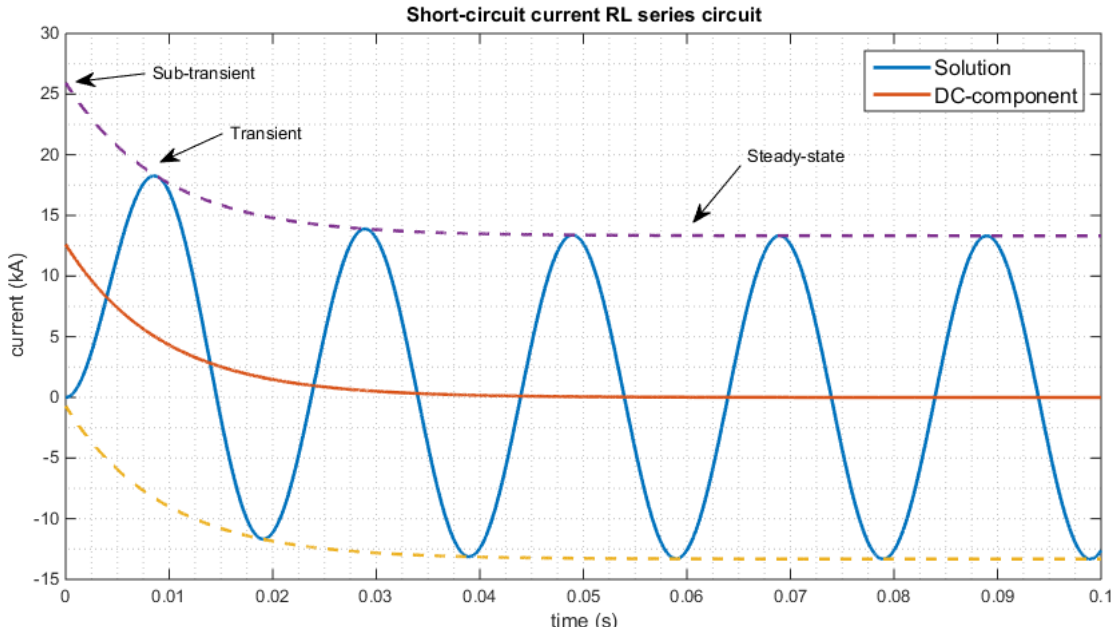

Figure 3.3: Short-circuit transient, U_{grid} = 13kV, S_{grid} = 300 MVA, R/X = 0.341

The maximum short-circuit power the external grid can deliver during a fault is given by the variable S_{grid}. This variable is usually dominant regarding the current magnitude during a fault inside the distribution system. Furthermore the ratio R/X of the external grid is given, which resembles the equivalent reactance and resistance of the external grid. Equations 3.4 and 3.5 are applied for determining the corresponding reactance en resistance of the external grid, which are taking into consideration during the short-circuit computation in figure 3.3.

$$Z_{grid} = \frac{U_{grid}^2}{S_{grid}} \tag{3.3}$$

$$R_{grid} = \frac{Z_{grid}}{\sqrt{1 + \frac{1}{(R/X)^2}}} \tag{3.4}$$

$$X_{grid} = \frac{Z_{grid}}{\sqrt{1 + (R/X)^2}} \tag{3.5}$$

3.1.2. Symmetrical components

The current contribution of the external grid during a fault is a function of time, as seen in the previous section and figure 3.3. The transient behavior consist of a sub-transient, transient and steady-state period, where each of these periods corresponds with an equivalent impedance (Xd", Xd' and Xd). These impedances can be used to calculate the short-circuit current magnitude for each of these periods with the help of symmetrical components. Symmetrical components make use of the transformation of a symmetrical n-phase system and decouples this system into n separated one phase systems, see figure 3.4. For a three-phase system the following one phase systems are obtained:

- Positive sequence network
- Negative sequence network
- Zero sequence network

The positive sequence system is the only system active during a symmetrical load/fault. However when the network is subjected to an unsymmetrical load/fault, a coupling exists between the three sequence networks, where the voltages and currents are the sum of all the coupled symmetrical components as can be seen in figure 3.5. The three-phase voltages or currents can be represented by phasors which can be expressed through a power-invariant transformation given in equations 3.6-3.8.

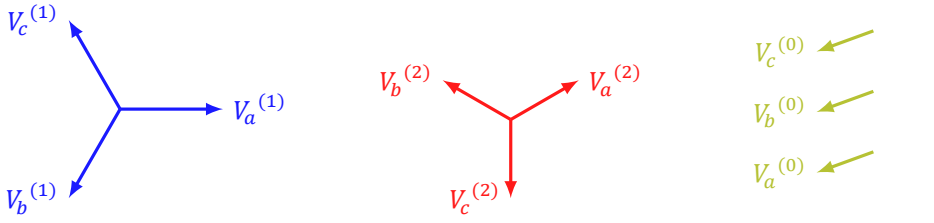

(a) Positive sequence (b) Negative sequence (c) Negative sequence

Figure 3.4: Symmetrical components

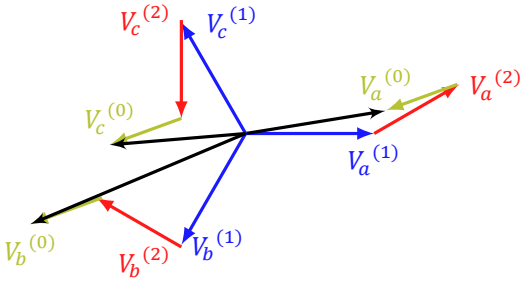

Figure 3.5: Unbalanced three phase system

$$V_a = \frac{1}{\sqrt{3}}(V_a^{(0)} + V_a^{(1)} + V_a^{(2)}) \tag{3.6}$$

$$V_b = \frac{1}{\sqrt{3}}(V_b^{(0)} + V_b^{(1)} + V_b^{(2)}) \tag{3.7}$$

$$V_c = \frac{1}{\sqrt{3}}(V_c^{(0)} + V_c^{(1)} + V_c^{(2)}) \tag{3.8}$$

It can be observed from figure 3.4 that the positive sequence phasors are nearly equal to the negative sequence phasors. The only difference is that the negative sequence network is rotating in the opposite direction of the positive sequence network. The symmetrical components given in equations 3.6-3.8 can also be written in the following matrix form.

$$\begin{bmatrix} V_a \\ V_b \\ V_c \end{bmatrix} = \mathbf{V} = \frac{1}{\sqrt{3}} \begin{bmatrix} 1 & 1 & 1 \\ 1 & a^2 & a \\ 1 & a & a^2 \end{bmatrix} \begin{bmatrix} V_a^{(0)} \\ V_a^{(1)} \\ V_a^{(2)} \end{bmatrix} = \mathbf{AV'} \tag{3.9}$$

The matrix given in equation 3.9 applies a complex variable (a), which has the following characteristics: $a = e^{j\frac{2\pi}{3}}$ and $0 = 1 + a + a^2$. **A** is a unitary 3 x 3 transformation matrix, where unitary is defined as a complex matrix whose columns (or rows) constitute an orthonormal basis. The symmetrical components can moreover by applied to the currents of the given unbalanced system as seen in equation 3.10. An example will be given in the following section by applying symmetrical components to a symmetrical three-phase fault.

$$\begin{bmatrix} I_a^{(0)} \\ I_a^{(1)} \\ I_a^{(2)} \end{bmatrix} = \mathbf{I'} = \frac{1}{\sqrt{3}} \begin{bmatrix} 1 & 1 & 1 \\ 1 & a & a^2 \\ 1 & a^2 & a \end{bmatrix} \begin{bmatrix} I_a \\ I_b \\ I_c \end{bmatrix} = \mathbf{A}^{-1}\mathbf{I} \tag{3.10}$$

3.1.3. Symmetrical fault

A symmetrical three-phase Y-impedance fault is connected between a three-phase system and ground, through a resistance (Z_n) (see figure 3.6). The following conditions apply for this type of fault: $I_a = I_b = I_c$, and $I^{(0)} = \frac{1}{\sqrt{3}}(I_a + I_b + I_c) = \frac{1}{\sqrt{3}}I_n$. Equation 3.11 is obtained by applying the given conditions together with the symmetrical components given in the section above.

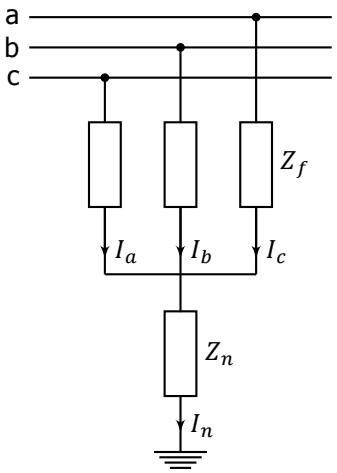

Figure 3.6: Representation of a symmetrical three-phase fault

$$\begin{bmatrix} V_a \\ V_b \\ V_c \end{bmatrix} = Z_y \begin{bmatrix} I_a \\ I_b \\ I_c \end{bmatrix} + Z_n \begin{bmatrix} I_n \\ I_n \\ I_n \end{bmatrix} = Z_y \mathbf{A} \begin{bmatrix} I^{(0)} \\ I^{(1)} \\ I^{(2)} \end{bmatrix} + Z_n \sqrt{3} \begin{bmatrix} I^{(0)} \\ I^{(0)} \\ I^{(0)} \end{bmatrix} \tag{3.11}$$

A decoupled equivalent sequence network is realised for a Y-impedances symmetrical three-phase fault by converting the voltage in the abc-domain on the left side of equation 3.11 to the 012-domain. This result is obtained by multiplying the left and right side with the complex matrix **A**. The result of this mathematical expression is given by equation 3.12, where the right side of this equation will be taken into consideration for the equivalent symmetrical component circuits.

$$\begin{bmatrix} V^{(0)} \\ V^{(1)} \\ V^{(2)} \end{bmatrix} = Z_y \begin{bmatrix} I^{(0)} \\ I^{(1)} \\ I^{(2)} \end{bmatrix} + Z_n I_0 \sqrt{3} \mathbf{A}^{-1} \begin{bmatrix} 1 \\ 1 \\ 1 \end{bmatrix} = Z_y \begin{bmatrix} I^{(0)} \\ I^{(1)} \\ I^{(2)} \end{bmatrix} + 3 Z_n I^{(0)} \begin{bmatrix} 1 \\ 0 \\ 0 \end{bmatrix} = \begin{bmatrix} (Z_y + 3Z_n) & 0 & 0 \\ 0 & Z_y & 0 \\ 0 & 0 & Z_y \end{bmatrix} \begin{bmatrix} I^{(0)} \\ I^{(1)} \\ I^{(2)} \end{bmatrix} \tag{3.12}$$

The equivalent symmetrical system of the external grid connected to the symmetrical three-phase fault can be modelled as a symmetrical synchronous induction machine. This symmetrical machine only has an internal voltage source in the equivalent positive-sequence system network and moreover has a zero (Z_0), positive (Z_1) and negative (Z_2) impedance in the corresponding sequence networks which have to be taken into account for the realization of the equivalent symmetrical networks [15]. The equivalent sequence network of the symmetrical three-phase Y-impedance fault, connected to ground, becomes equal to figure 3.7. This figure shows that there is only current present in the positive sequence network, due to the connected voltage source. The external grid is still symmetrically loaded even after the occurrence of the fault. This is because the same fault impedance is present in each line. Current will flow only in the positive sequence network, which can be calculated by equation 3.13, where V_f is the phase-to-neutral voltage.

$$I^{(1)} = \frac{V_f}{Z_1 + Z_y} \tag{3.13}$$

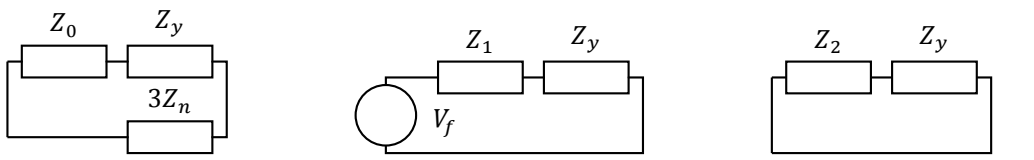

(a) Zero sequence network (b) Positive sequence network (c) Negative sequence network

Figure 3.7: Sequence network of a three-phase fault

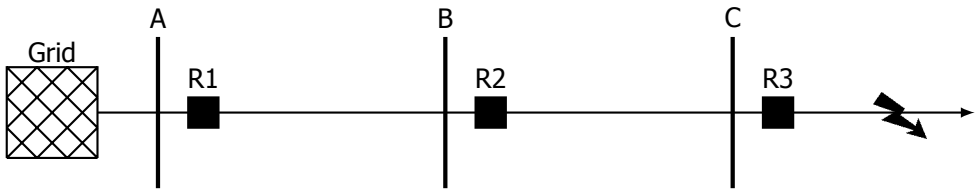

Figure 3.8: Protection scheme long feeder

3.2. Protective relays

Protective relays have the function to protect the components inside the distribution system against mechanical stresses and thermal damage, due to magnetic forces and heat exchange caused by a rise of the current magnitude during a short-circuit. The currents and voltages are measured by instrument transformers which provide the measured data to the protective relays. Over the years the protective relay technology have seen some significant changes, each change bringing with it reductions in size and improvements in functionality [16]:

- **Electromechanical**: work on the principle of a mechanical force, generated by current flow in one or more windings on a magnetic core or cores, operating relay contacts.
- **Static**: Absence of moving parts to create the relay characteristics. These characteristics are created by analogue electronic circuits instead of coils and magnets. However the output contacts are still generally attracted armature relays like in most of the electromechanical relays.
- **Digital**: Microprocessors and microcontrollers replaced analogue circuits applied in static relays for creating the characteristics. The measured quantities are converted from analogue to digital and supplied to the microprocessor which applies a counting technique or use of discrete fourier transform to implement the algorithm. These microprocessors have a limited processing capacity and memory and therefore the functionality is limited.
- **Numerical**: This relay is a development of the digital relay due to advances in technology regarding the use of one or more digital signal processors optimised for real time signal processing, running the mathematical algorithms. For fast real time processing and more detailed analysis of the waveforms, several digital signal processors can be run in parallel. The numerical relay has the ability that previously required several discrete relays, therefore a single numerical relay has build many protection functions inside it. Currently this relay is the most preferable relay technology applied inside energy distribution systems due to the many protection functions build inside and the function to communicate between numerical relays. These many functionalities give the power protection engineer a lot of freedom during the design of a correctly operating protection scheme.

It has to be noted that not all relay types require both the voltage and current to operate; this depends mainly on the function of the relay. These relays are decentralized decision makers inside a protection scheme which undertake protective coordination when the operational limits are surpassed of the components that are being protected. The protective coordination is created by operating a specific circuit breaker to isolate the fault. The current, voltage, frequency and power are one of the several variables these relays can measure. The component which is subjected to a fault is isolated from the distribution system by activating the nearest circuit breaker, where in most cases safe operations can continue without the loss of energy supply. It have to be taken into account that this is not always feasible, and that the energy supply is lost with severe faults like critical N-1 situations. A simple protective scheme for a long feeder can be observed in figure 3.8. This example will be extensively applied during the following sections to show the characteristics of the different types of protective relays.

3.2.1. Overcurrent relay

The overcurrent relay is the most common protective device found inside a protective scheme. This type of relay protects a single or multiple components against overcurrents which could be caused by overloading or a short-circuit. This type of relay only requires a current transformer to determine if the

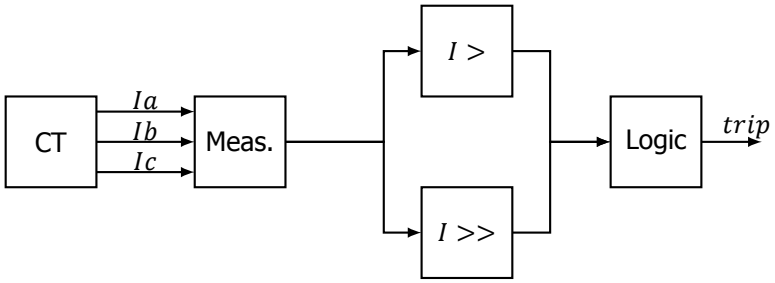

Figure 3.9: Model overcurrent relay

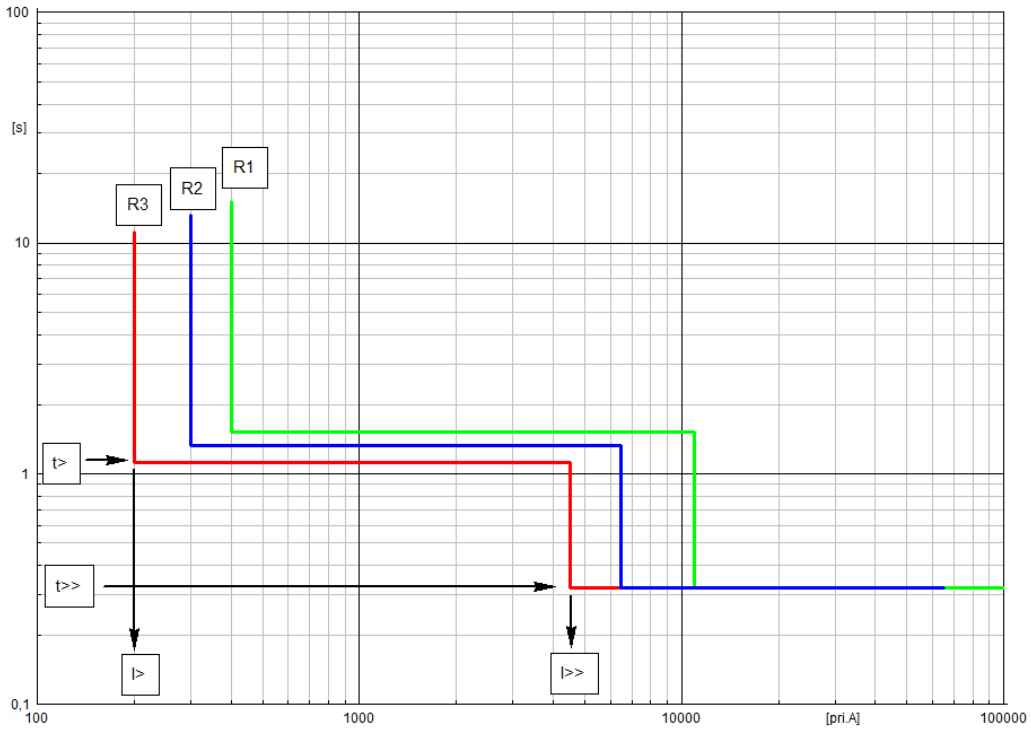

Figure 3.10: Characteristic definite time over-current relay

system is operating in (ab)normal working condition. See figure 3.9 for the applied model of this relay. This relay will send a (un)delayed tripping signal to the circuit breaker when it detects an abnormal current magnitude (usually 1.5 times nominal current of the component that is being protected) in one of the three phases. The time it takes the protective relay to send a tripping signal to the circuit-breaker depends on the magnitude of the short-circuit current and the tripping characteristic applied inside the relay. Regardless of the equipped tripping characteristic it is still important that the circuit-breaker closest to the fault reacts faster than the other relays. This must be realised to achieve a protection scheme with a selective characteristic. Overcurrent relays are normally equipped with a definite or inverse time switching characteristic [17] which will be further explained in this section.

The definite time overcurrent relay operates instantaneously or with a user defined set delay time when the current magnitude surpasses a predetermined value (pick-up current) for a specific period of time, see figure 3.10. In this figure two stages are defined regarding the pick-up current (overcurrent and instantaneous overcurrent) with the corresponding operating time. The overcurrent stage functions as back-up protection for the instantaneous overcurrent stage when the fault current does not surpass the instantaneous overcurrent stage. This characteristic is preferred by all the DNOs in the Netherlands.

- I>: overcurrent stage.
- I>>: instantaneous overcurrent stage.
- t>: overcurrent stage operating time.
- t>>: instantaneous stage operating time.

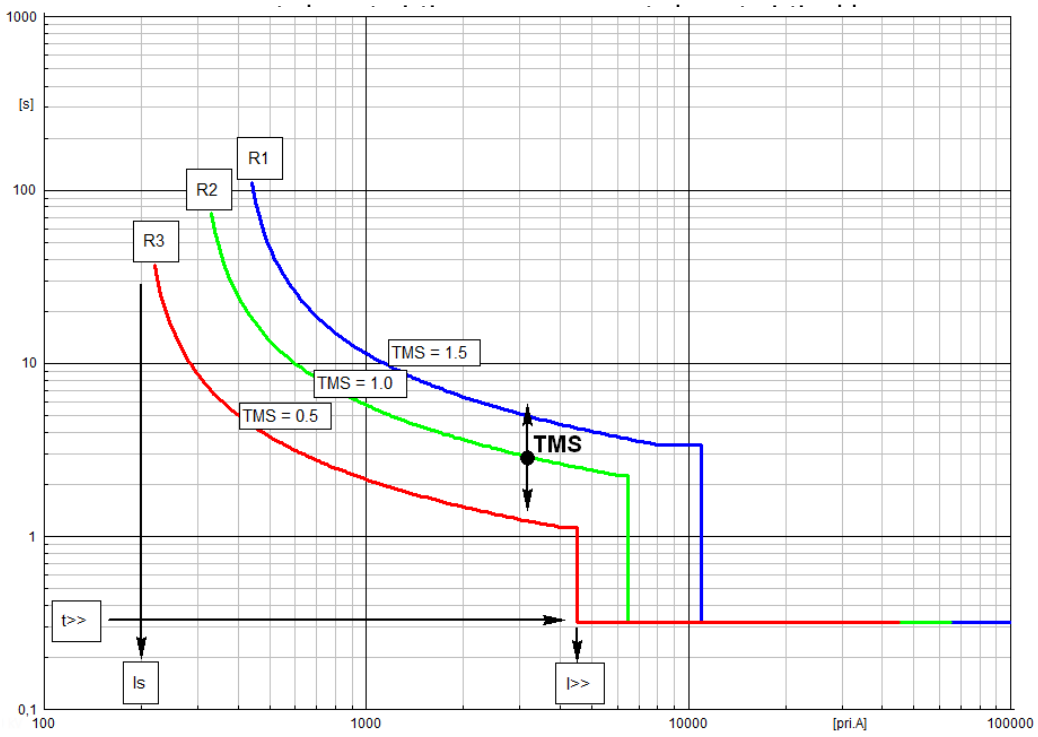

Figure 3.11: Characteristic inverse time over-current relay

Type	**k**	α
Inverse	0.14	0.02
Very inverse	13.5	1
Extremely inverse	80	2

Table 3.1: IEC 60255 constants for defining inverse time relays

The operating time is adjusted such that the relay closest to the fault will operate first while the other relays function as back-up protection by applying time grading (usually 0.3s). This time grading strategy will create time discrimination inside the protection scheme providing selectivity and reliability. An example is given in the situation that a short-circuit arises in the last part of the feeder, depicted in figure 3.8. Relay 3 will be the first to undertake protective coordination, while the operating time of relay 2 will be delayed longer for providing the correct protective coordination in the event that relay 3 malfunctions. The disadvantage of this protection strategy is that the operating time of the relay near the external grid becomes longer. This will subject the components to an overcurrent for a longer period of time. This needs to be taken into consideration when designing the distribution system.

The inverse time relay characteristic is also a function of the current magnitude even though that the delayed tripping signal differs for each short-circuit magnitude, see figure 3.11. The tripping curves of a inverse time relay are defined by the standard IEC 60255 with equation 3.14. These curves are being classified between inverse, very inverse or extremely inverse time characteristics. The constants for these curves are given in table 3.1.

$$t = TMS\left(\frac{k}{\left(\frac{I}{I_s}\right)^{\alpha} - 1}\right) \tag{3.14}$$

- t: operating time for constant current I (sec),
- TMS: time multiplier setting,
- I: energizing current (A),
- I_s: overcurrent setting (A),
- k, α: constants defining the applied curve.

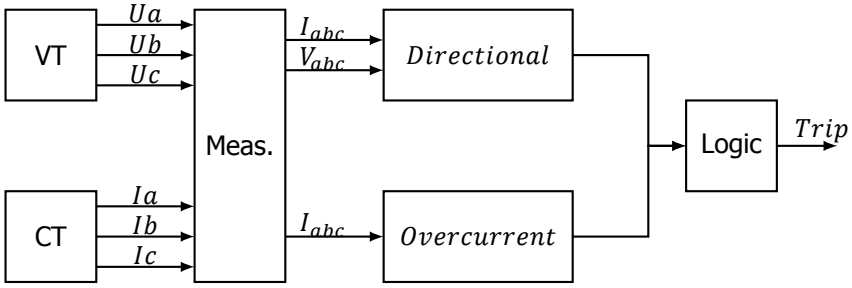

Figure 3.12: Model overcurrent relay with additional directional unit

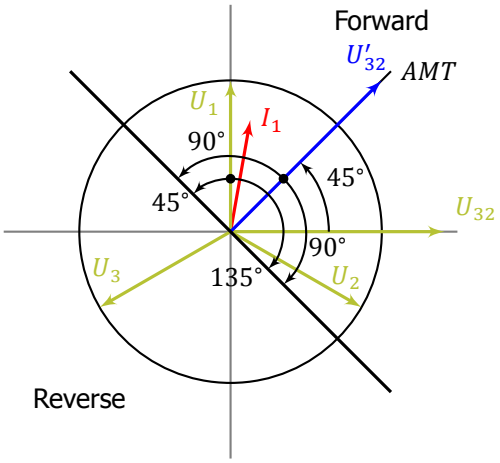

Figure 3.13: Directional relay principle for protecting phase 1, feeding the relay I_1 and polarization voltage $U'_{32} = U_{32} + 45°$

3.2.2. Directional overcurrent relay

The directional relay is equipped with an overcurrent relay and a directional unit which determines the direction of the current during (ab)normal working conditions, see figure 3.12. This directional relay can discriminate if the current is flowing forward (from load to the external grid) or reverse (from the external grid to the load). This directional unit determines the direction of the power flow by comparing the angle between the ”polarization” voltage phasor and the ”operating” current phasor. The polarization voltage phasor is determined by measuring the line voltage between the opposite two phases of the phase which is providing the operating current phasor. This phasor is responsible, together with the polarization technique, for determining the region of operations. In the case that phase a is providing the operating current phasor the line voltage between phase b and c will be applied for computing the polarization voltage phasor.

Various polarization techniques are available inside the model of the relay. The most common polarization technique is the, ”voltage, cross 90” better known under the name, ”Maximum Torque Angle” (MTA) which is derived from the older mechanical relays with a directional unit. The MTA is the angle by which the polarized voltage phasor is rotated by the so-called angle of maximum torque (AMT). In the case of figure 3.13 the AMT is equal to $45°$. In this figure phase 1 is used as a operating current phasor (I_1), where the line-voltage of phase 2 and 3 is used for the ”polarization” voltage phasor (U'_{32}). The angle of operation (forward direction) is when the operating current phasor, in the case of figure 3.13, is between $45°$ leading to $135°$ lagging the voltage phasor U_1. It is not desired to apply the voltage of phase 1 for voltage polarization when the current of phase 1 is measured to determine the operating current phasor. This is because the voltage over the faulted phase will collapse during a fault which will also be measured by the directional relay.

An example situation where a directional relay is desired is in the situation where the distribution system is subjected to an energy flow from multiple energy sources, or when parallel lines are needed for providing the correct transport capacity. These scenarios create a fault current inside the distribution system which flows in multiple directions. The example in figure 3.14 shows the application of a parallel feeder where directional relays are employed to provide a selective operating protection scheme. Relay 1, 2 and 3 don’t apply a directional units inside the protective relay and will operate when the current

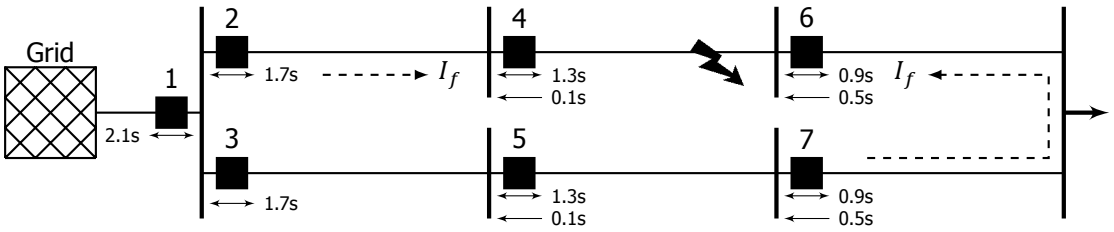

Figure 3.14: Application overcurrent relays with directional unit

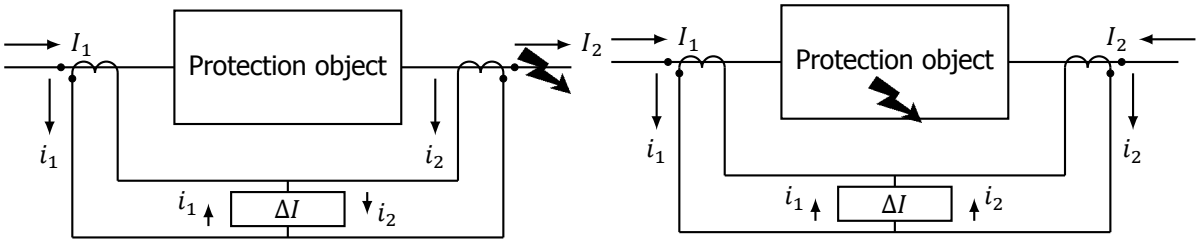

(a) Normal operations

(b) Operating conditions

Figure 3.15: Differential protection

is flowing reverse or forward (seen from the relay position). Time-grading between the directional and non-directional relays towards the source create a selective protective scheme. Relay 4 till 7 have a relay that measures the current both ways with a directional measurement unit looking forward. Without the use of these directional relay it would be very hard to realize a protection scheme with a selective characteristic. Because each current direction for relay 4 till 7 are set with a different time setting a selective protection scheme is realised with a high protective coordination speed.

3.2.3. Differential relay

Differential protection is applied for measuring the differences between incoming and outgoing currents between two or more connections. This type of relay determines if the net sum of the measured currents is equal to zero. If not a fault must be present inside the zone that is being protected and the relay will undertake protective coordination. Differential protection is popular due to its short tripping time, which provides a reliable and fast protective scheme. Moreover the distribution system is divided into protection-zones due to this type of relay, which makes it easy to locate the faulted component. This will ultimately shorten the maintenance time needed to restore the energy flow.

Under normal operating conditions, the differential relay will not generate any tripping signal, even when a fault is present outside the protection-zone, see figure 3.15a. A fault outside the protection zone will create a so-called through current with the same magnitude at both the CT positions. No tripping signal will be created in this situation because the net sum of the currents provided to the differential relay is equal to zero, see figure 3.15b. The net sum of the currents will not be equal to zero when a fault does appear within the protection-zone, due to the configuration of the CT's. This will create a differential current which will trip the differential relay [18].

When the current magnitude falls inside the linear range of the CT hysteresis the error between the CT will be proportional and the differential relay will operate appropriately. In the event of a large through current magnitude the CTs providing the measuring signals will usually not provide identical secondary currents for the same primary current. This because of their usual difference in magnetising characteristics, which will result in a rapidly increase of false differential current. This could ultimately lead to false tripping of the differential relay. To resolve this problem a differential relay setup can be applied which applies an additional variable-percentage characteristic, better know as a percentage biases. This biased differential relay increases the pick-up threshold when the through current increases. This will produce a more stable operating characteristic which prevents unnecessary tripping of the relay when CT saturation is expected during a large through current.

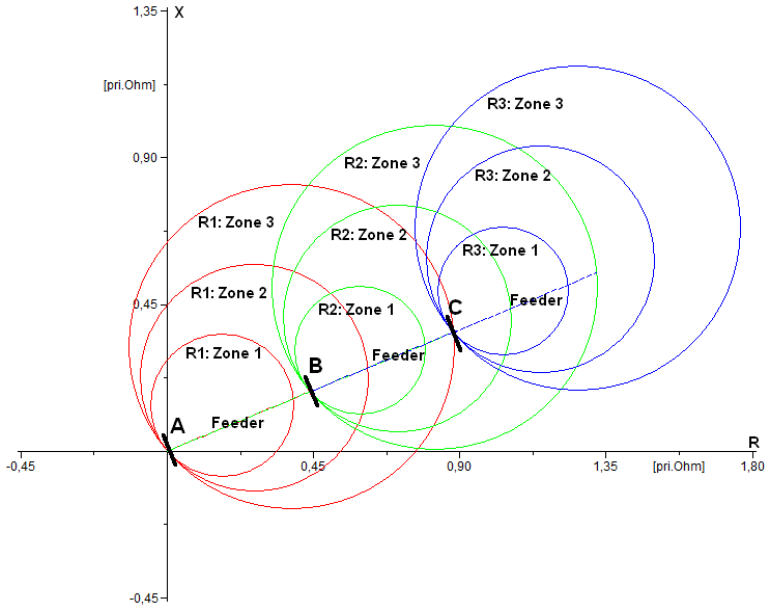

Figure 3.16: R-X plot distance relay with mho characteristic

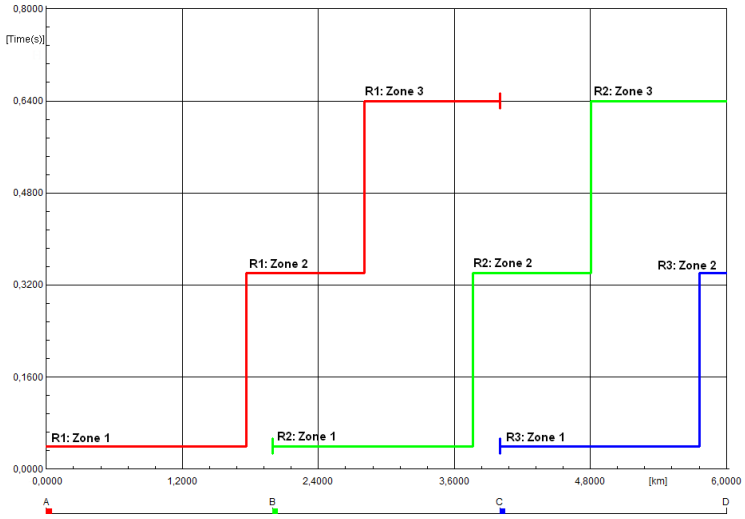

Figure 3.17: Time-distance plot between multiple distance relays

3.2.4. Distance relay

Distance protection has the characteristic to discriminate between different fault locations inside the feeder for both forward and reverse positions. This is achieved by measuring the voltage and current at the location of the relay, to determine the magnitude of the impedance seen by the relay between the relay position and the fault location. The main advantage of choosing this kind of relay is that the protection zone depends on a predetermined point. This point depends on the impedance of the feeder which is a constant during every circumstance. The zone dependency between distance relays gives this protection scheme a highly selective characteristic with appropriate back-up protection.

It is common practice to provide three protection zones for each distance relay to cover several components inside the distribution network and for providing back-up protection in the case of a malfunctioning relay/circuit-breaker. Each of the three zones have a specific tripping time for creating time discriminating between the distance relays (see figure 3.17). Zone 1 usually covers 80% of the total distance of the feeder. The remaining 20% is a safety margin for measurement errors created by transformers and line impedance calculations. Zone 2 covers the remaining 20% distance of the feeder including 30% of the next feeder. Zone 3 can cover multiple feeders as like in the example of figure 3.16. In this figures the zones are defined by using a commonly applied mho characteristic. This characteristic determines the region for each protection zone in the complex impedance plane.

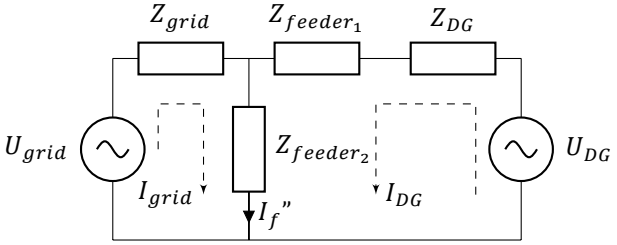

Figure 3.18: Short circuit contribution DG

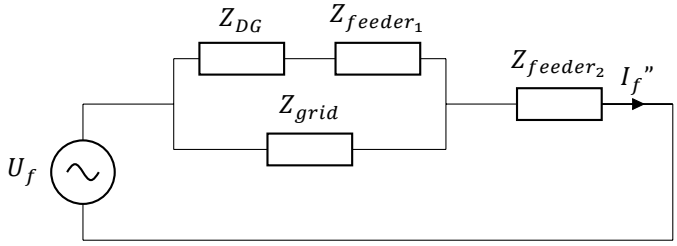

Figure 3.19: Equivalent Thevenin scheme for a three phase sub-transient short circuit calculation

3.3. Protection Problems with the implementation of DG

The protection scheme in the future will be subjected to bidirectional energy flows, which is different compared to present unidirectional energy flow. The main reason behind this change is the penetration of several DG units types inside the distribution systems where each of these units will also contribute current (next to the external grid) to a short-circuit location. The DG unit will not contribute current during a unsymmetrical phase-to-ground fault due to de decoupling between the DG unit and the distribution system during this type of fault which is caused by the configuration of the transformer (star-delta) connected between the DG unit and the distribution system.

The protection schemes mostly found in the distribution systems of the Netherlands are rather straightforward, where a reliable scheme is provided by the right current and time grading between multiple overcurrent relays. This section will explain the problems the overcurrent protection schemes will encounter when they are subjected to a larger penetration of DG units. Furthermore additional computed examples of symmetrical three-phase fault will be given for obtaining a higher understanding of the current contribution of DG units during a sub-transient short-circuit. The transient and steady-state short-circuit contribution are neglected in this study due to the different behavior of each DG unit during a fault event. Especially when power electronics are applied which are able to regulate the current contribution of the DG unit, even during a short-circuit.

3.3.1. Short-circuit contribution of DG

As mentioned in the earlier sections, a typical distribution system is connected to a external grid via a power transformers, where the energy is flowing from the external grid at the top, towards the end-users at the bottom of the system. The external grid is currently the main source that contributes current during a short-circuit event inside the distribution system. This changes when multiple DG units are connected inside the distribution system, see figure 3.21. In this scheme the DG units are connected to feeder 1, where a fault is initiated in feeder 2. The equivalent lumped element circuit for this diagram during a symmetrical fault is depicted in figure 3.18.

By converting the circuit given in figure 3.18 to the equivalent Thévenin circuit (see figure 3.19), a rather simple circuit is realized for computation. The corresponding equations for this Thévenin circuit to calculate the total short-circuit current at a specific fault location inside feeder 2 are given by equation 3.15 and 3.16 [15].

$$Z_{th} = Z_{feeder2} + \frac{Z_{grid} \cdot \left(Z_{DG} + Z_{feeder1}\right)}{Z_{grid} + Z_{DG} + Z_{feeder1}} \tag{3.15}$$

$$I_f{}'' = \frac{U_f}{Z_{th}} = \frac{U_L}{\sqrt{3}} \cdot \frac{Z_{grid} + Z_{DG} + Z_{feeder1}}{\left(Z_{feeder2} \cdot \left(Z_{grid} + Z_{DG} + Z_{feeder1}\right)\right) + \left(Z_{grid} \cdot \left(Z_{DG} + Z_{feeder1}\right)\right)} \tag{3.16}$$

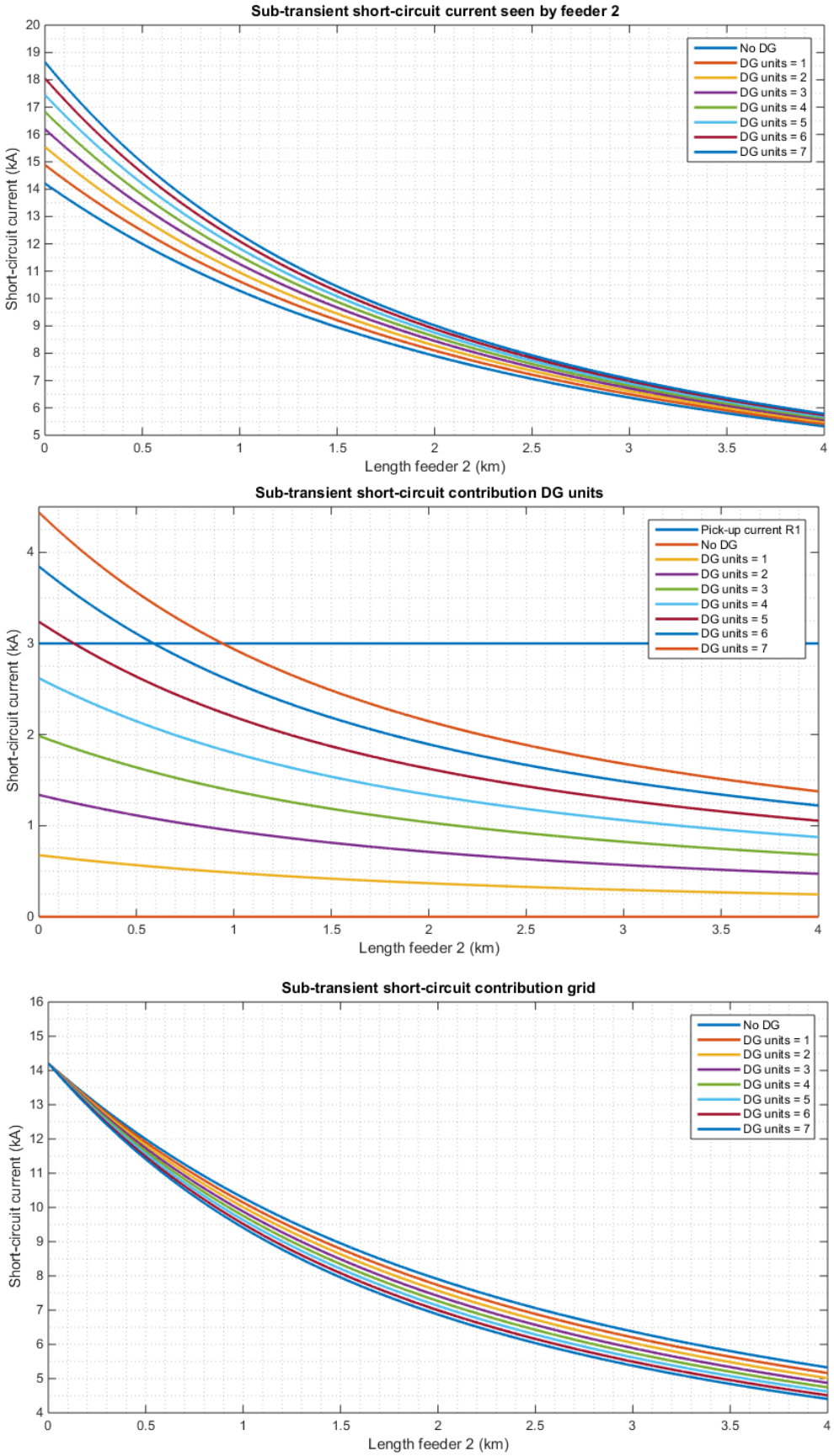

Figure 3.20: Short-circuit calculation of a distribution network subjected to DG units. From top to bottom: short-circuit calculation over the full length of feeder 2, short-circuit contribution of DG, short-circuit contribution of the grid.

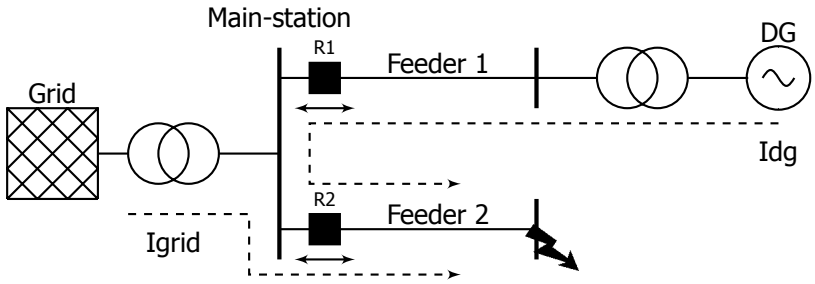

Figure 3.21: False tripping

An example is given in figure 3.20 to show the effect DG-units will have on the short-circuit contribution of the external grid during a symmetrical three-phase fault. For this example typical variables of a 13kV distribution system found in the Netherlands are applied for providing a realistic example. The following variables are applied for this example:

- S_{grid} = 320 MVA (max. short circuit)
- U_{grid} = 13kV
- R/X = 0.35
- S_{DG} = 2.7 MVA
- $X_{DG}"$ = 0.168 p.u.
- R_{stator} = 0.0504 p.u.
- $\cos\varphi$ = 1.0
- $Feeder1$ = 2 km, 3x3*1*150 AL XLPE (R = 0.205 Ω/km, X = 0.125 Ω/km, Inom = 3x290)
- $Feeder2$ = 4 km, 1x3*1*150 AL XLPE (R = 0.205 Ω/km, X = 0.125 Ω/km, Inom = 1x290)

It is clear from figure 3.20 that the amplitude of the short-circuit current will rise at both the beginning and end of feeder 2 when more DG units are connected in parallel to feeder 1. This is due to the fact that each DG unit will contribute current to each fault location inside feeder 2. The short-circuit current in feeder 1 rises with each extra DG unit, which may ultimately result is false tripping because the current could surpass the pick-up current of the overcurrent relay. In the lower image of figure 3.20 the contribution of the external grid is depicted. This figure shows that the contribution of the external grid decays with each additional DG unit. This is especially true when the fault is further away from the sub-station which may contribute to protection blinding. Both false tripping and protection blinding will be explained in the following sections

3.3.2. False Tripping

The principle behind false tripping can be seen in figure 3.21. The short-circuit fault location in feeder 2 creates a short-circuit current contribution supplied by both the external grid and the DG units. Figure 3.21 shows that the DG units will generate a short-circuit current, which is flowing from the healthy feeder 1 toward feeder 2. This energy flow will be detected by the overcurrent relay (with no directional component) which is protecting feeder 1. This fault can result in an unnecessary disconnection of the healthy feeder 1 when the short-circuit current magnitude contributed by the DG units exceeds the pick-up current of this overcurrent relay, see figure 3.20. This protective problem could arise when the fault inside feeder 2 is near the sub-station or when the DG units are connected closely to the sub-station and belongs to the selectivity issues regarding the overcurrent protection scheme.

False tripping could be resolved by increasing the pick-up current of the overcurrent relays which is protecting feeder 1. It is not desirable to increase this pick-up current for faults far away inside feeder 1. During these faults the current magnitude will be lower and the pick-up current could be set to high. Another solution could be the use of overcurrent relays with an additional directional component. This relay could discriminate the fault current direction (forward or reverse) coming from the external grid or the DG units. This ultimately increase the selectivity of the protection scheme. The only disadvantage

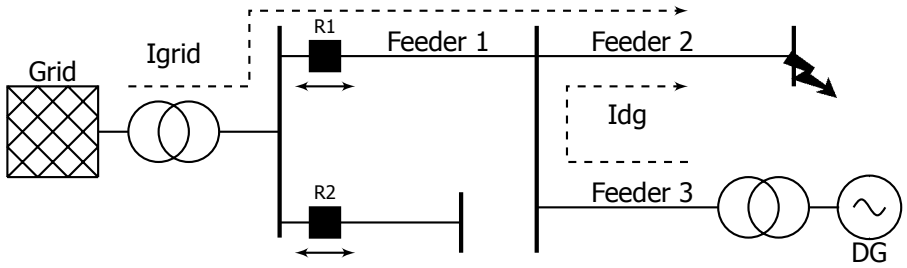

Figure 3.22: Blinding of protection

of these directional relays is the investment cost in an extra voltage transformer next to the existing current transformer to operate the relay appropriately.

It has to be noted that this problem will only occur when the overcurrent relay protecting feeder 1 is set with an instantaneously tipping time (t=0.0s), where the DG units can supply a high current magnitude for a longer period of time during a short-circuit event. This will be especially true for DG units applying synchronous machines (CHP units) but could be different for DG units applying an asynchronous machine (DFIG wind turbine). This last type of DG unit is mostly able to regulate the current contribution of the DG unit, even during a short-circuit, due to the applied power electronics with its corresponding controller.

3.3.3. Protection blinding

Figure 3.22 represents the concept behind protection blinding for a overcurrent protection scheme. In this example the DG units are connected (feeder 3) to the same sub-station as the feeder where the fault is initiated (feeder 2). The external grid is connected several kilometres far away from this sub-station by feeder 1. All the feeders are protected by one overcurrent relay which is connected inside feeder 1. Again as in the false tripping situation both the external grid and the connected DG units will contribute current to the short-circuit location. The short-circuit contribution of both these sources will make the amplitude of the current at the fault location larger than in the situation when the DG units are not connected. Nevertheless the fault current measured by the overcurrent relay will be smaller in the case when the DG units due are connected. In figure 3.22 an example is given where the protection relay is blinded due the short-circuit contribution of the DG units. The following variables are applied during this example:

- S_{grid} = 230 MVA (min. short-circuit power)
- U_{grid} = 13kV
- R/X = 0.4737
- S_{DG} = 2.7 MVA
- $X_{DG}"$ = 0.168 p.u.
- R_{stator} = 0.0504 p.u.
- $\cos\varphi$ = 1.0
- $Feeder1$ = 12 km, 3x3*1*150 AL XLPE (R = 0.205 Ω/km, X = 0.125 Ω/km, Inom = 3x290)
- $Feeder2$ = 12 km, 1x3*1*150 AL XLPE (R = 0.205 Ω/km, X = 0.125 Ω/km, Inom = 1x290)
- $Feeder3$ = 0.05 km, 3x3*1*150 AL XLPE (R = 0.205 Ω/km, X = 0.125 Ω/km, Inom = 3x290)

The applied overcurrent relay has a pick-up current of 1.5 times the nominal current of feeder 1 (1.5*3*290A). This is the smallest fault current (I>) that can be detected by the overcurrent relay and functions as a back-up protection for the instantaneously overcurrent protection (I>>). In this example feeder 1 and 2 have a corresponding length of 12km each. The smallest short-circuit power the external grid can supply is chosen for this example. This magnitude has the most effect toward protection blinding.

When multiple DG units are connected to the sub-station the short-circuit contribution of the external grid will decay during a short-circuit event inside feeder 2. Because the overcurrent relay relies on

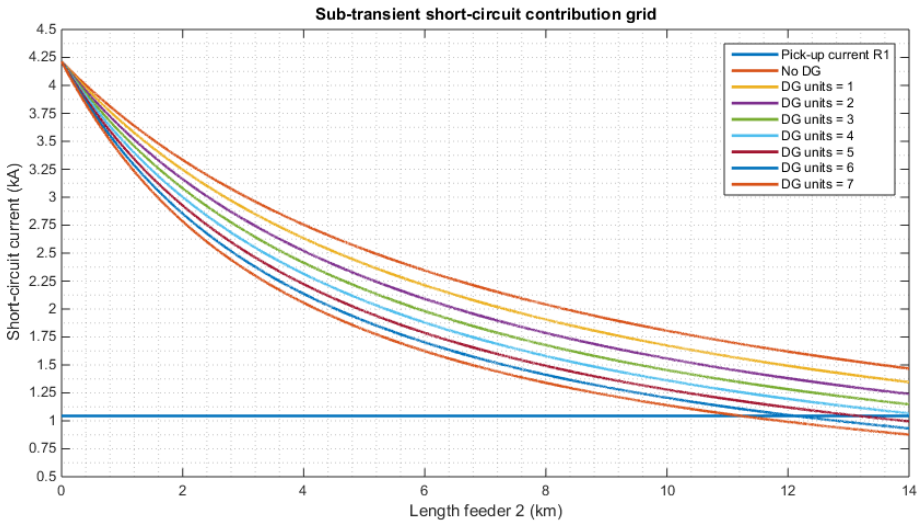

Figure 3.23: Example protection blinding

the current contribution of the external grid to operate correctly it is very important that this current magnitude will not be lower than the set pick-up overcurrent protection (I>). Nevertheless during the given example the situation will occur that the overcurrent relay will be blinded when the fault is situated at approximately >8.3km of feeder 2. Due to protection blinding the fault will not be detected anymore by the overcurrent relay and no protective coordination is undertaken by the protection scheme. This will create a very dangerous situation for maintenance personnel working on the distribution system. The location where protection blinding occurs changes when more (or less) DG units are applied, see figure 3.23.

Blinding of protection occurs at very long feeders or when the concentration of DG units with enough generated capacity at one specific location inside the feeder is very high. This situation can be resolved by decreasing the pick-up current of the overcurrent relay protecting feeder 1. It has to be noted that this contradicts with the increasing of the pick-up current for resolving the false tripping problem. Another solution could be the implementation of another protective relay deeper inside the feeder, after the DG units, with a smaller pick-up current to guarantee selectivity and reliability of the protection scheme. Again (as in the false tripping situation) the current contribution of the DG-units during a short-circuit is a key factor if protection blinding will occur or not. DG units that apply synchronous generators (CHP units) will have a higher short-circuit current contribution over several cycles compared to DG units which apply asynchronous generators (DFIG wind turbine).

3.3.4. Instantaneous current protection

The overcurrent relays are protecting the components against large overcurrent magnitudes which could be created by overloading or a short-circuit. When there are multiple relays present downstream the feeder a selective protection scheme is provided with the help of current- and time-grading as mentioned in the earlier sections. It is also possible to create a protection scheme which only applies current grading between the overcurrent relays whereby time grading is neglected. In this type of protection scheme all the overcurrent relays are set with an instantaneous pick-up current (I>>) which is equal to the calculated short-circuit magnitude at a length of 80% (rule of thumb for taking into consideration the measurement error of the instrument transformer and relay) of the feeder that is being protected, see figure 3.24. This current grading will only be applied inside a protection schemes where the difference in short-circuit current magnitude between two busses at each end of the feeder or transformer is large enough to discriminate (usually 1kA). The operating time for each overcurrent relay can be set to operate instantaneously (t=0.0s) without losing selectivity inside the scheme. An advantage of this type of protection scheme is the speed where protective coordination will take place compared to a protection scheme which is applying time grading. A disadvantage of this type of protection scheme is that it heavily relies on pre-calculated short-circuit magnitudes which could very when some of the feeders inside the distribution system are taking out of operations, when the short-circuit power of the external grid varies or, as will be showed in this section, DG units are taking in or out of operations inside the feeder due to their intermitted behavior.

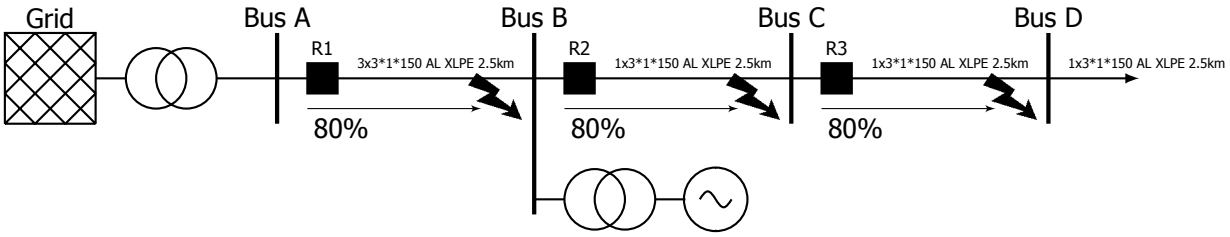

Figure 3.24: Instantaneous current grading protection

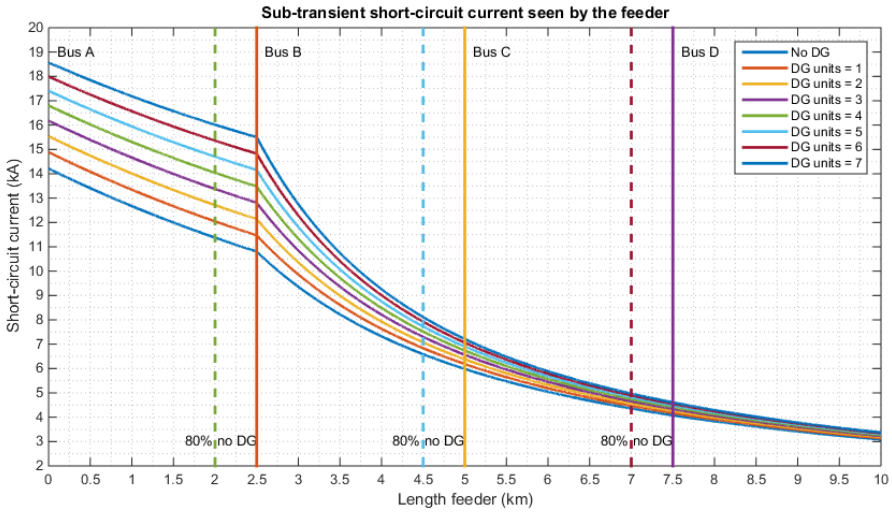

Figure 3.25: Short-circuit current magnitude seen by the feeder

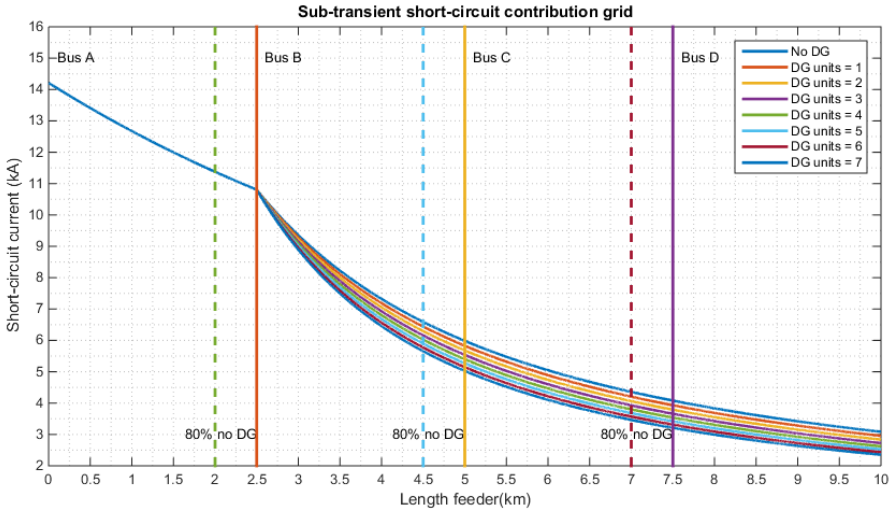

Figure 3.26: Short-circuit current contribution of the external grid

In the example of figure 3.24 a three phase short-circuit is initiated at each location inside the feeder (between bus A and end-user) where the current magnitude is calculated and depicted in figure 3.25 during the case when the DG units are disconnected, partially operating or operating at full capacity at the location of bus B. This figure shows that the current magnitude during a fault will rise due to the fault current contribution of the connected DG units. This is especially noticeable for faults near bus B. This rise in fault current means that the initially set pick-up current for the overcurrent relay 2 and 3 during no DG will overreach the desired protection zone (>80% length feeder). This occurs because relay 2 and 3 are loaded with the current delivered by both the external grid and DG units during a fault. This situation could result in the loss of selectivity inside the protection scheme when these relays are not adjusted accordingly. The current seen by relay 1 (subjected by only the current

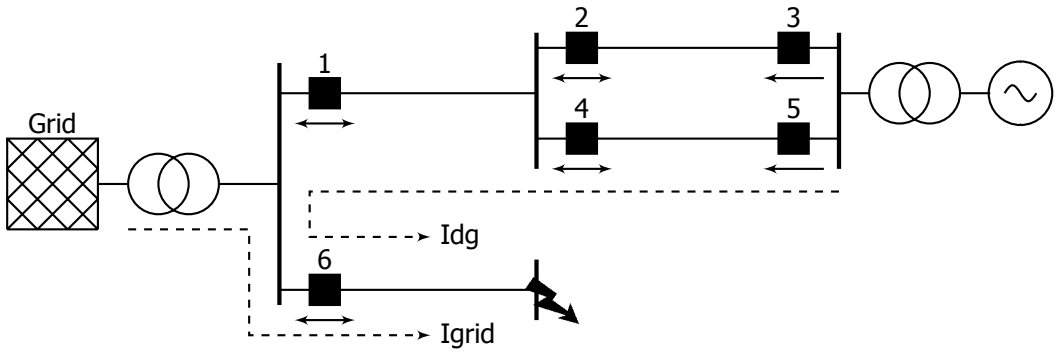

Figure 3.27: Directional current protection

contributed of the external grid) is shown in figure 3.26 which shows that regardless the connection of DG units the current magnitude of the external grid will stay the same for each fault location between bus A and B. This means that relay 1 will operate correctly even in the case when multiple DG units are connected to bus B.

3.3.5. Directional protection

The directional relay provides protective coordination for parallel operated feeders. These relays are usually set with a pick-up current (I>) of 1.2 times the rated current of the component that the directional relay is protecting Usually these relays are also set with an instantaneous pick-up current (I») which is equal to the short-circuit current at 80% of the full length of the feeder, with an instantaneously operating time (t=0.0s).

The implementation of DG may create selectivity problems regarding the use of directional relays inside the protection scheme. In the example of figure 3.27 a fault is initiated in the feeder below. Due to this fault the DG units will contribute current which could be detected by the directional relays 3 and 5 when the available power of the DG unit is high enough to surpass the pick-up current of these directional relays. This will ultimately result in false tripping of the directional relay which could also be the case when a fault is initiated in one of the parallel feeders.

3.3.6. Islanding

Islanding may occur when the main feeder of an area is disconnected (loss of main) from the distribution system and the area is still able to supply power to the loads due to the installed DG units (applying synchronous generator technology). Islanding inside a distribution system is undesirable because of the following reasons:

- power quality issues regarding voltage and frequency which could lead to an abnormal voltage or frequency,
- safety problems for maintenance personnel due to the de-energized circuits,
- reconnection to the distribution system is problematic.

A loss-of-main (LOM) protection is applied for acquiring an adequate safety and reliability level and is therefore necessary in the protection scheme. LOM protection is required in many of the relating rules and guidelines which vary from country to country [19]. The requirements often given are:

- DG units should be disconnected from the network in the case of abnormality in voltage or frequency,
- if one or more phases are disconnected from the grid, supply of the DG should be rapidly disconnected from the network,
- if auto-reclosing is applied, the DG units must disconnect clearly before the reclosing, so that there will be enough time for the fault arc to extinguish.

4

Protection Schemes for Meshed Operated Distribution Systems

A reliable protection scheme is essential for both the consumers and producers of electrical energy in any distribution system. This will be especially true in the coming years where the flow of electrical energy will change over the course of a day with the application of distributed generation and changing loads, like charging of electric cars and the demand response strategy towards end-users. The distribution system will evolve towards a so-called Smart Grid which applies a communication infrastructure next to the existing electrical infrastructure to increase the reliability of the system. This communication infrastructure allows the use of substation automation systems (SAS) and data exchange between the IEDs (intelligent electronic device) systems inside the protection scheme which could be used in advantage of the DSO.

The DG units that are currently being installed inside the distribution system are preferably connected directly to the main-station via relatively long feeders. The protection scheme for these feeders are simple and straightforward with the help of overcurrent relays, with additional differential or directional relays. The question that arises is, if it is always necessary and feasible to install more feeders for connecting DG units or loads directly to the main-station, without taking into consideration the surrounding infrastructure already available in the area with possibly nearby sub-stations. Another reason is the dense population of the Netherlands where installing one feeder of multiple kilometres has big consequences on both the surrounding inhabitants and environment. It is moreover very efficient to connect the loads closely to the generation units. The first reason is that the transport losses are reduced when the feeders between the loads and generation units are short of length. The second reason is that this situation will take away the existing loads of the feeders between the main-station and the sub-stations. This extra transport capacity can be utilized for installing additional DG units or supplying directly more power to the end-users without installing extra feeders. Hence investment costs toward the distribution network to guarantee continuity of the distribution system can be ruled out for a longer period of time.

This chapter will first give a global impression about how the current distribution system is protected and why this system is operated in a radial topology. The numerical relay REF630 from ABB will be briefly explained and why this numerical relay will provide the correct protective functions in the proposed protection schemes described in this chapter. With this relay type in mind an explanation will be given how the current protection scheme can be improved for changing the distribution system from a radial topology towards a meshed topology, by taking into consideration SAS and the application of a communication infrastructure between the IEDs. Multiple versions for improving the current protection scheme will be given in this chapter with the corresponding advantages and disadvantages. A meshed operated distribution system is also bound by operating constraints regarding the maximum short-circuit power. These constraints will be investigated in the last part of this chapter.

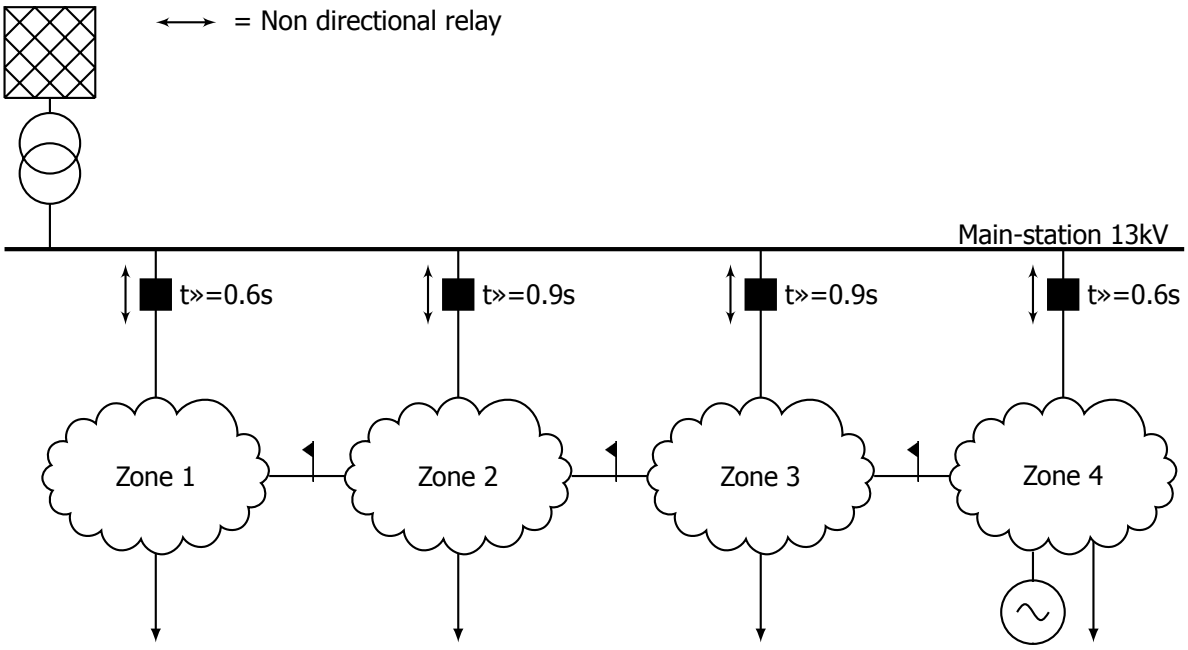

Figure 4.1: Typical protection scheme with overcurrent protection relays

4.1. Current protection scheme

The majority of the current protection schemes inside the distribution systems found in the Netherlands are designed for a radial topology. This topology is created by making use of physical net openings inside specific parts of the feeder, see figure 4.1. A result of these net openings is a radial operated distribution system which creates several zones inside the network. The main reason for applying this radial topology is the realization of a simple and straightforward protection scheme with mainly non-directional overcurrent relays with in some cases additional differential or directional relays for providing extra security and reliability. This protection scheme can be created due to the vertical energy flow inside each zone. Another reason is in the situation that one of the zones is disconnected from the main-station due to a fault, energy towards the end-users can be rerouted by closing the appropriate net openings.

The advantage of operating the distribution system radially is that the protection scheme can be designed with primarily decentralized overcurrent relays, without the use of an additional communication infrastructure between the protective relays. The selectivity for this protection scheme is usually created by introducing current- and time-grading between the overcurrent relays. Another advantage of radially operated distribution system is that the components during a short-circuit are subjected to a smaller fault-current magnitude compared to a meshed operated distribution system. This is due to the fact that the total impedance seen by the fault, in a radial operated system, is higher than in a meshed operated system.

A disadvantages of radially operated distribution systems is that transport capacity is being lost by not fully utilizing the total infrastructure. For example in figure 4.1, where power for the loads in zone 1 can only be transported by the feeder between the main-station and zone 1. An additional feeder has to be installed when the demanded power in zone 1 is surpassing the transport capacity of this single feeder. One of the possibilities for this problem is closing the net opening between zone 1 and zone 2, to increase the total transport capacity of the infrastructure. In the current situation it is not desired to close these openings for the reason that selectivity will be lost in the protection scheme. Selectivity is considered as the most import characteristic of a protection scheme during normal operations. Another disadvantage of this protection scheme is the application of time grading between the relays. Each time grading step will extend the duration of the voltage dips when the fault is initiated near the main-station. This can cause problems toward power-quality which is considered to be a very important characteristic in the coming years.

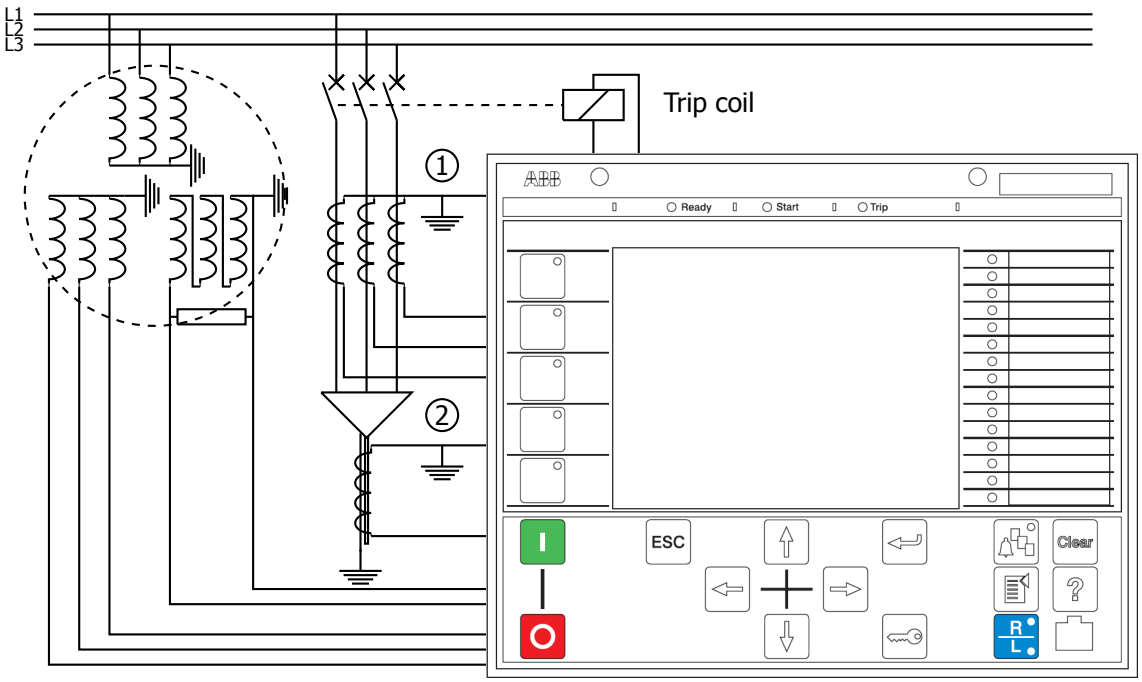

Figure 4.2: Numerical directional overcurrent protection with sensitive earth fault detection, ABB REF630

4.2. Numerical relay ABB REF630

The proposed protection schemes in the following sections are based on the REF630 numerical relay from the Relion 630 protection and control series, manufactured by ABB (see figure 4.2). This relay type is currently one of the preferred feeder protection relays by Stedin (DNO operating in the west of the Netherlands) and is mainly implemented during projects which require SAS. An advantage of this relay type is the presence of multiple protection features inside this single relay which provides a lot of flexibility towards the protection engineer during the design of the protection system. The extensive use of this relay is due to the flexibility in the pre-configured application configurations, scalability (integrating more in- and outputs) and the programmable logic for implementing bay-control logic. This relay is suitable to provide protection in either resistance-earthed, compensated, effectively earthed or isolated neutral distribution networks. In resistance-earthed and isolated neutral systems the earth-fault current will be as high as or higher than the load current. Still this relay is able to detect if a earth fault is present inside the distribution system togehter with the implemented algorithm found inside this relay. The resistance-earthed distribution network is the most common type of system found in the distribution systems operated by Stedin which will be also true for the study case found in the following chapter.

Dependent on the applied protective functions activated inside the programmable environment of the relay (PCM600 for ABB) a current and/or voltage instrument transformer needs to be connected to the analog inputs of the relay. The wiring scheme for this type of relay is given in figure 4.2. This relay is capable of measuring an earth-fault by decomposing the three-phase current offered by the current transformers into three separate single phase systems (positive, negative an zero). In the current protection schemes, found in the distribution system of Stedin, an earth fault is located by monitoring the residual-current of the earthed star connection of the current transformers measuring the current through the in/outgoing feeder (see circle number 1 figure 4.2). This residual-current is provided to the appropriate inputs of the relay which will trip the circuit-breaker when this current magnitude is exceeding the pick-up current magnitude by energizing the trip coil. With this type of connection it is possible to monitor a earth fault current magnitude with a sensitivity up to 10% (this number is chosen due to practical experience) of the nominal current of the applied current transformers. When more sensitivity is required, except of measuring the residual-current of the earthed star connection, a separate current transformer can be connected around the earth screen of the cable (see circle number 2 figure 4.2) for detecting an earth fault current magnitude lesser than 10% of the nominal current.

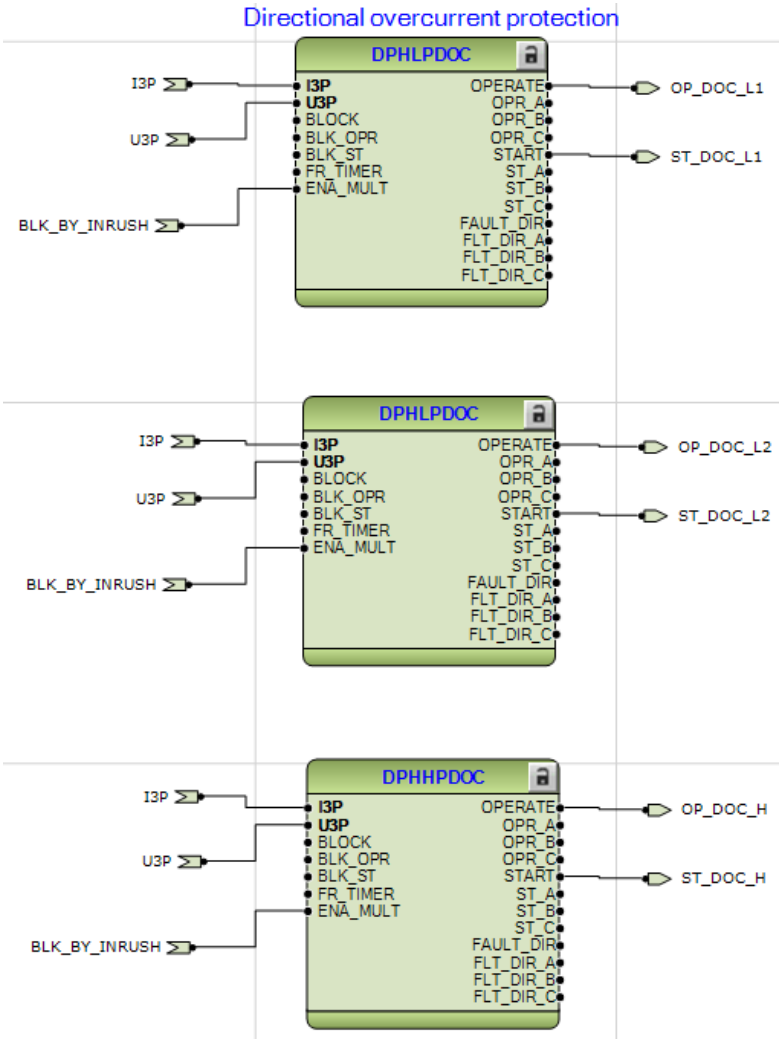

Figure 4.3: Programmable environment REF 630 including protection blocks. Top to bottom: directional overcurrent stage (forward), directional overcurrent stage (reverse) and directional instantaneous overcurrent stage (forward or reverse).

DPHHPDOC: 1					
Operation		On			
Base value Sel phase		Phase Grp 1			
Measurement mode		DFT			
Num of start phases		1 out of 3			
Min operate current		0,01	pu	0,01	1,00
Min operate voltage		0,01	pu	0,01	1,00
Curve parameter A		28,2000		0,0086	120,0000
Curve parameter B		0,1217		0,0000	0,7120
Curve parameter C		2,00		0,02	2,00
Curve parameter D		29,10		0,46	30,00
Curve parameter E		1,0		0,0	1,0
Reset delay time		0,020	s	0,000	60,000
Minimum operate time		0,040	s	0,040	60,000
Voltage Mem time		40	ms	0	3000
Allow Non Dir		Not allowed			
Setting Group1					
Directional mode		Forward (Non-directional / Forward / Reverse)			
Pol quantity					
Start value			pu	0,10	40,00
Characteristic angle		0	Deg	-179	180
Max forward angle		90	Deg	45	135
Min forward angle		90	Deg	45	135
Max reverse angle		90	Deg	45	135
Min reverse angle		90	Deg	45	135
Start value Mult		1,0		0,8	10,0
Time multiplier		1,00		0,05	15,00
Operating curve type		IEC Def. Time			
Type of reset curve		Immediate			
Operate delay time		0,04	s	0,04	200,00

Figure 4.4: Programmable environment REF 630 parameters inside protection blocks

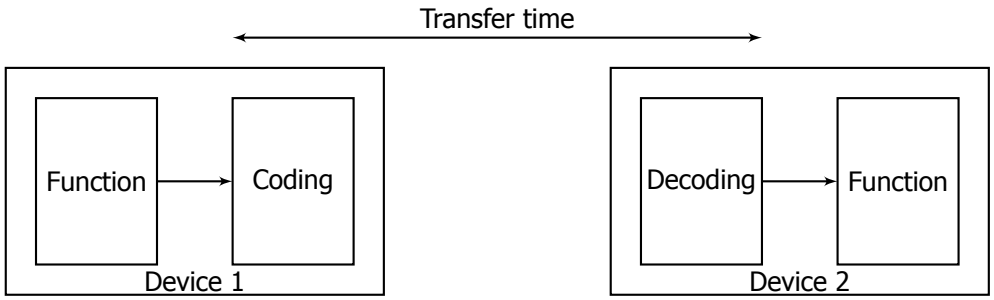

Figure 4.5: Definition of transfer time by IEC61850

Type	Name	Examples	Transfer time
1A	Fast message - trip	Trips	≤10ms
1B	Fast message - others	Commands, simple message	≤20ms
2	Medium speed messages	Measurements	≤100ms
3	Low speed messages	Parameters	≤1000ms
4	Raw data messages	Output data instrument transformers	≤10ms
5	File transfer function	Large files	≤10000ms
6A	Time synch. message a	Time synchronisation station bus	-
6B	Time synch. message b	Time synchronisation process bus	-
7	Command message with access control	Command from station (HMI)	≤10ms

Table 4.1: Message types and required transfer time according to IEC 61850-5 [3]

All the protection functionalities inside this relay can be activated by introducing the correct function blocks, see figure 4.3. For each of these function blocks a parameters list can be filled in for proper protective coordination, see figure 4.4. One of the other reasons for making use of this type of relay is the ability to discriminate the current in both the forward and reverse direction. This functionality will be further utilized during the following sections.

4.3. IEC 61850

The REF 630 relay explained in the earlier section is furthermore equipped with the latest IEC61850 communication protocol which is currently the standardized communication protocol for SAS and SCADA (Supervisory Control And Data Acquisition) systems. This protocol replaces the traditional wiring schemes between feeders, control switches and signaling devices by applying an ethernet based communication network. This data communication network is usually carried out over an single wired fibre-optic ethernet network, designed for quick data exchange. This network can be designed into a ring topology to increase the overall reliability of the network. With this protocol it is even possible to detect if one of the communications paths has failed. This results in high availability and reliability because operations can continue in a ring configuration even if one of the communication path fails, where the faulted communication path will be indicated by the system.

One of the several functions inside the IEC61850 protocol is the application of a fast communication multicast/broadcast function called Generic Object-Oriented Substation Event (GOOSE), which is capable of sending packages for auto-reclosing (between relay and CB), intertripping (between relay and relay) and interlocking (between bay-controller and relay) from one single server (IED) to multiple clients. This GOOSE message has the advantage that it is directly mapped on the ethernet link layer (layer 1 and 2) of the ISO/OSI model. This is needed for realizing a fast transfer time (≤10ms). In table 4.1 a summary is given of the different messages applied inside the IEC61850 protocol with the corresponding defined transfer time for each of these messages.

4.4. Smart Grid protection scheme

As mentioned in the earlier sections the current distribution system is operated with a radial topology. Due to this topology possible transport capacity will be lost which could be considered as a disadvantage. A main advantage of this topology is a protection scheme which applies simple rules for providing the correct protective coordination. When it becomes desirable to close certain connections inside a radial operated system to increase the transport capacity due to growing loads/generation, selectivity may possibly be lost when only conventional protection strategies are incorporated. This because each non-directional overcurrent relay will measure any fault initiated inside a fully radial operated system which could lead to possibly false tripping when the settings are not adjusted accordingly. In this section two proposed versions for electrically protecting meshed operated distribution system will be given which will apply the conventional protection techniques together with a communication infrastructure which will apply the IEC61850 protocol to realize fast tripping. The proposed schemes found in this section are created with respect to the following assumptions:

- The topology of the system can only be altered when protection and safety can be guaranteed.
- The present protection scheme already applied inside each distribution system must be respected as much as possible without making any major alterations.
- The proposed protection schemes must be easily to understand without the use of complex algorithms.
- Each extra interconnection that is being installed to increase the transport capacity can be integrated into the protection scheme without major changes towards the algorithm.
- During normal operations selectivity is the most important characteristic of the protection scheme.
- During abnormal operations (e.g. loss of communication) fast isolation of the fault will be preferred above selectivity.

4.4.1. Version 1

As mentioned earlier in this section conventional protection strategies inside a meshed operated distribution system may lead to false tripping when only non-directional overcurrent relays are applied. This issue is related to selectivity problems which could possibly be resolved by making use of a communication infrastructure, with the latest IEC61850 protocol, next to the existing electrical infrastructure. Besides communication the relays between the zones will be set with the appropriate protection functionality (see numerical relay REF630 ABB).

The protective functionality of the relays between each zones are set with a directional overcurrent component to discriminate in both the forward and reverse direction, see figure 4.6. This protective function needs an additional voltage transformer besides the current transformer to determine the direction of the fault current. In the earlier chapter about directional relays forward was defined as current flowing from load to the external grid and reverse as current flowing from the external grid to the load. This will not be true in a meshed operated system because the current will flow between the interconnected zones, as indicated in figure 4.6. In this case forward and reverse current direction is defined corresponding to the applied relay name as follows:

- R_{ij}, relay placed in zone i, connected to zone j
- Forward: current flowing from zone i to j
- Reverse: current flowing from zone j to i

Relay R12 In figure 4.6 is taken as an example:

- R12, relay placed in zone 1, connected to zone 2
- Forward: current flowing from zone 1 to 2
- Reverse: current flowing from zone 2 to 1

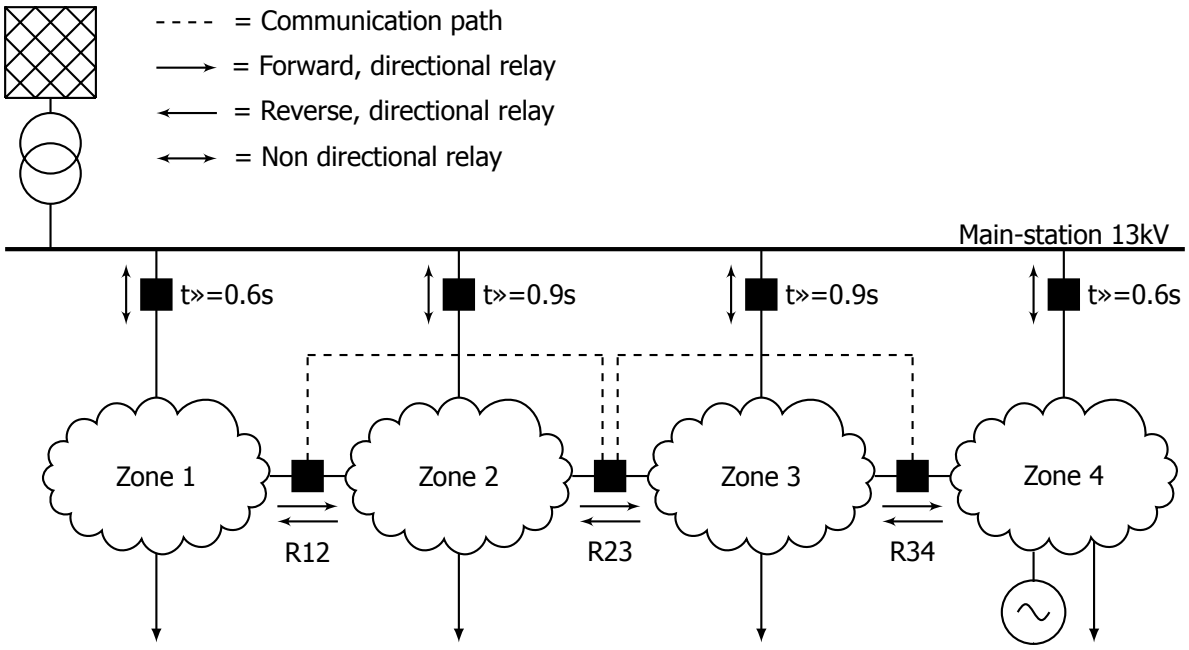

Figure 4.6: Protection scheme version 1: overcurrent relays with and without directional unit

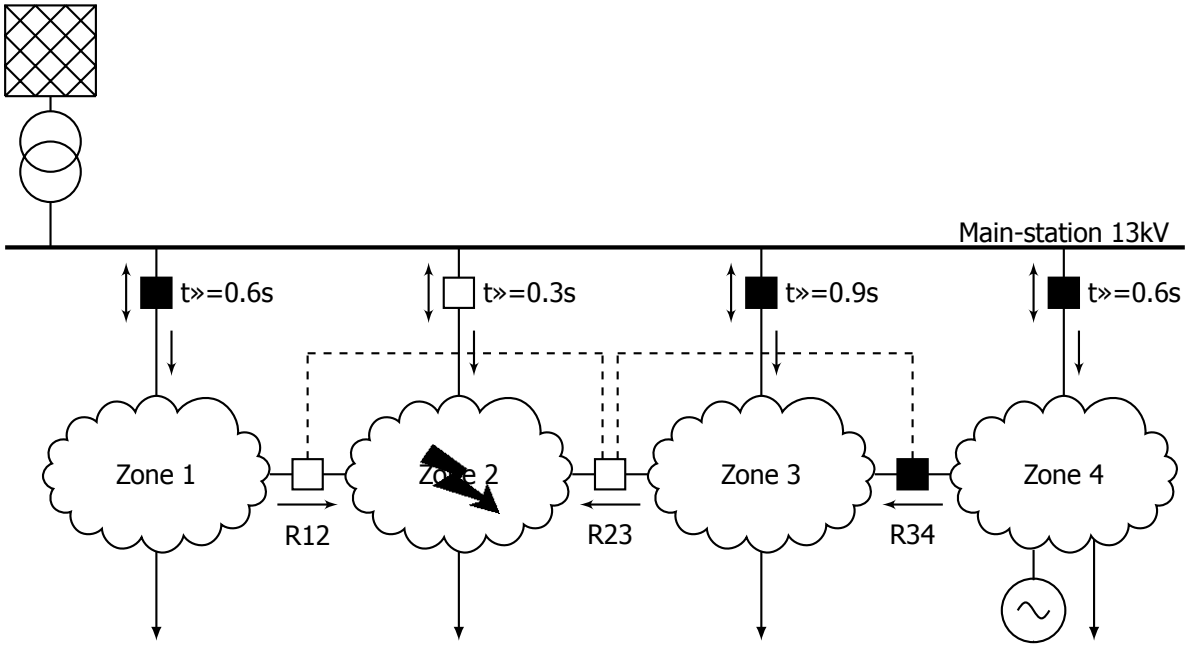

Figure 4.7: Protection scheme version 1 with fault in zone 2

One of the most important characteristics of a protection scheme besides selectivity is the simplicity to understand the protective coordination. Protective coordination in the radially operated distribution system is realized due to the unidirectional energy flow which will mostly occur during a fault and the current- and time-grading strategy applied between the protective relays. In a meshed operated distribution system this will be completely different because the current will flow from multiple directions towards the fault which makes it complex to provide the correct protective coordination. With both the directional overcurrent relays and communication infrastructure a simple algorithm can be obtained with the desirable characteristics towards protective coordination.

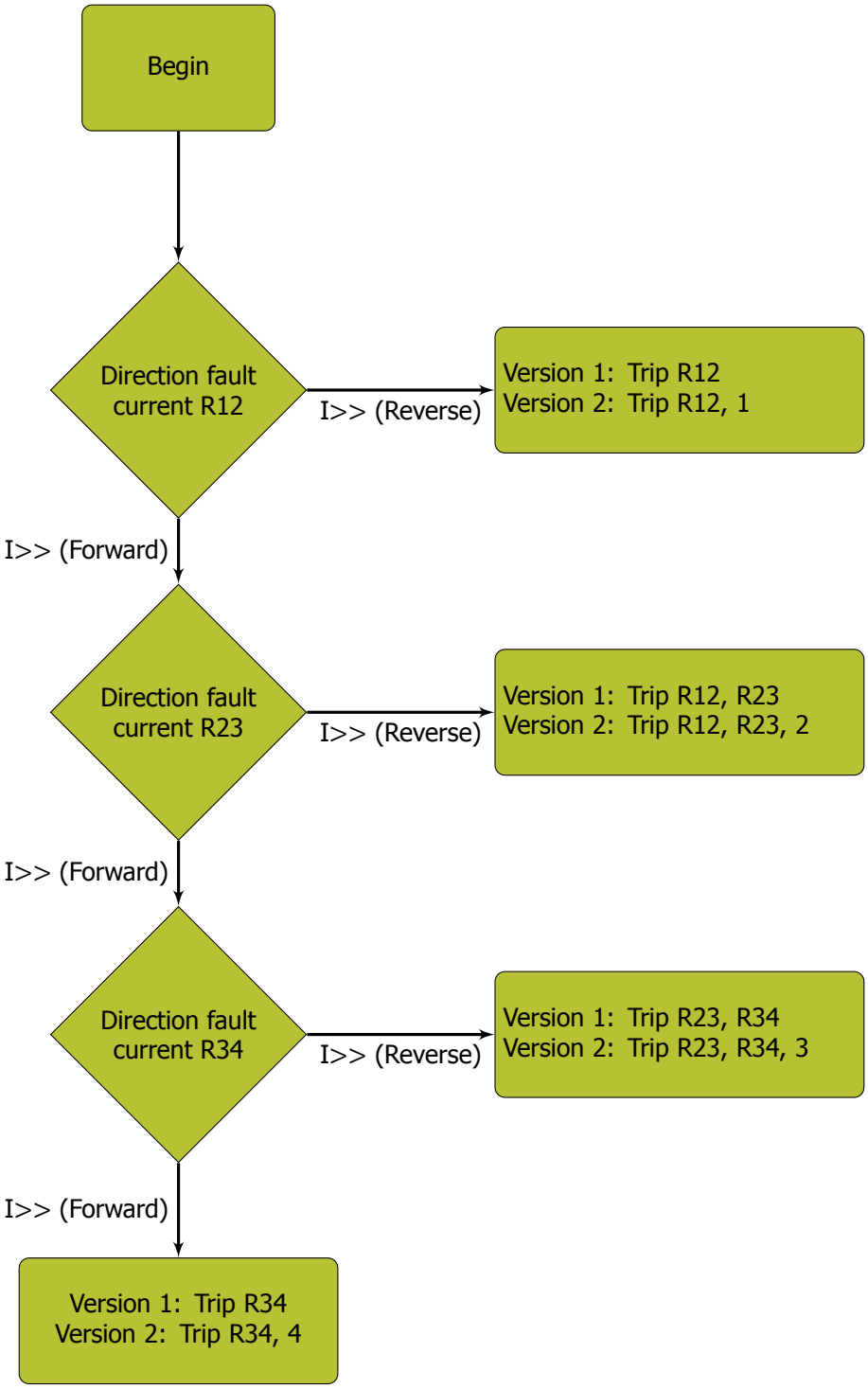

Figure 4.8: Flow chart protection scheme version 1 and 2

When a fault is initiated in one of the interconnected zones the current magnitude and direction will be monitored by each directional overcurrent relay. In the case of figure 4.7 this will be true for relay R12, R23 and R34. When the fault current magnitude surpasses the set pick-up current in the forward or reverse direction a signal will be send to a (de)centralized bay-controller. This bay-controller will compare all the received signals from the directional relays R12, R23 and R34 to locate in which zone the fault is initiated. By applying the flowchart in figure 4.8 a decision will be made inside the controller in which zone the fault is initiated and what the desired protective coordination will be to alter the topology of the faulted zone from meshed to radially.

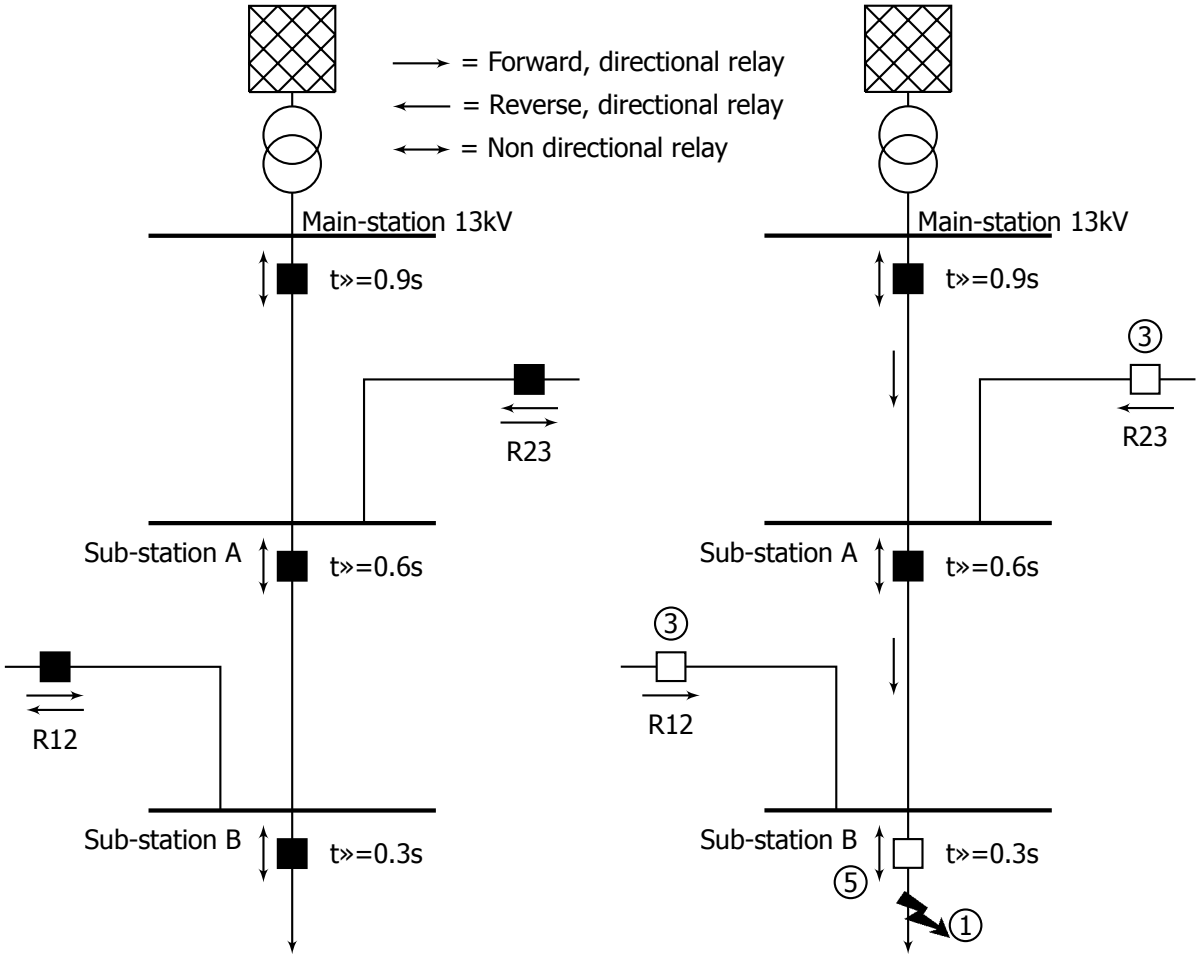

(a) Normal operations (b) Protective coordination

Figure 4.9: Example protective coordination scheme version 1 applied to zone 2

The algorithm used for this protection scheme is depicted in figure 4.8 which indicates that the decisions in this flow chart are determined by the fault current direction (forward or reverse) measured by each directional overcurrent relay. These relays are illustrated in figure 4.6 by R12, R23 and R34. In figure 4.9a an example is shown of zone 2 which is connected to the neighbouring zones 1 and 2. These interconnections are protected with the help of the proposed protection scheme by relay R12 and R23. As can be seen in this figure the protection scheme with overcurrent relays and the time-grading philosophy is not altered. In this example a fault is initiated in the feeder connected to sub-station B (figure 4.9b). The following steps, which are also indicated in figure 4.9b, will be realized to isolate the faulted feeder correctly:

1. Short-circuit is initiated in feeder connected to sub-station B ($t \leq 0.0s$)
2. The algorithm will locate the faulted zone 2.
3. The circuit-breakers connecting to the faulted zone (circuit-breakers R12 and R23) will be tripped instantaneously ($0.1s \geq t \geq 0.0s$)
4. Now the topology of the faulted zone has changed from meshed to radially.
5. The existing protection scheme can isolate the faulty component by using time grading ($t \geq 0.3s$).

Because this protection scheme applies time-grading to isolate the faulted feeder the voltage dip duration can last for a long period of time ($t \geq 0.9s$) when a short-circuit is located near the main-station. The duration of this dip needs to be as short as possible when multiple DG units are connected to the neighbouring zones. This because each of these DG units are protected with an undervoltage protection. When the duration of the dip is to long DG units will be disconnected from the healthy neighbouring zones which can be considered as undesirable for the DG owners.

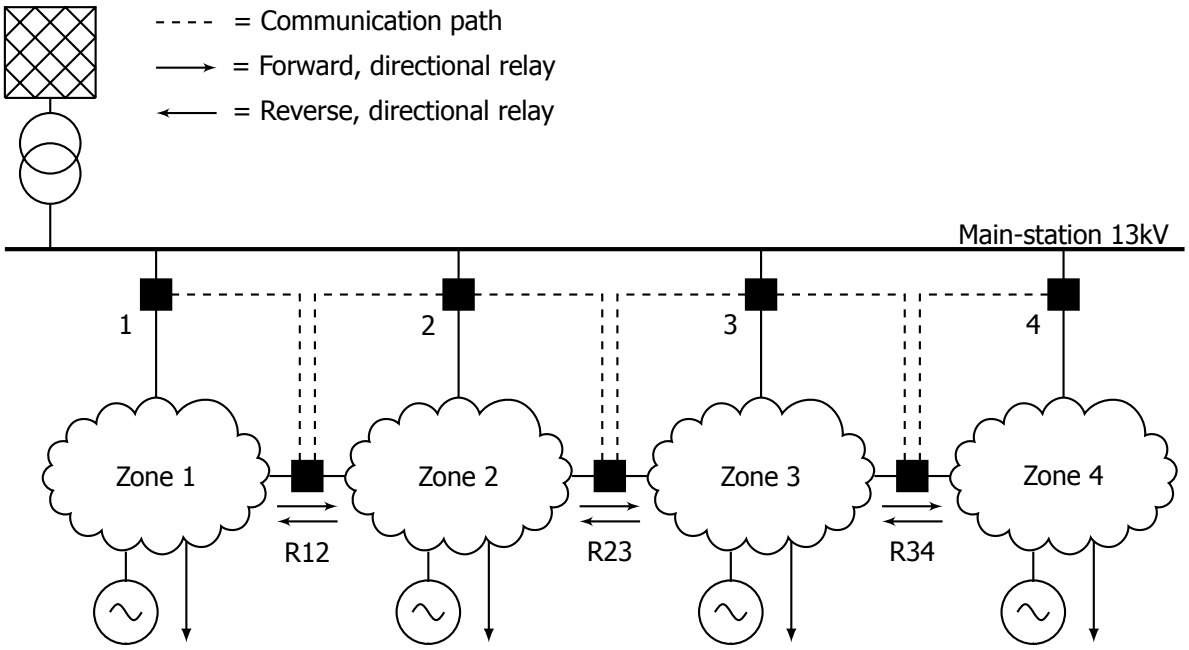

Figure 4.10: Protection scheme version 2, overcurrent relays with directional unit

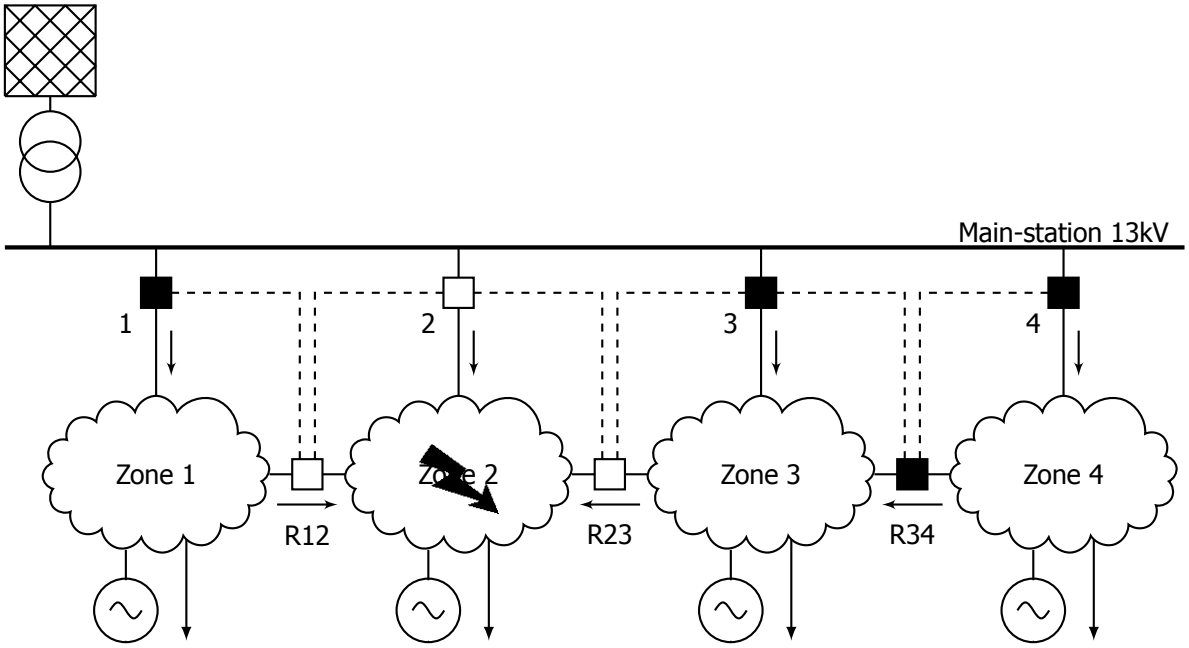

Figure 4.11: Protection scheme version 2 with fault in zone 2

4.4.2. Version 2

The protection scheme proposed in this section is an extension of scheme version 1. In this version an additional communication path is situated between the directional protection relays R12, R23 and R24 and the relays directly connected to the 13kV main-station, see figure 4.10. This protection scheme is designed for areas with multiple DG units in several zones, where quickly isolation of the fault is essential for the continuity of the DG units. The main reason for proposing this protection scheme is the fact that each DG unit inside a distribution system is protected for voltage dips with the help of an undervoltage relay. These voltage dips will occur during a short-circuit inside the distribution system and will have an effect on the DG units. The severity of the voltage dip depends on the type of fault, where the three-phase fault has the largest dip.

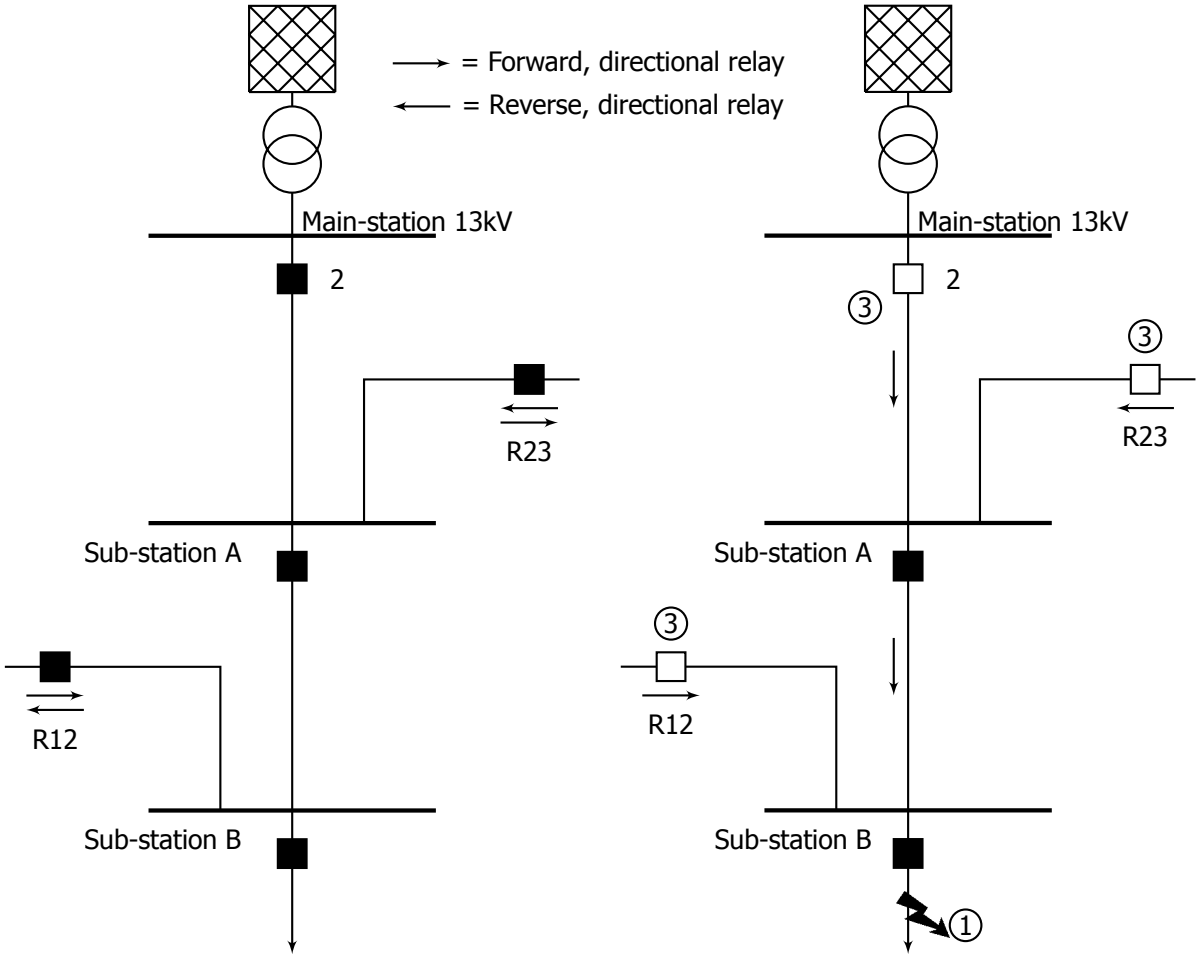

(a) Normal operations (b) Protective coordination

Figure 4.12: Example protective coordination scheme version 2 applied to zone 2

The voltage magnitude inside the distribution system will drop when a short-circuit is initiated inside one of the connected zones. This voltage dip will have an effect on all the interconnected zones, especially for zones which are connected closest to the faulted zone. Multiple DG units inside the distribution system will be disconnected when this voltage dip holds for a longer period of time below the pick-up voltage of the undervoltage relays. For this reason the zone with the faulted component must be isolated as quickly as possible from the entire distribution system to guarantee that the DG units in the healthy zones will stay connected after the occurrence of a short-circuit.

The algorithm for protection scheme version 1 is extended with an additional tripping signals towards the circuit-breaker located in the main feeders coming from the main-station, see figure 4.8. The main reason for this additional tripping signal is to isolate the faulted zone as quickly as possible from the distribution system, see figure 4.11. Again in the case a fault is initiated in zone 2 (see figure 4.12b) the following steps will be taken:

1. Short-circuit is initiated inside a component of zone 2.
2. The algorithm will locate the faulted zone 2.
3. Circuit-breakers R12, R23 and 2 connected to the faulted zone will be tripped instantaneously.
4. Now the faulted zone is isolated from the healthy zones.

The time it takes for this algorithm to isolate the faulted zone can be set as quickly as possible, preferably less than 300ms. According to the netcode of the Netherlands [8] the undervoltage relays, protecting the DG units, are set for an overvoltage magnitude of 1.1 p.u. for 2 seconds (U>) and an undervoltage magnitude of 0.7 p.u. for 300ms (U<<).

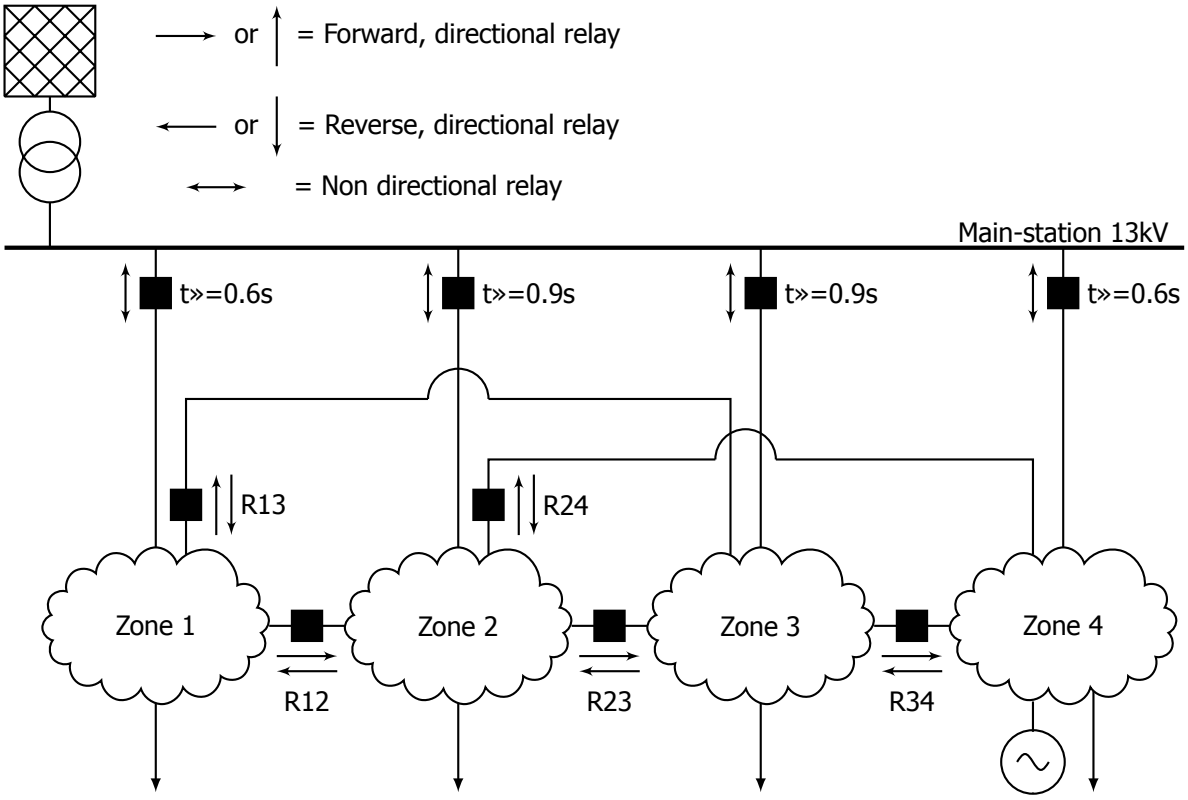

Figure 4.13: Protection scheme with connection between more than 2 zones, overcurrent relays with and without directional unit

A major disadvantage of this protection scheme is the loss of selectivity inside the distribution system with the applied protective coordination of version 2. This because the main feeder is instantaneously disconnected from the zone even when the fault is situated inside the feeders connected to sub-station B. This problem could be resolved by introducing each relay of all the zones inside the logic diagram, but consequently will overcomplicate the overall protection scheme. In the current system this loss of selectivity and complexity is not desirable and that is why this scheme is considered to be very radical and the least likeliest of the two proposed schemes to occur in the future.

4.5. Connecting with multiple zones

In the example of figure 4.6 it is shown that an interconnection can be made between two or three zones. In this figure zone 1 can only be interconnected to zone 2, where zone 2 is interconnected to both zone 1 and 3. In the distribution systems found in the Netherlands it is often possible to interconnect more than 3 zones with each other. For example in the real life example found in the following chapter it is even possible to interconnect a multiple of five zones. To still provide protection with the appropriate protective coordination the flow chart found in figure 4.8 can no longer be applied.

As an example figure 4.13 shows a meshed operated distribution system with more than three interconnected zones. In this particular example a multiple of four zones are interconnected when zone 2 is closer examined. The protection scheme for this example is derived from the protection scheme found in version 1, where the protective coordination inside each zone is still provided by time-grading. The logic diagram according to figure 4.14 will be applied for this example to open the appropriate circuit-breakers during a fault. This diagram is only applicable to relays R12, R13, R24, R23 and R34 and will decide in which zone the fault is initiated. When the diagram has located the faulted zone the correct circuit-breakers will be tripped instantaneously (t>>0.0s) for changing the topology of the zone from meshed to radial. After this switching event the protection scheme inside the zone will finally isolate the faulty component from the system by applying time-grading.

It could be possible that the transport capacity of the infrastructure is enhanced by installing an additional interconnection after the installation of the proposed protection scheme. The fault current direction flowing through this connection must be taken into consideration in the logic diagram as well.

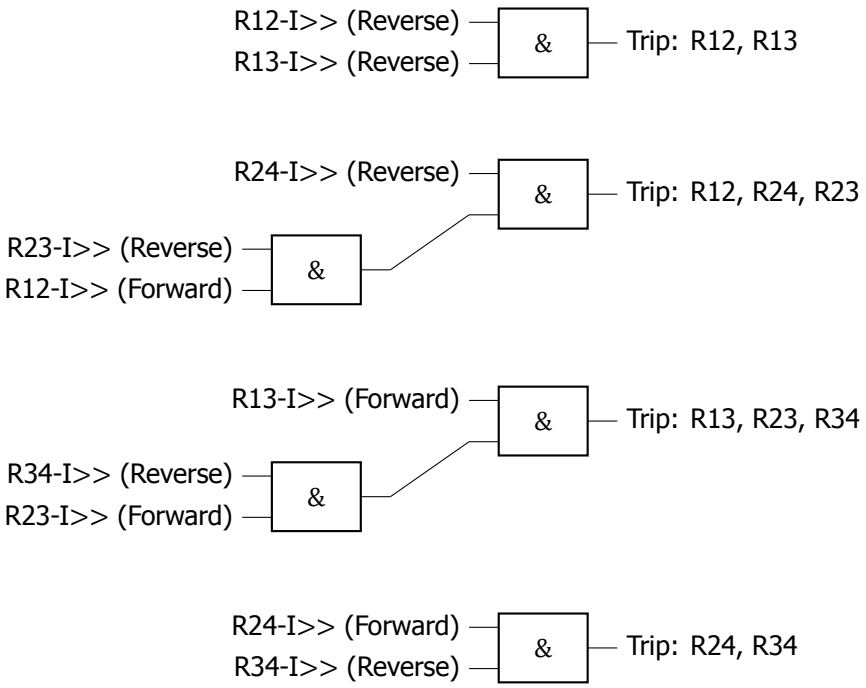

Figure 4.14: Logic diagram for relays R12, R13, R24, R23 and R34

Additionally it could be needed to alter the set values for the pick-up currents for each directional relays to incorporate this extra interconnection properly inside the protection scheme, which could be considered as a drawback of the system.

4.6. Back-up protection

During normal operations any fault inside one of the connected zones needs to be isolated, where selectivity is the most important characteristic. It could be a possibility that a fault will occur during a abnormal situation, e.g. the loss of communication which is needed to decide in which zone the fault is initiated, the circuit-breakers and/or relays is not able to operate appropriately during a fault or the circuit-breaker is undergoing maintenance. In such a case it is the most desirable to isolate the fault as quickly as possible.

4.6.1. Maintenance of feeder/circuit-breaker

When the circuit-breaker is undergoing maintenance between two interconnected zones and needs to be taken out of order, the current will no longer flow through this interconnection when a short-circuit is initiated in the neighbouring zones. This can create problems in the logic diagram regarding protective coordination if no proper measures are taken into consideration. This problem can be resolved by incorporating a so-called maintenance input for each circuit relay output, see figure 4.15. This input will be set to high (”1”) during maintenance and hereby still deliver the satisfactory functionality for the logic diagram. This because each of the fault current directions of the circuit-breaker under maintenance are already set to high. When a fault does appear during this abnormal situation protective coordination inside the logic diagram will only depend on the circuit-breakers still under operations.

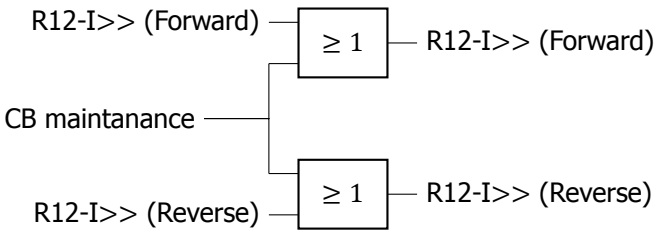

Figure 4.15: Logic diagram adaptation for including maintenance

4.6.2. Loss of communication

A rather direct back-up protective system, in the case of loss of communication is by neglecting the logic diagram considered in the earlier section. Each directional relay will decide independently if a protective tripping action is required during this abnormal situation. The applied directional relays can each be set with a desired pick-up current for both the forward and reverse direction which will improve the overall reliability of the protection scheme during this kind of emergency operation. The applied delay time for the directional relays during this situation can be set to react instantaneously (t>>0.0s) for isolating the fault as quickly as possible.

4.6.3. Malfunction of circuit-breaker

When a fault is initiated in one of the zones, it could be a possibility that one of the circuit-breakers and/or relay malfunctions. Again a possibility of back-up protection could be that the directional relays can each be set with a delayed tripping time (t>>0.3s), where each relay will decide independently if protective coordination is required.

4.7. Research towards Smart Grid protection

Smart Grid technology enables freedom for designing multiple protection concepts which rely on fast communication and data exchange between the IEDs present inside each sub-station. Due to this technology several studies are conducted for designing such a protection scheme inside a Smart Grid infrastructure with each a different approach towards protective coordination. This research attempts to design a protection scheme (philosophy) with existing protection techniques and with the enhancement of a communication infrastructure, where the settings for each relay is set by a static value for providing the right protection during several fault type situations. This allows the concept behind the protective coordination to be still understandable for people designing and maintaining the protection scheme.

A more complex approach towards protective coordination can be found in [20] where wavelet based fault location is applied to locate the faulty component. This is realised together with communication support. In [21] a proposal is given for realizing the appropriate protective coordination by applying an adaptive protection scheme which enables and disables certain protection functions during different situations and changes these settings appropriately. This scheme is proposed when certain parts inside the distribution system are connected or disconnected from the distribution system (operated as an island) during the day due to the large implementation of DG units in that specific area. Again as in the previous research communication is applied for providing the correct settings inside each IED during these different scenarios. In [22] the distribution system like in the case of this research is separated in several zones. In this case it is assumed that each zone can operate stand alone with the help of frequency control applied to the DG unit connected to the zones. This concept also relies on off online load flow and short-circuit calculations of each significant change in load which is incorporated to realise an adaptive protection scheme. These are one of the multiple researches that can be found toward Smart Grid protection in the IEEE library, which indicates that this topic also enjoys much interest in the academic world.

5

Modelling and Simulation Results

The proposed protection schemes version 1 and 2, found in chapter 4, will be modelled and tested inside the simulation environment of Digsilent PowerFactory. In the first case study of this chapter these schemes will be implemented into a simplified distribution system for research purposes. The results obtained during the simulations are provided in this chapter by tables and figures to show what the impact will be of the proposed protection schemes on the loadability of the infrastructure and protective coordination.

In the second case study of this chapter the discussed protection scheme version 1 will be applied to a distribution system with a topology largely found in the Netherlands. The topology of the studied distribution system is related to the distribution system found in Goeree-Overflakkee, an island in the south-west of the Netherlands (see red marked island in figure 5.11). In this distribution system it is possible to interconnect a multiple of zones with each other which will ultimately test the proposed schemes for the correct protective coordination.

The information for realizing this case-study is provided by the Vision files (steady-state power system analyzing software for calculating load flow and short-circuit faults, used by all the network operators in the Netherlands) generated by Stedin (distribution network operator of the distribution system found on Goeree-Overflakkee). In these files information can be found of the applied infrastructure and corresponding protection scheme. This information is implemented in PowerFactory for studying the dynamic behavior of the system during fault situations. This functionality is currently not available in the software package of Vision.

5.1. Case study 1

This case-study is created to show the effect the proposed protection schemes of chapter 4 will have on a simplified distribution system. Not only will the effect on the loadability of the infrastructure be studied but furthermore the protective coordination of the protection schemes, with the help of time simulations.

5.1.1. Distribution system

The distribution system applied during this case study is depicted in figure 5.1. Initially this distribution system is operated radially, due to the physical net openings between the four zones. These net openings allow the use of a simple protection scheme with only nondirectional overcurrent relays. Time-grading is applied between these protective relays to guarantee selectivity inside the scheme.

The configuration of the power-transformer between the external grid and the main-station is of the type Wye-delta (star-delta). The distribution system is operated with an additional grounding transformer (better known as a zig-zag transformer), connected to the main-station, to provide the appropriate path for the fault current during a phase-to-ground fault. This transformer is often found in the distribution systems operated by Stedin. The earth fault current coming from the earth connection to the windings of the zig-zag transformer is evenly divided over the three connected phases of the transformer. One of the main reasons to apply a zig-zag configuration is that not the full voltage is required over the windings (phase-to-ground/$\sqrt{3}$). This makes it more cost effective to apply this

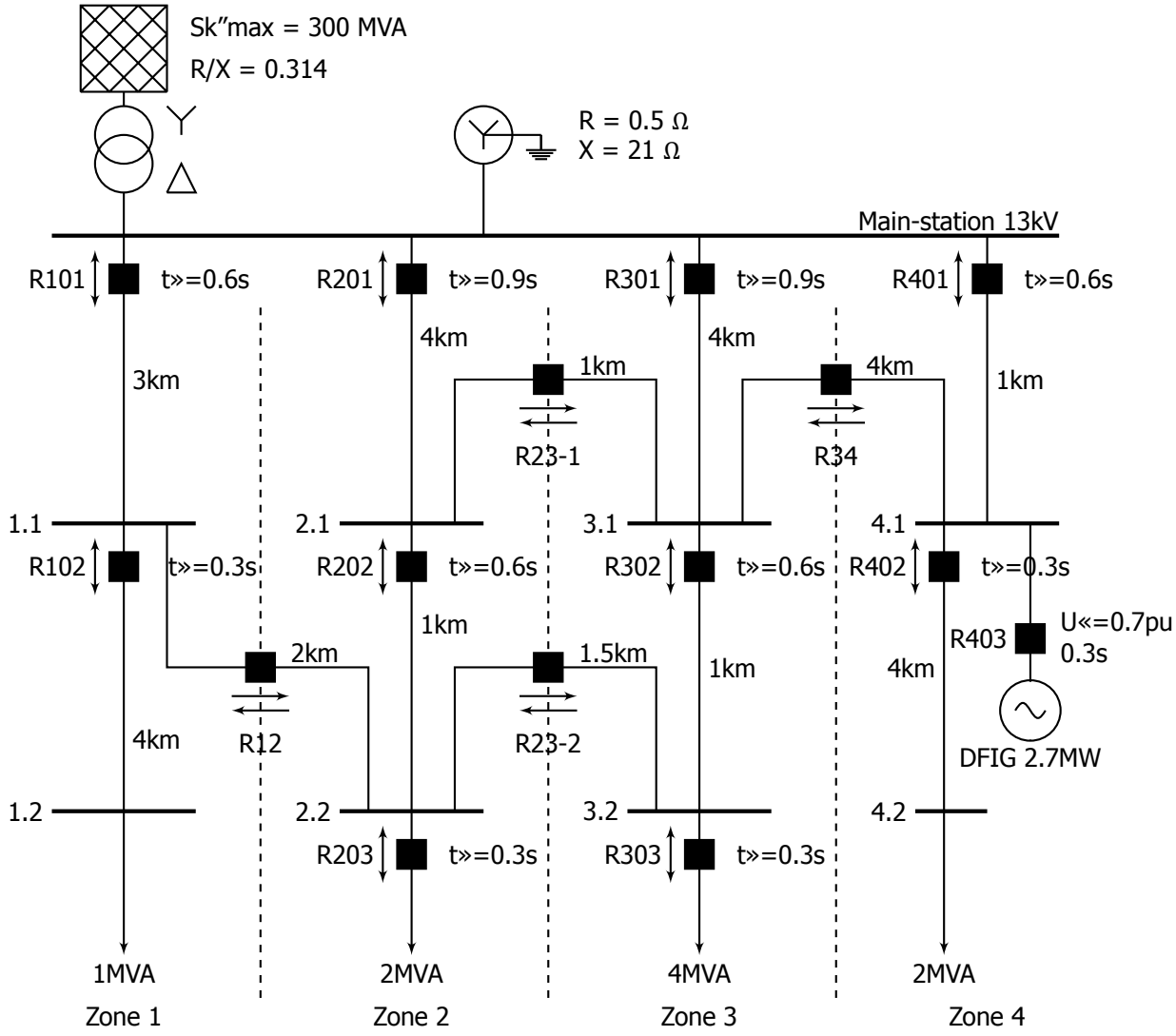

Figure 5.1: Distribution system case study 1

winding configuration compared to a wye winding configuration which is also an applicable winding configuration for a grounding transformer.

The power-transformer applies a high short-circuit voltage (Uk = 9%) to reduce the current contribution of the external grid during a fault inside the distribution system. This is currently a common technique inside the distribution systems operated by Stedin. In this example a DG unit is connected to bus 4.1 to show the effect the proposed protection schemes will have on the behavior of this DG unit. For this example a doubly fed induction generation (DFIG) wind turbine is applied with a total generating capacity of 2.7 MW. The model for this machine is a generic model already available inside PowerFactory. The derivation of this model is explained in appendix A. Lastly the underground cables applied for this case study are provided with the following characteristics:

- 3x95 mm^2 (R = 0.22 Ω/km, X = 0.091 Ω/km), for interconnecting the zones
- 3x120 mm^2 (R = 0.17 Ω/km, X = 0.088 Ω/km), the other connections inside each zone

Because the proposed protection schemes allow the use of a meshed operated distribution system, the net openings between zone 1,2,3 and 4 will be closed. Hence the transport capacity for some main feeders will be increased (between main-stations and sub-station 1.1, 2.1, 3.1 and 4.1). Figure 5.1 doesn't depict the applied communication infrastructure needed for this protection scheme to function properly. This is done in order to keep the figure clear for the reader, but still it have to be noted that this infrastructure is vital for providing the correct protective coordination.

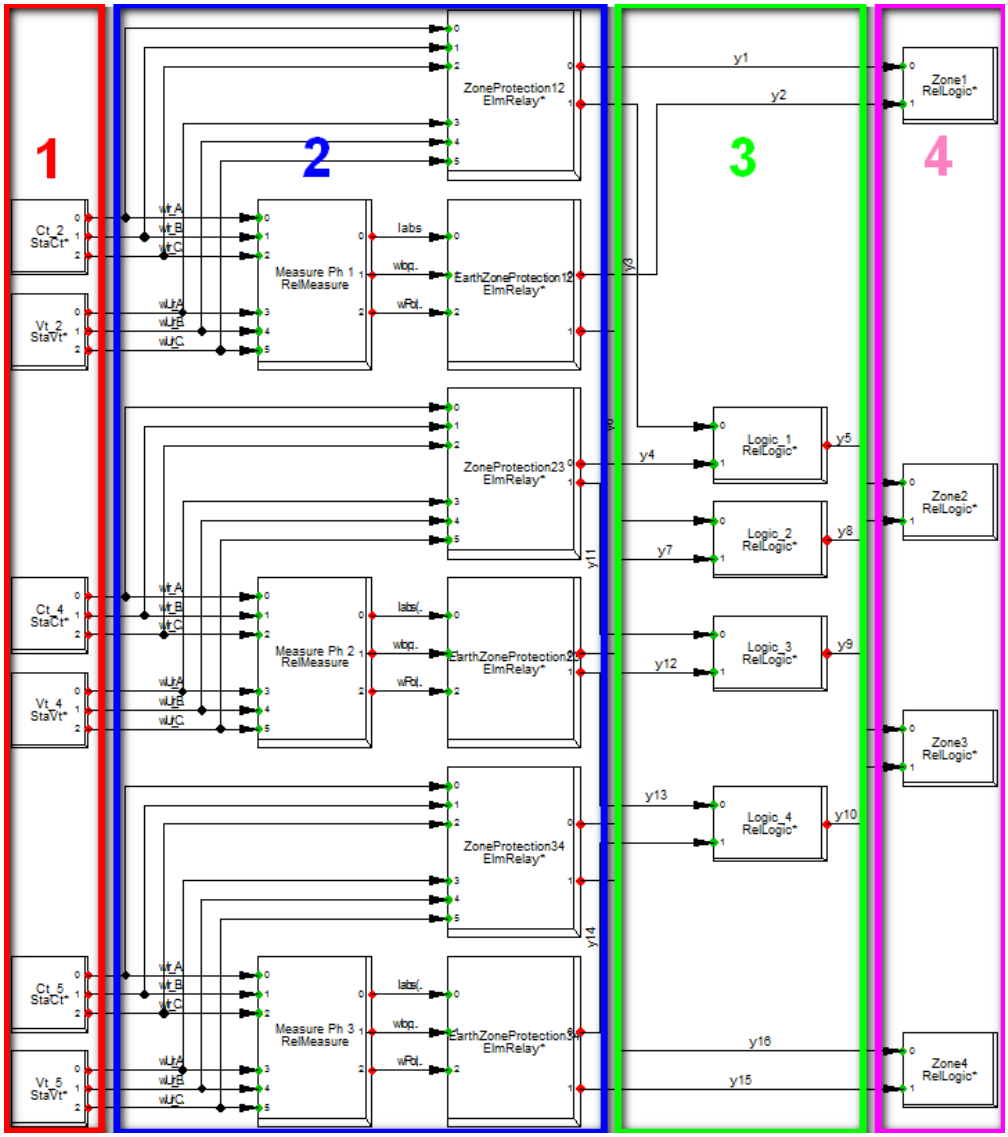

Figure 5.2: Relay model

5.1.2. Relay model

The proposed protection schemes, version 1 and 2 require a logic diagram to determine in which zone the fault is initiated, as discussed earlier in chapter 4. None of the generic protective relay models inside PowerFactory are able to provide the correct operations for the proposed protection schemes. Due to this an own relay model for both protection schemes is built inside PowerFactory by the author to provide the correct protective coordination during the simulations, see figure 5.2. This model can be separated in 4 parts which have the following functions:

- 1: this part is responsible for collecting the measured data of the instrument transformers (voltage and current transformers) between each interconnected zone;
- 2: collects the measured data of part 1 and determines the fault current direction, for both phase-to-phase and phase-to-earth faults, when the current is surpassing the corresponding pick-up current. Each fault current direction can be set independently with its own pick-up current;
- 3: determines which zone has to be isolated, and sends a tripping signal to the corresponding zone with the help of logic operators;
- 4: here the circuit-breakers are defined for each zone that will isolate the zone from the interconnecting zones.

Loading feeders							
Feeder	+0%	+10%	+20%	+30%	+40%	+50%	+60%
Main-station - 1.1	15%	19%	19%	20%	21%	23%	25%
Main-station - 2.1	31%	34%	38%	41%	44%	48%	51%
Main-station - 3.1	64%	**71**%	**78**%	**85**%	**92**%	**99**%	**108**%
Main-station - 4.1	18%	16%	15%	14%	14%	14%	15%
1.1 - 1.2	16%	18%	19%	20%	22%	24%	26%
2.1 - 2.2	31%	35%	38%	41%	45%	48%	51%
3.1 - 3.2	65%	**71**%	**78**%	**85**%	**92**%	**99**%	**109**%
4.1 - 4.2	32%	35%	38%	42%	45%	48%	52%
1.1 - 2.2	0%	0%	0%	0%	0%	0%	0%
2.1 - 3.1	0%	0%	0%	0%	0%	0%	0%
2.2 - 3.2	0%	0%	0%	0%	0%	0%	0%
3.1 - 4.1	0%	0%	0%	0%	0%	0%	0%

Table 5.1: Loading of feeders when loads are increased for each step by 10% for radially operated distribution system

Loading feeders							
Feeder	+0%	+10%	+20%	+30%	+40%	+50%	+60%
Main-station - 1.1	33%	36%	40%	43%	47%	51%	54%
Main-station - 2.1	28%	32%	35%	38%	41%	44%	48%
Main-station - 3.1	29%	32%	35%	39%	42%	45%	48%
Main-station - 4.1	16%	20%	23%	27%	32%	36%	40%
1.1 - 1.2	16%	18%	19%	21%	23%	24%	26%
2.1 - 2.2	27%	30%	33%	36%	39%	42%	44%
3.1 - 3.2	51%	56%	61%	66%	**72**%	**77**%	**82**%
4.1 - 4.2	32%	35%	38%	42%	45%	48%	52%
1.1 - 2.2	22%	25%	27%	29%	32%	34%	37%
2.1 - 3.1	3%	3%	3%	4%	4%	4%	5%
2.2 - 3.2	17%	19%	21%	23%	25%	27%	28%
3.1 - 4.1	26%	28%	31%	33%	35%	37%	39%

Table 5.2: Loading of feeders when loads are increased for each step by 10% for meshed operated distribution system

5.1.3. Loadability

The differences in loading of the feeders between a radially and meshed operated distribution system are calculated for the distribution system given in figure 5.1. The results of the load flow calculations are given in table 5.1 and 5.2 for the distribution system with a radially and meshed topology respectively.

The results in table 5.2 shows that feeder, "Main-station - 3.1" is less loaded in the initial 0% situation for the distribution system with a meshed topology compared to the radial topology. This is because the current provided to the loads are more evenly divided over all the main feeders coming from the main-station. It can be concluded from the tables that more transport capacity is generated in a meshed operated system. Due to the increase in transport capacity the load/generations units can grow in size compared with a radial operated system, without investing in additional feeders.

It has to be noted that the results obtained in the tables above are only true for the distribution system depicted in figure 5.1, and that these results do not reflect on any desirable distribution networks. Research needs to be done, when it is decided to change the topology of a distribution system, in order to understand if it is even feasible.

Table 5.3 and 5.4 represent the steady state voltage profile of a radial and meshed topology respectively. The overall voltage profile of a meshed operated distribution system is improved in comparison to the radial situation as can be seen in the last column of the tables. This is due to the fact that the equivalent impedance of the meshed system is smaller than that of a radial system, due to the multiple interconnections. Furthermore this lower equivalent impedance improves the overall transport losses of the system. For the distribution system depicted in figure 5.1 it means that the losses are slightly reduced, by 1.3 % which could be considered as negligible.

Voltage profile							
Sub-station	+0%	+10%	+20%	+30%	+40%	+50%	+60%
1.1	1.00	1.00	1.00	1.00	1.00	0.99	0.99
1.2	1.00	0.99	0.99	0.99	0.99	0.99	0.99
2.1	1.00	0.99	0.99	0.99	0.99	0.99	0.98
2.2	0.99	0.99	0.99	0.99	0.98	0.98	0.98
3.1	0.99	0.98	0.98	0.98	0.97	0.97	0.97
3.2	0.98	0.98	0.97	0.97	0.97	0.96	0.96
4.1	1.00	1.00	1.00	1.00	1.00	1.00	1.00
4.2	1.00	0.99	0.99	0.99	0.99	0.98	0.98

Table 5.3: Voltage profile measured for each substaton when loads are increased by 10% for each step, radial topology

Voltage profile							
Sub-station	+0%	+10%	+20%	+30%	+40%	+50%	+60%
1.1	1.00	1.00	0.99	0.99	0.99	0.99	0.99
1.2	0.99	0.99	0.99	0.99	0.98	0.98	0.98
2.1	1.00	0.99	0.99	0.99	0.99	0.99	0.99
2.2	0.99	0.99	0.99	0.99	0.99	0.98	0.98
3.1	1.00	0.98	0.99	0.99	0.99	0.99	0.98
3.2	0.99	0.98	0.99	0.99	0.98	0.98	0.98
4.1	1.00	1.00	1.00	1.00	1.00	1.00	1.00
4.2	0.99	0.99	0.99	0.99	0.99	0.98	0.98

Table 5.4: Voltage profile measured for each substaton when loads are increased by 10% for each step, meshed topology

5.1.4. Emergency operations

Any faulted zone that is being isolated from the distribution system will result in a loss of the overall transport capacity. The loading of the components during an emergency operation of the distribution system are calculated and summarized in table 5.5. Because the distribution system is operating in a meshed configuration the initial loads are increased by 40%. This is done to show that even during emergency operations the interconnected feeders aren't loaded above 100%.

The results in table 5.5 are given for a short-circuit initiated on bus 1.1, 2.1, 3.1 and 4.1. These fault locations will disconnect the main feeder coming from the sub-station, which will have the most severe impact on the overall transport capacity. It can be concluded from this table that, regardless which zone is isolated from the distribution system, none of the feeders will be loaded above the 100% burden.

		Isolated zone			
Feeder	Normal	Zone 1	Zone 2	Zone 3	Zone 4
Main-station - 1.1	47%	0%	22%	37%	53%
Main-station - 2.1	41%	53%	0%	30%	50%
Main-station - 3.1	42%	53%	58%	0%	54%
Main-station - 4.1	32%	72%	76%	44%	0%
1.1 - 1.2	23%	0%	23%	23%	23%
2.1 - 2.2	39%	55%	0%	30%	37%
3.1 - 3.2	72%	79%	90%	0%	66%
4.1 - 4.2	45%	45%	45%	45%	0%
1.1 - 2.2	32%	0%	0%	15%	40%
2.1 - 3.1	4%	3%	0%	0%	16%
2.2 - 3.2	25%	15%	0%	0%	31%
3.1 - 4.1	35%	36%	40%	0%	0%

Table 5.5: Loading of feeders during isolating of one zone from the distribution system

	Three-phase Ik"		Phase-to-phase Ik"	
Bus	Radial (kA)	Meshed (kA)	Radial (kA)	Meshed (kA)
Main-station	9.7	9.7	8.4	8.4
1.1	6.5	7.6	5.6	6.6
1.2	4.2	4.7	3.7	4.1
2.1	5.8	8.0	5.0	7.0
2.2	5.2	7.9	4.5	6.8
3.1	5.8	8.2	5.0	7.1
3.2	5.2	7.7	4.5	6.6
4.1	8.7	**8.9**	7.6	7.7
4.2	5.3	5.3	4.5	4.6

Table 5.6: Short-circuit calculation for three phase and phase-to-phase fault with a duration of 1 second

5.1.5. Rated short-time withstand current

Transition from a radial to a meshed topology has consequences regarding the short-circuit current magnitude experienced by the infrastructure. The meshed operated distribution system will create a lower equivalent impedance between the external grid and the fault location. The components in the distribution system are designed to experience a certain short-circuit magnitude for a duration of 1 second, which is a standard test condition to compare components of different manufacturers. This current magnitude is better known as the rated short-time withstand current. During both normal and abnormal operating conditions the component (feeder or transformer) will create transport losses. These losses are the amount of energy dissipated (E) as heat given by equation 5.1.

$$E = \int_0^T P(t) \cdot dt$$

$$E = U(t) \cdot I(t) \cdot t$$

$$E = Z_{comp.} \cdot I^2(t) \cdot t \tag{5.1}$$

In the following example a cable is used to compare the total time needed for the cable to dissipate the same amount of energy for different current magnitudes, see equation 5.2.

$$E_1 = E_2$$

$$Z_{cable} \cdot I_1^2 \cdot t_1 = Z_{cable} \cdot I_2^2 \cdot t_2 \tag{5.2}$$

The manufacturers of cables will provide rated short-time withstand current (I_1) of the cable for usually a period of 1 second (t_1). As mentioned this is the standard test condition applied by all the manufacturers. Because t_1 is equal to one, equation 5.2 can be rewritten as equation 5.3. With the help of this equation each maximum fault current magnitude (I_2) can be linked to a specific maximum fault clearing time (t_2). This equation will be needed to determine the impact the change in topology will have on the maximum fault current magnitude for each component inside the infrastructure.

$$\frac{I_1}{\sqrt{t_2}} = I_2 \tag{5.3}$$

E.g. a 3x95 mm^2 underground cable designed for a rated short-time withstand current of 12.7 kA for 1 second is connected to bus 4.1 in a meshed operated distribution system (see highlighted value table 5.6). The maximum fault clearing time corresponding to this short-circuit magnitude is calculated as follows:

$$t_2 = \left(\frac{12.7}{8.9}\right)^2 = 2.04s$$

This concept will be applied more in dept in the following case study. This because a typical distribution system is equipped with cables with a thickness even lesser than 3x95 mm^2.

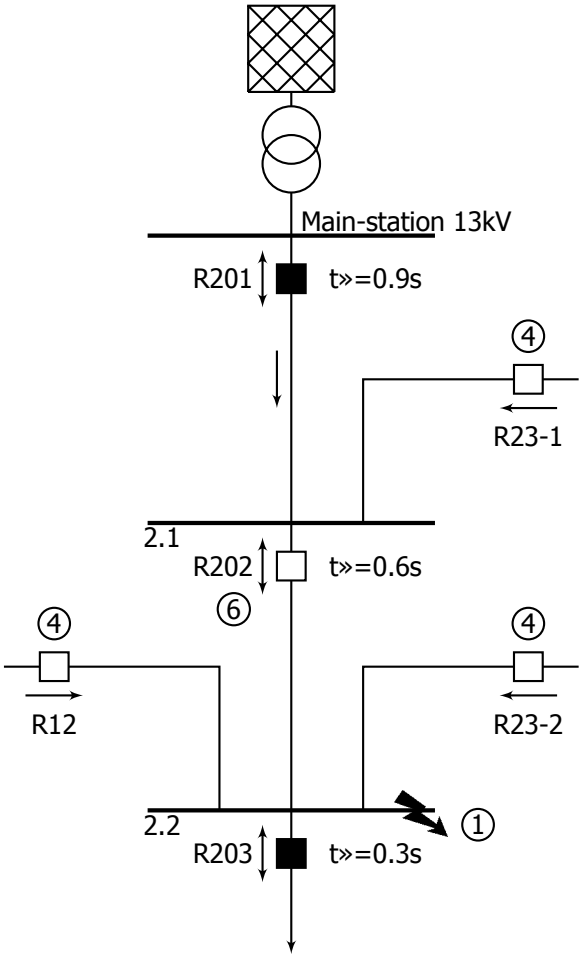

Figure 5.3: Protective coordination for a fault in zone 2, with protection scheme version 1

5.1.6. Protective coordination

One of the major advantages of PowerFactory is the computation of simulations in the time domain. PowerFactory is able to introduce events inside the distribution system which is being studied, for both the RMS- and EMT-simulation environment. Events inside a power system could be for example: (un)symmetrical faults, variation in load, operation of a switch, parameter change, tap change, power plant shut down or an synchronous machine event. These are one of the several events that can be initiated inside the model during the simulations in the time domain. With the help of these simulations the proposed protection schemes are simulated and tested to study if the correct protective coordination is applied during a (un)symmetrical fault event inside one of the interconnected zones. With the time simulations it is possible to simulate a more realistic scenarios towards fault current magnitudes over time by incorporating the sub-transient, transient and steady state behavior of the applied components.

For this simulation a fault is initiated in bus 2.2 (see figure 5.3) for simulating a phase-to-phase fault between phase a and b, where the fault impedance is set equal to 0Ω. This short-circuit type is chosen because the current magnitude for this type of fault is lower compared with a three-phase fault. When the proposed protection schemes are generating the correct protective coordination for a phase-to-phase fault, it can be concluded that this will be the case for a three-phase fault. The time simulation are carried out with the help of a RMS-simulation. In appendix B an explanation is given about the difference between a RMS- and EMT-simulation in PowerFactory and how the models applied during these simulations are created with the help of this software package.

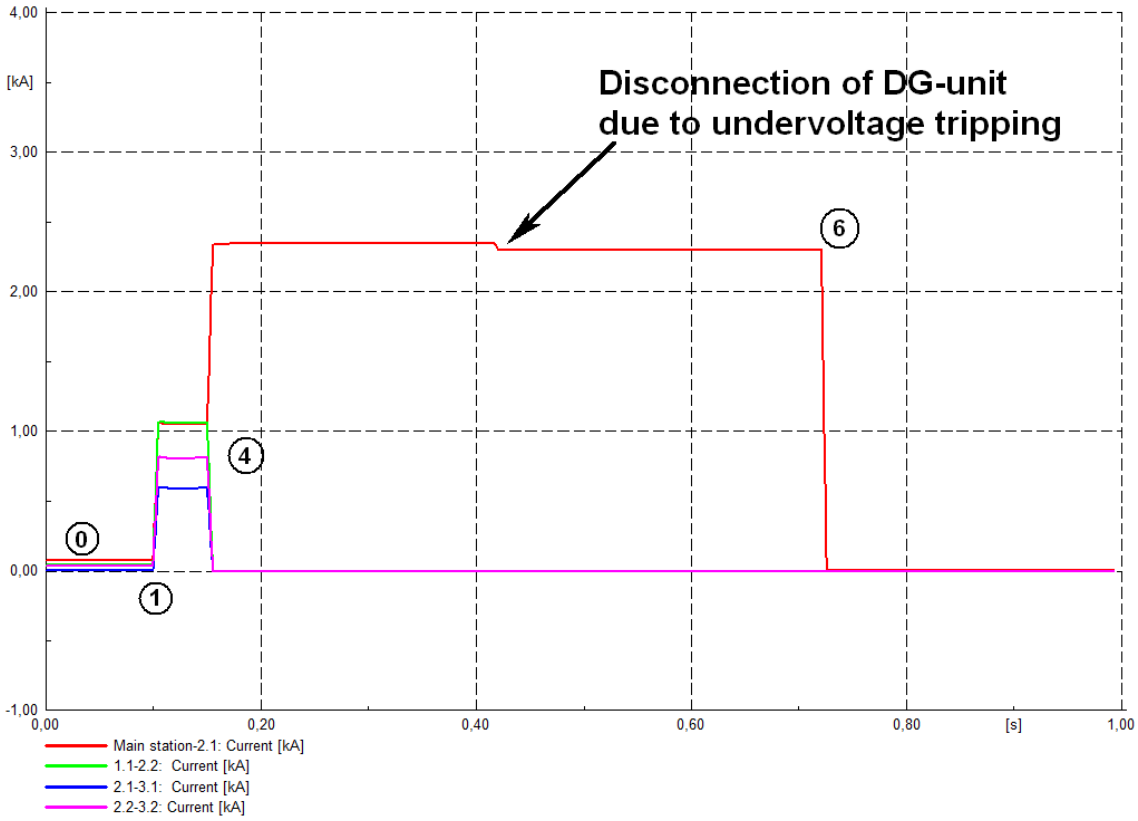

Figure 5.4: Protective coordination of a phase-to-phase fault on bus 2.2 for protection scheme version 1

The following protective coordination steps are taken by the protection scheme version 1 during a phase-to-phase fault initiated in bus 2.2:

1. A phase-to-phase fault event is initiated at t=0.1 seconds on bus 2.2.
2. The current magnitude experienced by each interconnection will increase and hereby each directional relay will determine the fault current direction.
3. The signals from the directional relays are collected and the logic diagram will determine in which zone the fault is located.
4. The appropriate circuit-breakers are tripped between the healthy and faulty zones (R12, R23-1 and R23-2).
5. Now the topology of the faulty zone has changed from meshed to radially.
6. The existing protection scheme will isolate the component corresponding for the short-circuit by using the time grading approach (R202).

In both figure 5.3 and 5.4 the protective coordination steps taken by the protection scheme are also indicated. The numbers found in these figures correspond with the numbers in the enumeration above. As can be seen in figure 5.4 is that the current magnitude in the feeders ”main-station-2.1”, ”1.1-2.2”, ”2.1-3.1” and ”2.2-3.2” will grown above the nominal operation current during a phase-to-phase fault (step 1). The faulty component has to be isolated as quickly as possible without losing selectivity inside the protection scheme. To achieve this the proposed protection scheme first isolates feeder ”1.1-2.2”, ”2.1-3.1” and ”2.2-3.2” from zone 2 after approximately 0.15 seconds by tripping circuit-breaker R12, R23-1 and R23-2. The delayed response time is created due to the applied circuit-breaker (step 4). It has to be noted that the delayed operating time created by the communication is neglected during this example. This communication time falls outside the scope of this research but needs to be studied to ensure that the algorithm is fast enough to operate. After zone 2 is isolated feeder ”sub-station-2.1”

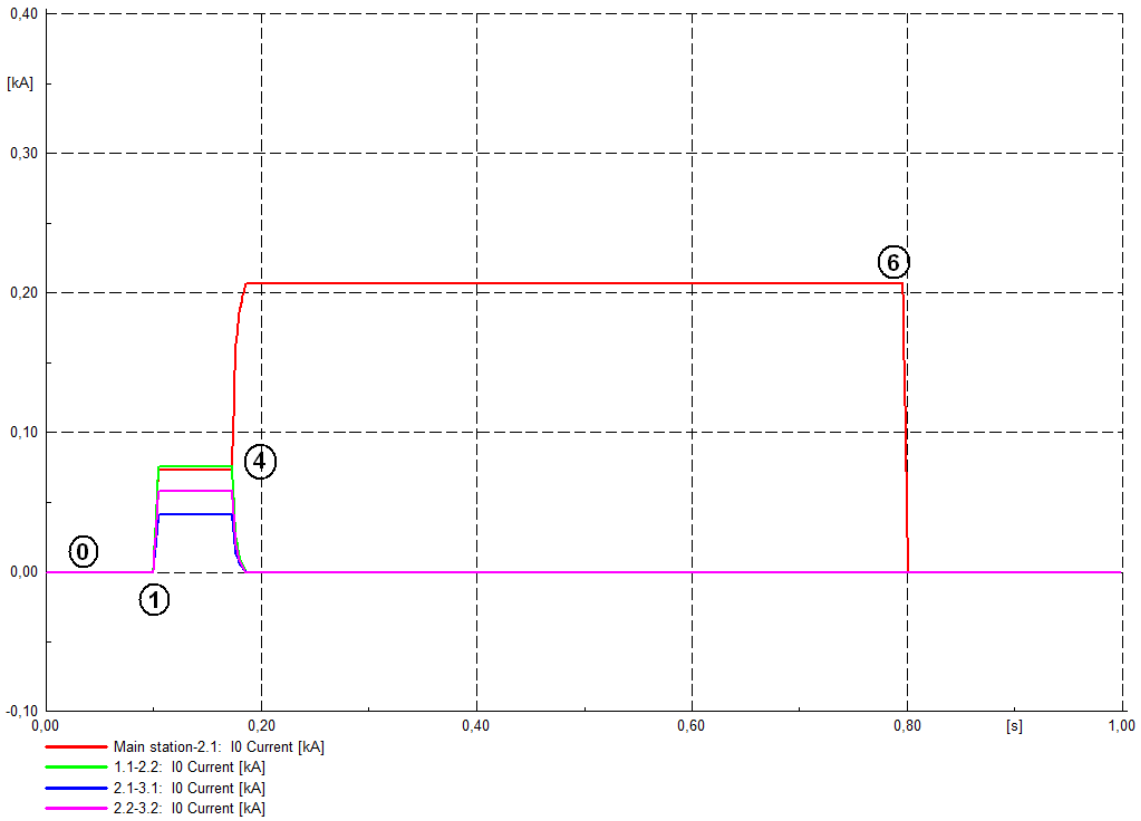

Figure 5.5: Protective coordination of a phase-to-earth fault on bus 2.2 for protection scheme version 1

is still subjected to a high overcurrent. The main task of relay R21 is to disconnect the faulted bus 2.2 from zone 2. This relay (R202) is set with a delay tripping time of 0.6 seconds. Again with the delayed response time coming from the circuit breaker a safe situation is realised after bus 2.2 is isolated from zone 2 after 0.72 seconds (step 6).

With the relay model shown in the earlier section it is possible to detect a phase-to-earth fault and realize the appropriate protective coordination to disconnect the faulted component with the same principle as described above for the phase-to-phase fault. The proposed protection relay is able to detect a phase-to-earth fault by monitoring the zero-sequence current (I_0) between the interconnecting zones, which will rise in magnitude during this type of fault. This current type is chosen because the earth-fault current will be as high as or higher than the load current. This makes it hard to provide the correct protective coordination without monitoring the zero-sequence current. As an example a phase-to-earth fault is again initiated on bus 2.2 with the corresponding protective coordination and current magnitude depicted in figure 5.5. When the fault is initiated the zero-sequence current component rises from zero to a certain magnitude for all the interconnections. This rise in zero-sequence current helps the protection scheme to decide in which zone the fault is initiated. Again the faulty component is isolated appropriately.

After this protective coordination certain feeders could come back into operation. This switching coordination can only be applied if the reconnected feeders are not creating a direct connection to the fault that is being isolated from the distribution system. This switching coordination allows the application of a so-called self healing grid inside the distribution system, where the system automatically determines which of the interconnections could come back in service to the system after the occurrence of a fault. This principle is different than the auto re-closure function applied in the current protective relays, found in the transport system. The auto re-closure function automatically re-closes the circuit-breaker regardless if the feeder is still feeding into the fault.

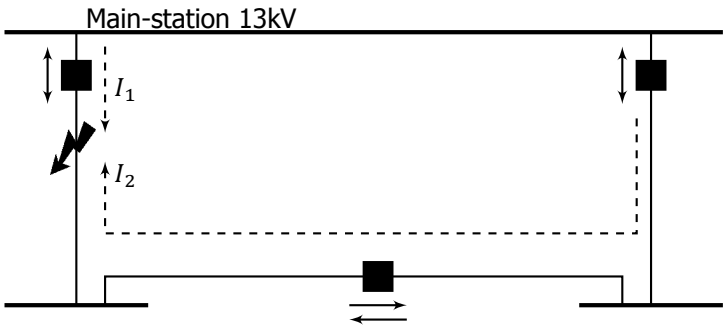

Figure 5.6: Concept behind blinding of the directional relays

5.1.7. Protective coordination problems

Problems can occur regarding the protective coordination when a fault is initiated near the main-station in one of the outgoing main feeders. This will occur at approximately the first 20% of the total length of all the outgoing main feeder regardless which type of fault (phase-to-phase or phase-to-earth). In the example explained above it was mentioned that first the relays between the interconnected zones will trip before the protection scheme inside the faulted zone will isolate the faulty component. In the case a fault is initiated around 20% of the total length of the main feeder this will be the other way around. First the relay protecting the main feeder will trip before the relays between the interconnected zones will trip. This problem is due to blinding of the directional relays where this principle is shown in figure 5.6. In this situation the current magnitude seen by the directional relays (I_2) will be much lower compared to the current magnitude of the external grid (I_1). This current magnitude will even be so low that the pick-up current of the directional relays will not detect the fault ($I_1 >> I_2$). It is not desirable to set the pick-up current values of the directional relays to sensitive. This because the scheme can even respond to normal load currents. To provide the appropriate protective coordination (when it is desirable to first let the relays trip between the interconnected zones before the relays protecting the main feeder) the current magnitude seen by the relays protecting the main feeder can be incorporating inside the logic diagram. When these relays detect a current magnitude surpassing the set pick-up current the relays between the interconnected zones will be tripped immediately.

5.1.8. Undervoltage tripping

The protective coordination of the protection schemes discussed in the previous sections will create net openings between the interconnected zones during a fault to guarantee selectivity inside the already applied protection schemes found in each zone. The protection scheme inside each zone depends on time-grading for providing the right protective coordination. A longer responds time will be needed when the fault is initiated closely to the main-station. This longer responds time will create a voltage dip with also a long duration. The magnitude of this voltage dip depends on the type of fault and the distance between the fault location and point of measuring. This voltage dip is especially noticeable for the neighbouring healthy zones which are connected the closest to the faulted zone. When DG units are connected to these neighbouring zones the duration of the voltage dip will have consequences regarding the undervoltage protection of these DG units. Due to this duration in voltage dip the fault must be isolated as fast as possible before the undervoltage protection will generate a trip signal and disconnect the DG units from the distribution system.

Figure 5.7 gives the computation of the rms voltage magnitude for bus 4.1 during a phase-to-phase fault on bus 2.2 at t=0.1 seconds. The voltage magnitude for zone 4 during this fault surpasses the 0.7 p.u. border for more than 300 ms. This is due to the applied time grading inside the protection scheme of zone 2. This means that the undervoltage protection will generate a tripping signal and will disconnect the DG unit from zone 4 which is very undesirable for the DG owner.

In protection scheme version 2 the protection of the main feeder for each zone are further integrated inside the protection scheme. This means that the faulted zone will instantaneously be disconnected from the distribution system when the fault is located by the protection scheme. This protective coordination ensures that the voltage dip won't last as long as in the case where the protection of the main feeder is not integrated inside the protection scheme. Again a phase-to-phase fault is simulated for bus 2.2 and the voltage magnitude is measured for bus 4.1, see figure 5.8. This figure shows that the voltage dip will not hold longer than the 300ms limit and that the DG unit will stay in operation.

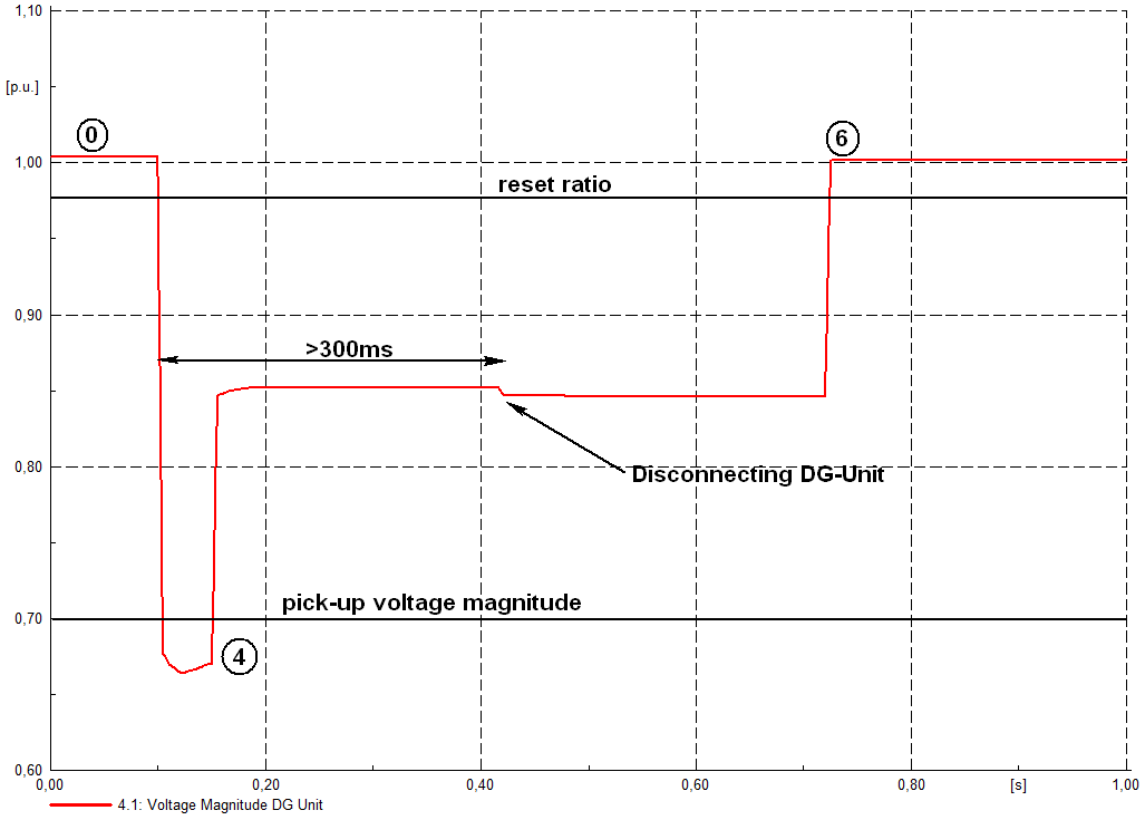

Figure 5.7: Voltage magnitude bus 4.1 during a phase-to-phase fault on bus 2.2 for protection scheme version 1

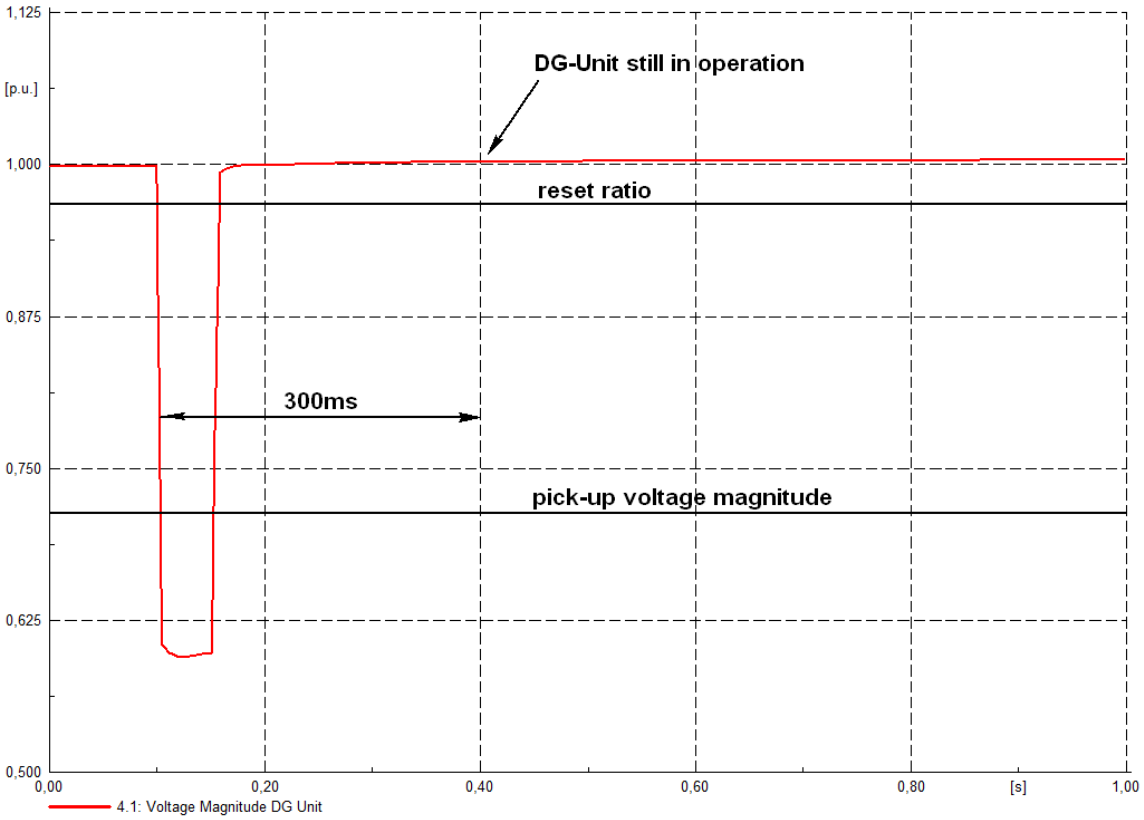

Figure 5.8: Voltage magnitude bus 4.1 during a phase-to-phase fault on bus 2.2 for protection scheme version 2

5.1.9. Self healing principle

A self healing grid applies a smart algorithm to determine the fault location, and will only automatically reconnect the feeders that will not feed into the fault. This to guarantee an even more reliable transport of energy for the end-users connected to the distribution system. The principle of a self healing grid could be a possibility due to the applied communication infrastructure of the proposed protection schemes. This self healing principle can be seen as a separate function after the correct protective coordination is applied. Figure 5.9 shows how it can be determined which interconnection can be re-closed after the fault is isolated from the distribution system. The protective relays of the protection scheme inside each zone determine the border for the decision of which interconnection can be re-closed after isolating the fault. In this example the second relay is tripped which means that interconnection 1 can be re-closed, and that interconnection 2 must stay open to prevent connection to the faulty bus three.

In figure 5.10 an example is given of how this self healing principle could be integrated inside the proposed protection scheme version 1 of the distribution shown in figure 5.1. Again a phase-to-phase fault event is initiated after 0.1 seconds on bus 2.2, where the protection scheme will first isolate the fault. After the fault is isolated feeder, ”2.1-3.1” can safely be put back into operation without the risk of feeding into the fault.

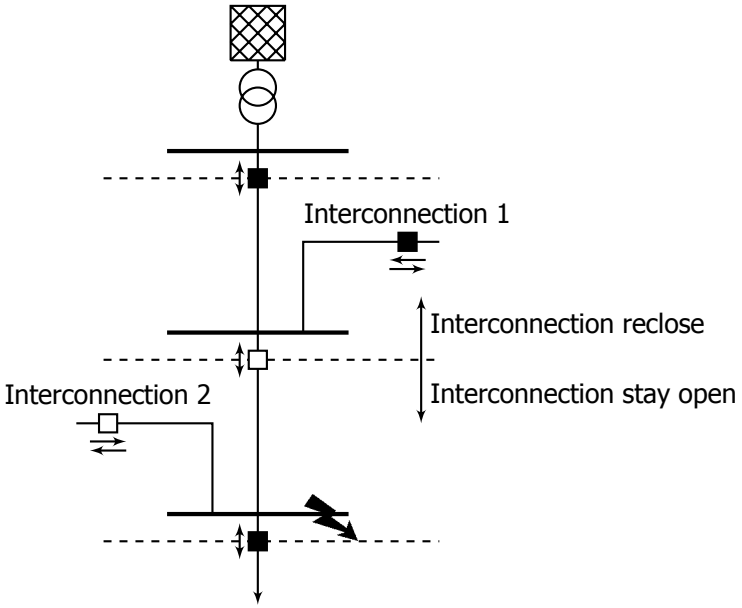

Figure 5.9: Principle behind self healing grid

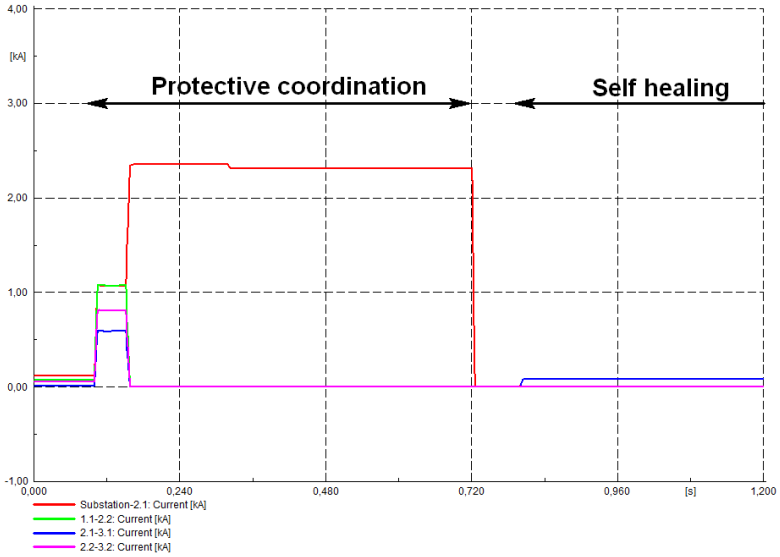

Figure 5.10: Self healing grid after a phase-to-phase fault on bus 2.2

Figure 5.11: Goeree-Overflakkee

5.2. Case study 2

This case-study is related to the distribution system found on the island of Goeree-Overflakkee. The distribution system on this island is divided between two major sub-stations, Stellendam and Middelharnis, each responsible for transporting energy for both consumers (small villages and agriculture) and producers (wind and solar energy production) of electrical energy. The proposed protection schemes will be integrated into the distribution system of Stellendam, where again the impact of this protection scheme on the distribution system will be studied in this section.

5.2.1. Goeree-Overflakkee

The municipality of Goeree-Overflakkee with a total area of 261 km^2 consist of 48.000 citizens spread over 19 small villages, which compared to the Netherlands corresponds to a low population density. This area is very popular during the summer days due to its location near the North sea, which results in 1.563.000 overnight stays during peak days [23].

The location of Goeree-Overflakkee has many benefits with regards to natural energy sources. This area has a lot of sun hours during the year with relatively high wind speeds, with tidal energy being a further in the coming years [6]. Goeree-Overflakkee has the ambition to become energy neutral in the year 2030, which means that the overall energy production is matched with the overall energy consumption during the course of one year. The distributed generation units for this island are expected to be realised in 2030 with the help of wind, solar, biomass and tidal energy.

The current energy consumption of this island is estimated to be 992GWh per year, where the ambition is to reduce this consumption to 553GWh per year due to energy savings. The expected energy production in 2030 is divided between solar (26GWh), tidal (155GWh), biomass combustion (46GWh), biomass fermentation (45GWh) and wind (284GWh). At the current moment 22% of the total energy demand is produced with the help of wind turbines.

5.2.2. Distribution system

The current distribution system of Goeree-Overflakkee is fed by a 52.5kV cable, which in turn is fed with an overhead line coming from the main land (Klaaswaal) to the village Ooltgensplaat. From there a 52.5kV underground cable is connected between a wind park with 12 2MVA wind turbines operating at a voltage of 23kV and to the sub-station of Middelharnis. Sub-station Stellendam is connected to sub-station Middelharnis via two 52.5kV underground cables.

This case study is focussed on the 13kV distribution system found on Goeree-Overflakkee. This is because the infrastructure is already extensively integrated over this island, which can be utilized to connect bigger loads or more DG units in the future. Moreover the topology of this system is related to the distribution systems mostly found in the Netherlands, which makes it easier to relate this research to other distribution systems in the Netherlands.

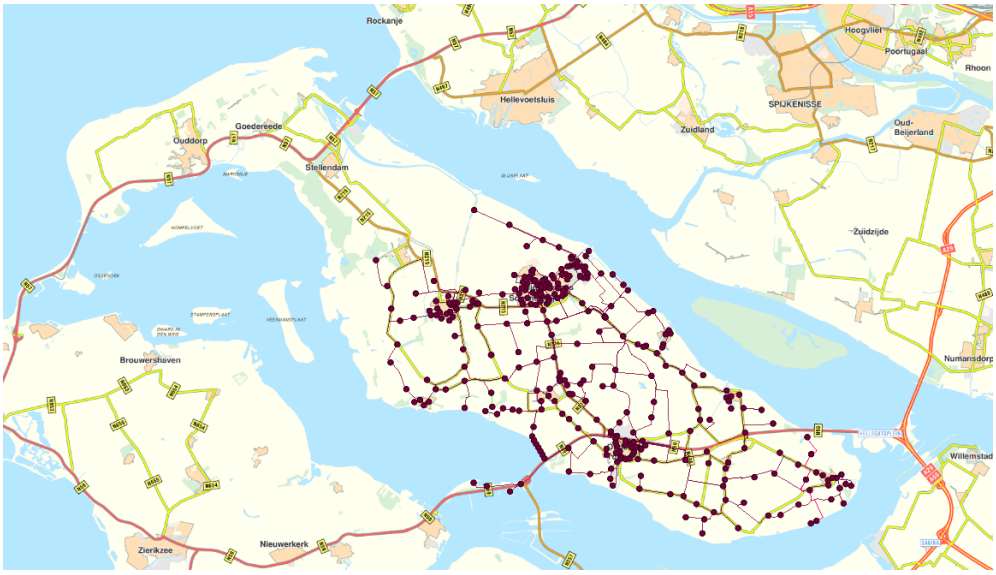

Figure 5.12: Infrastructure connected to main-station Middelharnis

Figure 5.13: Infrastructure connected to main-station Stellendam

The 13kV distribution systems on this island are connected to two main sub-stations. These corresponding main-station are Middelharnis and Stellendam, see figure 5.12 and figure 5.13 respectively for the applied infrastructure connected to each station. Both stations are earthed with a grounding (zig-zag) transformer. The distribution systems for both Stellendam and Middelharnis are operated radially, created by multiple net openings between certain connections. The protection schemes applied for both Middelharnis and Stellendam are both applied with overcurrent relays, while differential relays are used at station Middelharnis to protect the outgoing feeders.

This case study will focus on the 13kV distribution system connected to main-station Stellendam. The single line diagram of this distribution network is depicted in figure 5.14. The distribution network of Stellendam consist of several types of underground feeders with different characteristics. It has to be noted that usually a feeder consist of several types of underground cables with different thicknesses. These different kind of thicknesses are not taking into consideration during this case study. This is why also the original Visions files of this distribution system will be used. The external grid connected to distribution system Stellendam is modelled as a infinite strong voltage source with the corresponding R/X ratio (0.35) and short-circuit power (320 MVA).

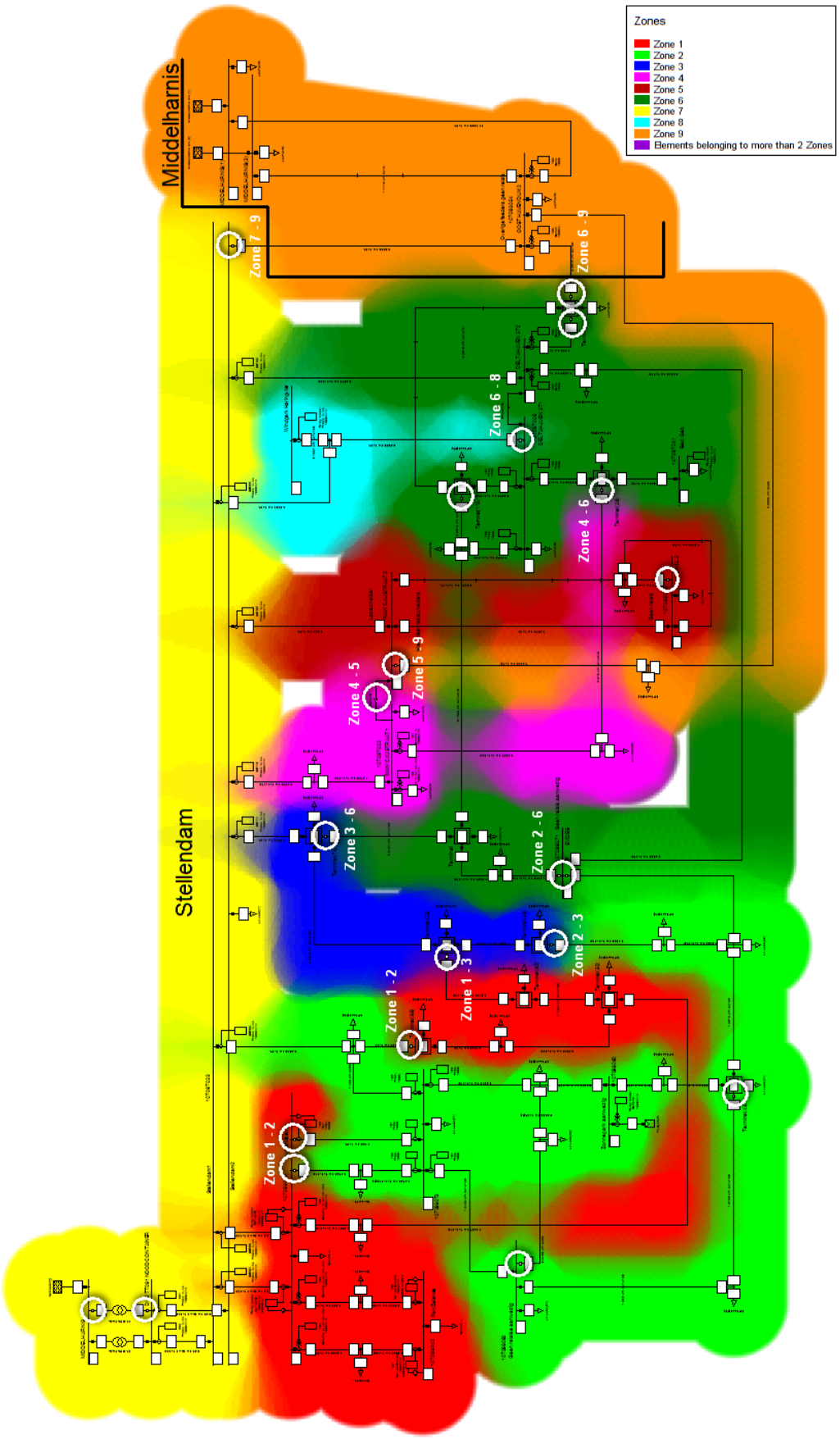

Figure 5.14: Single line diagram distribution network Stellendam with net openings indicated

Interconnections between zones									
Zone	1	2	3	4	5	6	7	8	9
1	X	X	X				X		
2	X	X				X	X		
3	X		X			X	X		
4				X	X	X	X		
5				X	X		X		X
6		X	X	X		X	X	X	X
7	X	X	X	X	X	X	X	X	X
8						X	X	X	
9					X	X	X		X

Table 5.7: Zone connection

The distribution network of Goeree-Overflakkee is radially operated, which means that there are multiple net openings inside this network. In figure 5.14 these net openings are indicated by white circles including a label with the corresponding neighbouring zones. The main reasons for applying these openings is for providing a simple overcurrent protection scheme. Furthermore the energy supplied to the end-user will be rerouted after a faulty component is isolated by re-closing some of the openings. This will decrease the average failure minutes. This case study is making use of these net openings to define multiple zones inside the distribution network of Goeree-Overflakkee. The net openings (18 in total) are responsible for creating 9 zones (main-station zone 7 included) in total. Table 5.7 summarizes the interconnections that can be made for each zone.

5.2.3. Protection scheme

In table 5.7 the interconnections are summarized that can be made between each zone. This table will be applied for projecting the proposed protection schemes of chapter 4 on the distribution system of Goeree-Overflakkee. Table 5.7 is translated into figure 5.15 for giving an overall representation of the proposed protection scheme. This figure shows all the interconnections that can be made between each zone, where the most interconnections can be created towards zone 6. In figure 5.15 the zones are rearranged such that the feeders inside the figure overlap each other as least as possible. This is done for representing a clear figure to the reader of this thesis, where in reality the order of the zones is as depicted in figure 5.14.

In figure 5.16 the single line diagram, including the applied relay interconnections, is given for distribution system Stellendam. The interconnections applied during this case study are again indicated with white circles with the corresponding relay number. This figure shows that even with the applied protection scheme not all the net openings are closed. This is done intentionally because only some of the closed net openings will increase the overall transport capacity of the infrastructure by several percents compared to others. Furthermore most of the closed net openings are directly connected to the underlaying sub-stations of main-station Stellendam when figure 5.14 and 5.16 are compared with each other. This method is applied because in practice it would make more sense to install a communication cable, which is needed for the proposed protection scheme, towards a sub-station. This example can be seen when a closer look is given to the interconnection between zone 3 and 6 in figure 5.14 and R63 in figure 5.16. This also counts for the interconnections R64 and R69. Only the interconnection between zone 1 and 3 is made at a transformer load.

The relay model in figure 5.2 is attended for measuring 4 locations in total, where in case study 2 a total of seven measuring locations will be applied. Figure 5.16 shows a total of nine interconnections that can be made inside distribution Stellendam, which implies the use of nine measuring locations inside the relay model. For this case study this will not be the case because the two interconnection towards zone 9 are neglected. This is due to the fact that zone 9 corresponds with the distribution system of Middelharnis. This distribution system is not modelled inside PowerFactory and could result in faulty simulation results. Each measuring location is applied with both a voltage and current transformer, where the data coming from these transformers is send to the relay model to determine the faulty zone.

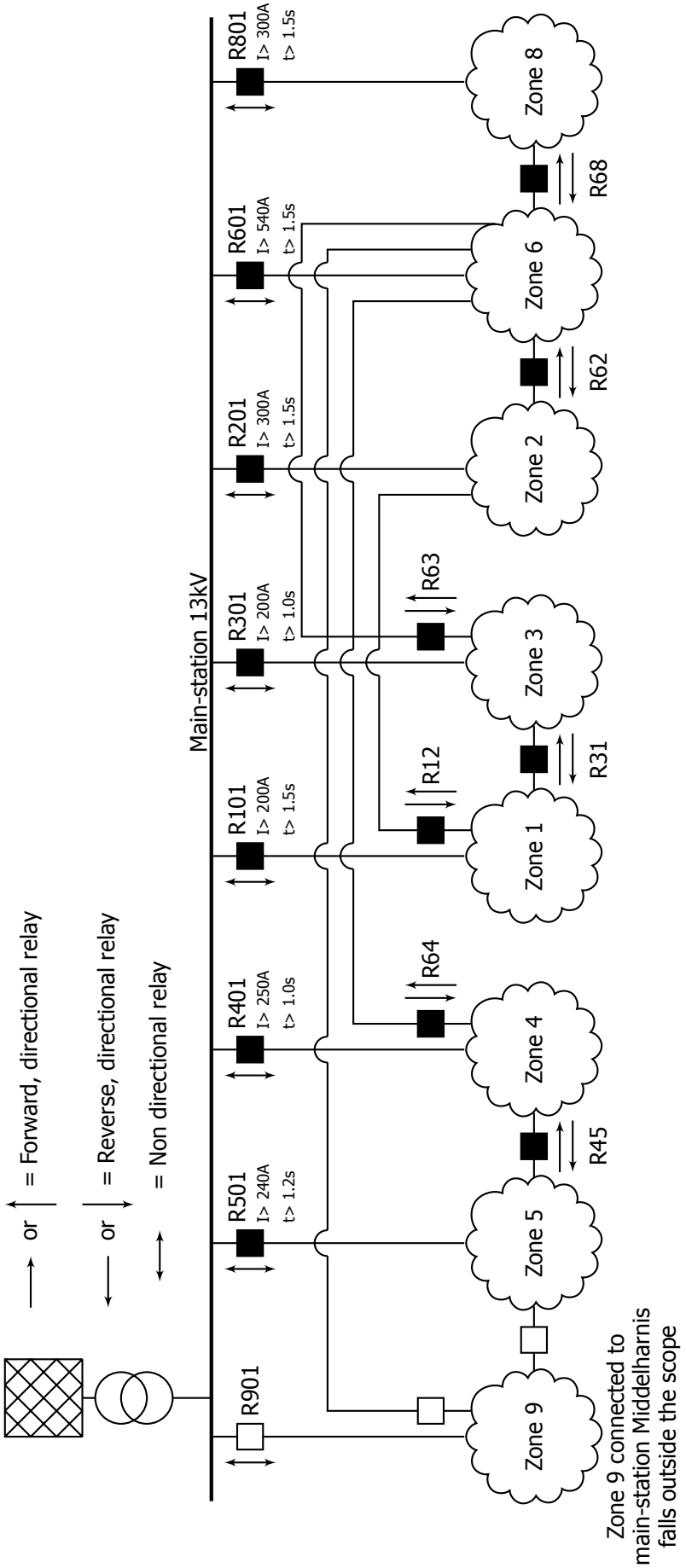

Figure 5.15: Protection scheme version 1 applied to distribution system of Goeree-Overflakkee

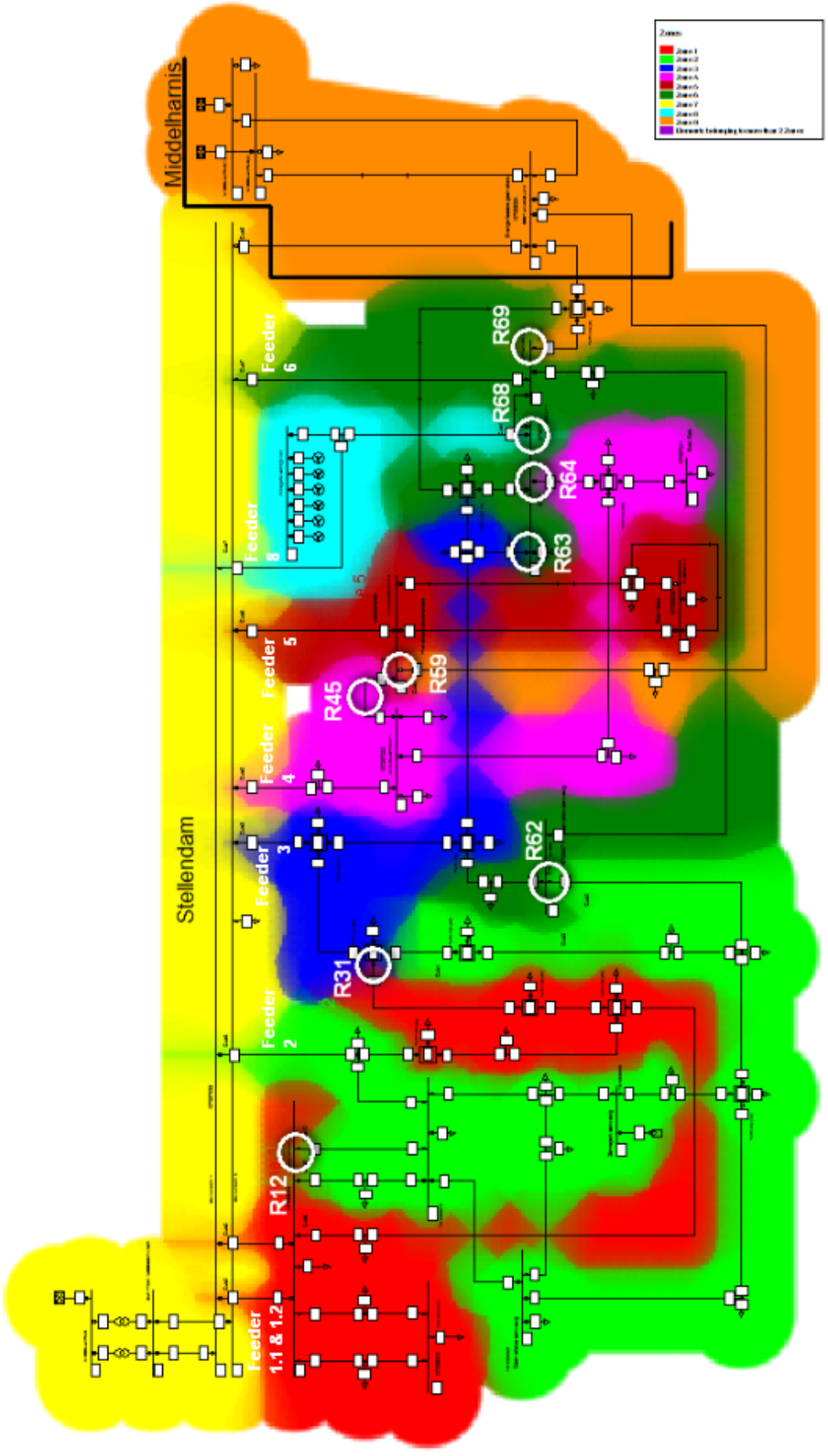

Figure 5.16: Protection scheme version 1 applied to distribution network of Stellendam with interconnected zones indicated

Relay	Current Direction	I>>(A)	3xI0 (A)
R12	Reverse	250	150
	Forward	160	150
R31	Reverse	80	120
	Forward	300	70
R62	Reverse	80	100
	Forward	160	80
R63	Reverse	90	100
	Forward	600	120
R45	Reverse	300	100
	Forward	800	150
R64	Reverse	200	40
	Forward	120	80
R68	Reverse	300	20
	Forward	800	150

Table 5.8: Settings for overcurrent relays with directional unit for protection scheme version 1

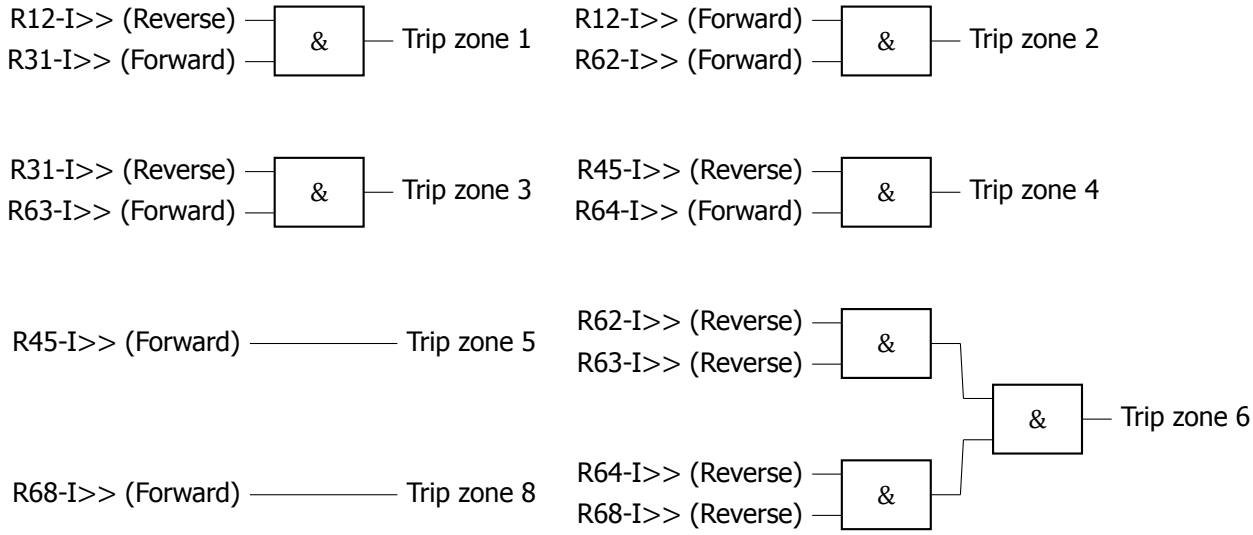

Figure 5.17: Logic diagram protection scheme version 1 for distribution system Goeree-Overflakkee

The settings for each interconnection inside the proposed protection scheme are given inside table 5.8, with the corresponding logic diagram shown in figure 5.17. This table shows that each interconnection and current direction can be set independently with a desired pick-up current magnitude. The pick-up currents shown inside this table are tested for both phase-to-phase and phase-to-earth faults at different locations inside each of the seven zones applied during this case study. The choice to set the pick-up current independently for each current direction is created to increase the sensitivity of the protection scheme to detect every kind of fault at each location inside the faulted zone. For some interconnections the set pick-up current is rather low compared to the others. This is due the low fault current contribution of certain interconnections during a phase-to-phase fault. Nevertheless the set pick-up current with a low magnitude will not introduce false tripping during normal operations due to the logic applied inside the relay model.

The already applied protection schemes inside each zone of distribution system Stellendam are slightly changed by including time grading (step of 0.3 seconds) for some of the definite overcurrent relays which are initially set be an instantaneously tripping time (0.0 seconds). Also some of the pick-up currents are altered. These changes in tripping time and pick-up current are done for firstly give the proposed protection scheme the change to create the correct protective coordinations without losing selectivity. Each of these relays are set with a minimum tripping time of 0.3 seconds, which means that the proposed protection scheme must react within 0.3 seconds (delay tripping time of the circuit-breakers and protective algorithm not included) to guarantee selectivity.

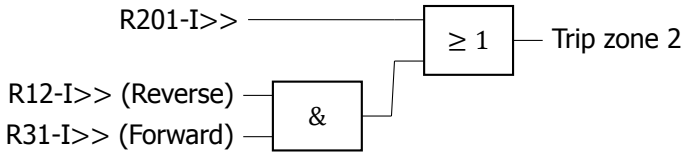

Figure 5.18: Example of an additional input measured from the main feeder for logic diagram zone 2

Again as mentioned in case study 1 the desired protective coordination will be hard to guarantee when a fault is located inside the main feeder near the main-station. Also in this practical example of the distribution system of Goeree-Overflakkee this will be true. The fault current magnitude seen by the directional relays will be to low to be detected by the set pick-up currents. As mentioned in the earlier section this could be resolved by incorporating the measured current magnitude of the relay position protecting the main feeder inside the logic diagram. For example the logic diagram for tripping the interconnected relays of zone 2, where the current magnitude measured by the relay protecting the main feeder (R201), will look according to figure 5.18. In this case only the current magnitude measured by relay R201 will be provided to the logic diagram. When this current magnitude surpasses the short-circuit seen at around approximately 80% of the total length of the main feeder an additional trip signal will be generated, where the current magnitude and direction of the current measured by the directional relays will will not be taken into consideration. This current magnitude for relay R201 is chosen because the protection blinding effect will occur between 0 and 20-40% (dependently of the type of fault) of the total length of the main feeder with the corresponding pick-up current values for the directional relays found inside table 5.8. Some of the pick-up current values found in table 5.8 are rather low compared to the nominal operating current magnitude. By incorporating this enhancement the values can be set much higher which allows the protection scheme to be less sensitive. As an example due to this extra input both the values for the reverse and forward current direction of relay R62 can be set to a pick-up value of 160A.

Loading of main feeders		
Feeder	Radial (%)	Meshed (%)
1.1	34.5	27.6
1.2	34.5	27.6
2	68.3	29.8
3	17.3	28.6
4	28.2	23.1
5	34.6	30.1
6	20.4	8.2
8	67.2	7.3

Table 5.9: Loading main feeders distribution system Stellendam

5.2.4. Loadability

To show the difference in loading of the main feeders the comparison is made between a radially and meshed operated distribution system for distribution system Stellendam. Only the interconnections R12, R31, R62, R63, R45, R64 and R68 are closed during this load flow study. In table 5.9 a summery is given between the two operating systems. As can be concluded from this table is that feeder 2 is less loaded during meshed operations because the load is evenly divided over the other main feeders. Feeder 8 is also less loaded when the two operations scenarios are compared with each other. This is not totally true because in zone 8 there are already 6 DG units present in the form of 0.63 MVA wind turbines that produce energy which is delivered directly to the end-user. Due to the meshed configuration the energy that is being generated by these wind turbines is directly injected into zone 6, which means that the 90 meter 3x95 GPLK connection between the wind turbines and the sub-station of zone 6 will be subjected to a higher load (0% radial to 73% meshed).

Name	From	To	Ik"1b	Ik"2b	tmax
88		HOFDIJKSWEG	1,88	2,94	0,196
154	INLAATSLUIS	OOST HAVENDIJK 20	2	2,87	0,205
117			1,88	2,54	0,684
55	AWZI		3,15	3,31	0,994
252	VAN DIS		2,52	3,2	1,065
303	SCHAKELH. STELLENDAM	RABOBANK	6,2	5,91	1,202
58			4,15	3,77	1,226
116	GEMAAL KRONINGSPOLDER		1,63	1,88	1,25
53	AWZI		2,48	2,73	1,46
64	TRAFO 1		2,69	2,51	1,508
63	TRAFO 1	TRAFO 3	2,69	2,66	1,508
145		IMAN CAUSTRAAT	4,86	5,51	1,523
1069	TRAFO 2		2,38	2,51	1,725
54	AWZI		2,48	2,36	1,774
16	RIDDERSTEE	GELDERSEROOS	2,25	2,39	1,904

Figure 5.19: Critical clearing time calculation radially operated distribution system Stellendam

Name	From	To	Ik"1b	Ik"2b	tmax
88		HOFDIJKSWEG	2,32	4,05	0,103
154	INLAATSLUIS	OOST HAVENDIJK 20	2	2,87	0,205
16	RIDDERSTEE	GELDERSEROOS	4,05	4,44	0,553
21	TOPPERSHOEDJE	NOORDZEEPARK	4,17	3,64	0,625
			3,82	4,09	0,65
15	KOOLMEES	RIDDERSTEE	3,69	4,05	0,663
117			1,88	2,54	0,684
53	AWZI		3,29	3,72	0,787
	KOOLMEES		3,69	3,32	0,798
20		NOORDZEEPARK	3,27	3,64	0,823
58			4,93	4,44	0,871
252	VAN DIS		2,59	3,31	0,995
54	AWZI		3,29	3,11	1,004
55	AWZI		3,29	3,13	1,004
64	TRAFO 1		3,04	2,82	1,175

Figure 5.20: Critical clearing time calculation meshed operated distribution system Stellendam

5.2.5. Rated short-time withstand current

The Vision files of distribution system Goeree-Overflakkee are applied during this section for providing the correct short-circuit study without simplifications found in the feeders of the PowerFactory model. Vision is applied for calculating the maximum fault clearing time accurately. This concept is explained in more detail in case study 1. By calculating the maximum short-circuit current seen by each feeder inside the system the rated short-time withstand current is calculated. This calculation for case study 2 shows that the bottleneck for applying a meshed distribution system are the 3x25 GPLK cables (oil filled lead paper cable) installed during the 1970s. The underground feeders that are currently being installed, inside the distribution system managed by Stedin, are of the type 3x150 XLPE cable. These type of cables can experience a relatively high rated short-time withstand current in comparison to the maximum short-circuit current these cables will experience during a fault.

The short circuit calculations (three-phase fault) done for the distribution system of Stellendam shows that in a meshed operated system Stellendam only eight additional feeders of the 200 feeders found in the distribution system of Stellendam (see figure 5.20) will have a shorter critical clearing time than 1 second compared to the radially operated system (see figure 5.19), which already has 3 feeders with a short critical clearing smaller than than 1 second. These feeders with the critical clearing time of less than 1 second are mainly the 3x25 GPLK cables, which are mostly installed far away from the main-station. When a fault is initiated inside these feeders, in a meshed operated network, the fault must be isolated by the protection scheme faster than the calculated critical clearing time found in the tables above. The responds time of the protection scheme mainly depends on the speed of the communication infrastructure, the algorithm and the reaction time of the applied circuit-breakers. This research question falls outside the scope of this thesis but needs to be studied to guarantee quick protective coordinations to isolate these feeders as quickly as possible. When this responds time is to low other measures have to be taken, like applying additional protective relays or lower the delayed tripping time of some relays to provide a fast responds time below the critical clearing time ($< t_{max}$).

6

Conclusion and Recommendation

6.1. Conclusion

The topic of this research is related to Smart Grid. The topic Smart Grid enjoys much attention with the many stakeholders in the energy market and is therefore the driving force behind this research. First the impact of DG units towards the overcurrent relay protection scheme is studied, where it is shown that the DG units will indeed have an impact on both the total short-circuit current magnitude experienced by the fault and the short-circuit contribution of the external gird. It is shown that in some cases this even can lead to non correct protective coordination. It have to be noted that this effect will mainly depends on the technique applied inside the DG unit. In the case synchronous machines are applied (CHP units) this effect can last for many cycles compared to the asynchronous machines (DFIG).

Further in this research two proposals are given for protection schemes inside a fully meshed operated distribution system together with Smart Grid solutions. This is done to fully utilize the infrastructure inside the distribution system and hereby increase the transport capacity, but still have the desirable characteristics that are being required from the protection scheme. In protection scheme version 1 loads are more respected than distribution generation units and in protection scheme version 2 the continuity of generations units are more respected than loads. These protection schemes rely on the conventional protection technique of the directional relay (which have to discriminate in both the forward and reverse current direction), a fast communication network and a logic diagrams for obtaining the right characteristics of a properly functional protection scheme. During the development of this research it was concluded that in the current strategy applied by the distribution system operators protection scheme 1 will be more practical compared to version 2. This because protection scheme version 2 will have a severe loss of selectivity which is extremely undesirable in the outage time averaged over one year.

To research the proposed protection schemes two case study were created. The first case study was a simplified representation of a distribution system and the second case study was related to the distribution system found on the island of Goeree-Overflakkee. Both the proposed schemes were tested were it was concluded that in protection scheme version 2 indeed the distribution generation units inside the distribution system were still in operation after the occurrence of a fault due the the fast isolation of the faulty zone. As a consequence a severe loss in selectivity was obtained. To increase the selectivity the protection relays inside the faulty zone need also to be taken into consideration of the protection scheme version 2 which will result in much more complexity. In the simulations it is shown that protection scheme version 1 will have the longest duration in voltage dips when the fault is initiated near the main station, but high selectivity will be maintained. This is mainly because a faulty zone will first change from a meshed to a radial topology. After this step the already applied protection scheme with the commonly found time-grading strategy (found in most of the distribution systems) will provide the correct protective coordination. Some settings of the already applied relays where altered by introducing additional time-grading steps and increasing the pick-up current to achieve the

right characteristics. In the second case-study it was shown that the critical clearing time for a limited amount of feeders was shortened below the 1 second barrier due to the change in topology from radially to meshed. When a fault is initiated inside these feeders the fault must be isolated by the proposed protection scheme faster than the calculated critical clearing time.

A drawback of both protection schemes is the application of a communication infrastructure to provide the appropriate protective coordination. In the present distribution system this will result in high investment costs because most of the substation are not provided with a communication infrastructure. Another disadvantage of the proposed protection schemes is that they both rely on the current magnitude to determine if a fault is initiated inside the distribution system. The current magnitude of the external grid will be much higher than the current magnitude experienced by the direction relays when a fault is located near the main station inside the main feeder of the faulty zone. This will create protection blinding which will result that first the relay protecting the main feeder will trip before the relays between the interconnection, still in this situation selectivity is maintained. A solution inside the logic diagram is provided to overcome this issue when it is desirable to first let the relays trip between the interconnections before the relay protecting the main feeder.

6.2. Recommendation for future work

In this research a proposal is given for meshed operated distribution systems inside a Smart Grid with the corresponding key advantages and drawbacks. The author gives the following recommendations for future work towards this research subject:

- include an automatic self healing function inside the relay model;
- include the proposed back-up system inside the logic diagram of the protection scheme;
- enhance the logic diagram for the protection scheme to detect faults initiated near the main station;
- the desired communication infrastructure needed for this proposed protection scheme to operate;
- the correct polarization technique inside the relay model for the earth-fault detection inside grounded distribution systems. This is true for interconnection R62 in case study 2;
- how this scheme can be realised with the station automation products found in today's industry;
- how the IEC61850 can be further utilized for the proposed protection schemes.

Bibliography

[1] Centraal bureau van statestieken, *Energiebalans; aanbod, omzetting en verbruik 2012-2013* (Centraal bureau van statestieken, 2015).

[2] European Technology Platform, *European SmartGrid Technology Platform, Vision and Strategy for Europe's Electricity Networks of the Future* (European Technology Platform, 2006).

[3] NEN, *NEN-EN-IEC 61850-5* (Communcation networks ans systems for power utility automation part 5, 2013).

[4] Rijksoverheid, *Nationaal actieplan voor energie uit hernieuwbare bronnen* (Richtlijn 2009/28/EG, 2009).

[5] Netbeheer Nederland, *Decentrale Duurzame Collectieven, van realisatie naar de toekomst* (Netbeheer Nederland, 2009).

[6] H+N+S Landschapsarchitecten, *Goeree-Overflakkee, duurzame energie in het landschap* (H+N+S Landschapsarchitecten, 2009).

[7] Schavemaker, P. and L van der Sluis, *Electrical Power System Essentials* (John Wiley and Sons, 2009).

[8] Autoriteit consumenten markt, *Netcode elektriciteit* (ACM, 2014).

[9] Netbeheer Nederland, *Betrouwbaarheid van elektriciteitsnetten in Nederland* (Netbeheer Nederland, 2013).

[10] European Technology Platform, *European SmartGrid Technology Platform, SmartGrids, Strategic Deployment Document for Europe's Electricity Network of the Future* (European Technology Platform, 2008).

[11] J. Tongeren P. Kadurek S.F.G. Cobben and W.L. Kling, *Operational data measurements in intelligent medium voltage networks* (Cired Workshop - Lisbon 29-30, 2012).

[12] J.I. Melnik F. Provoost and W. Bos, *"Intelligent distribution substation improves power quality* (Cired Frankfurt, 6-9, 2011).

[13] P. Kadurek J.F.G. Cobben and W.L. Kling, *Future LV distribution network design and current practices in the Netherlands* (IEEE, 2011).

[14] Dr. M. Popov, *Lecture Notes: Power System Grounding and Protection* (TU Delft, 2014).

[15] J.J. Grainger and W.D. Stevensorn, JR., *Power system analysis* (McGraw-Hill International Editions, 1994).

[16] Alstom, *Network protection and automation guide, protective relays, measurement and control* (Alstom, 2011).

[17] Phase to Phase, *Netten voor distributie van elektriciteit* (Phase to Phase, 2012).

[18] G. Ziegler, *Numerical differential protection, principles and applications* (Siemens, 2005).

[19] K. Kauhaniemi L. Kumpulainen, *Impact of distribution generation on the protection of distribution networks* (IEE, Michael Faraday House, Six Hills Way, 2004).

[20] R. V. R. de Carvalho F. H. T. Vieira S.G. de Araujo e C. R. Lima, *A Protection Coordination Scheme for Smart Grid Based Distribution Systems Using Wavelet Based Fault Location and Communication Support* (IEEE, 2013).

[21] S Voima H Laaksonen K Kauhaniemi, *Adaptive Protection Scheme for Smart Grids* (IEEE, 2014).

[22] Sukumar M. Brahma and Adly A. Girgis, *Development of Adaptive Protection Scheme for Distribution Systems With High Penetration of Distributed Generation* (IEEE, 2004).

[23] Gemeente Goeree-Overflakkee, *Overall information about Goeree-Overflakkee* (Website Gemeente Goeree-Overflakkee, www.goeree-overflakkee.nl, 2015).

[24] J.G. Slootweg, *Wind Power, Modelling and Impact on Power System Dynamics* (J.G. Slootweg, 2003).

[25] Lab-Volt, *Principles of doubly-fred induction generators* (Lab-Volt Ltd. Canada, 2011).

[26] H.A. Pulgar-Painemal and P. W. Sauer, *Doubly-fed induction machine in wind power generation* (University of Illinois at Urbana-Champaign, 0000).

[27] P. Krause O. Wasynczuk S. Sudhoff and S. Peparek, *Electric Machines and Drive Systems* (IEEE Presss, Wiley, 2013).

[28] J. Machowsk J.W. Bialek and J.R. Bumby, *Power System Dyanamics: Stability and Control* (Second Edition, John Wiley and Sons, 2008).

[29] GmbH Digsilent Germany, *Technical Reference Papers* (DIgSILENT Technical Documentation, 2014).

[30] P. Ledesma and J. Usaola, *Effect of Neglecting Stator Transients in Doubly Fed Induction Generators Models* (IEEE transactions on energy conversion, vol. 19, 2004).

Abbreviations and symbols

AMT:	Angle of Maximum Torque
CHP:	Combined Heat Power
CB:	Circuit Breaker
CT:	Current Transformer
DFIG:	Doubly Fed Induction Generator
DG:	Decentralised Generation
EMT:	Electromagnetic Transients
GOOSE:	Generic Object-Oriented Substation Event
DNO:	Distribution Network Operator
DSO:	Distribution System Operator
ETP:	European Technology Platform
HVDC:	High Voltage Direct Current
ICT:	Information and Communication Technology
IDS:	Intelligent Distribution Sub-stations
IEC:	International Electrotechnical Commission
IED:	Intelligent Electronic Device
LOM:	Loss of Main
MTA:	Maximum Torque Angle
MV:	Medium Voltage
POC:	Point Of Connection
RES:	Renewable Energy Sources
RMS:	Root Mean Square
SCADA:	Supervisory Control And Data Acquisition
SAS:	Substation Automation Systems
TMS:	Time Multiplier Setting
TSO:	Transport System Operator
VT:	Voltage Transformer

k, α:	Constants defining the applied curve
ω:	2πf
f:	Frequency
i:	Instantaneous Current
I:	RMS Current
I>:	Overcurrent stage
I»:	Instantaneous overcurrent stage
I_s:	Overcurrent setting
I_f"/I_k":	Subtransient short-circuit current magnitude
L:	Inductance
R:	Resistance
E_{max}:	U_{line}
X:	Reactance
U,V:	Voltage
U':	Polarization voltage
Z:	Impendance
S:	Apparent power
t>:	Overcurrent stage operating time
t»:	Instantaneous stage operating time

A

Wind turbine

Wind turbines are utilized to convert energy provided by the wind to electric energy. This conversion has two stages where the wind energy is mechanical converted with the help of the rotation of the blades. These blades produce a lift force integrated along the length of the blades. These blades, connected to a shaft, drive an induction machine through a gear box. This gear box steps up the rotational speed of the shaft around 1500rpm. After this stage, the mechanical energy is converted into electrical energy with an induction machine. This induction machine is attached to the grid with the help of a step-up transformer, which steps up the voltage from 690V to the connected voltage of the grid. There are many technologies regarding generator units for converting wind energy into electrical energy. This chapter will only explain the doubly fed induction generator technology which is mostly found in the present distribution systems.

A.1. Wind power

The maximum power that can be extracted from the wind with the help of a wind turbine is determined by the thermodynamic equation of the mass flow rate, see equation A.1. The mass flow rate ($\dot{m}$) is equal to the mass of a fluid (gas or liquid) flowing per unit of time. The fluids density, volume and shape can change within the domain with time, where the mass of the fluid will stay unchanged through this domain. In the case of a wind turbine this fluid is equal to the amount of air with a certain density passing through the blades of the wind turbine. During this process the same amount of mass leaves and enters the blades of the wind turbine, where no mass is destroyed during this process.

$$\dot{m} = \rho \dot{V} = \rho \mathbf{v} \cdot \mathbf{A} \tag{A.1}$$

- $\dot{m}$ = Mass flow rate,
- $\dot{V}$ = Volume flow rate,
- ρ = Mass density of the fluid,
- $\mathbf{v}$ = Flow velocity of the mass elements,
- $\mathbf{A}$ = cross-sectional vector area/surface.

Equation A.2 determines the average wind speed (v_{avg}) before (v_1) and after (v_2) the rotor blades. This equation can be substituted into equation A.1 to get equation A.3:

$$v_{avg} = \frac{1}{2}(v_1 + v_2) \tag{A.2}$$

$$\dot{m} = \rho \cdot v_{avg} \cdot A = \frac{1}{2}\rho A(v_1 + v_2) \tag{A.3}$$

Wind is developed by air that is moving from a high pressure area towards a low pressure area. This movement of air creates kinetic energy, due to the mass density of air (ρ) that the wind turbine can use to convert wind energy into electric energy. The equation for kinetic energy has to be applied to determine the energy that is subtracted from the wind by the rotor blades. The standard equation for kinetic energy is given by:

$$E = \frac{1}{2}mv^2 \tag{A.4}$$

The difference between the speed before and after the rotor blades is the amount of kinetic energy extracted from the wind to make the rotor blades spin. The speed of the wind after the blades is subtracted from the wind speed before the blades, because the wind speed before the blades is faster than the wind speed after the blades, due to the subtracted energy. The average wind speed is calculated as follows:

$$E = \frac{1}{2}m(v_1^2 - v_2^2) \tag{A.5}$$

The following equation is found by taking the derivative of both sides from equation A.5 and substitution of equation A.3. The result shows the amount of work extracted from the system. This system is equal to the rotor blades of the wind turbine. In thermodynamic work ($\dot{E}$) is defined as the energy transferred by the system to another that is accounted for by changes in the generalized external mechanical constraints on the systems. This is equivalent to the amount of mechanical work in physics.

$$\dot{E} = \frac{1}{2}\dot{m}(v_1^2 - v_2^2) = \frac{1}{4}\rho A(v_1 + v_2)(v_1^2 - v_2^2) \tag{A.6}$$

Equation A.6 can be rewritten in a simplified form for computational reasons. This form makes it easy to apply an answer for the theoretical maximum performance coefficient.

$$\dot{E} = \frac{1}{4}\rho A v_1^3 \left(1 - \left(\frac{v_2}{v_1}\right)^2 + \left(\frac{v_2}{v_1}\right) - \left(\frac{v_2}{v_1}\right)^3\right) \tag{A.7}$$

The theoretical maximum performance coefficient for a system can be calculated by differentiating $\dot{E}$ with respect to $\frac{v_2}{v_1}$, for a given fluid speed v_1 of the wind, swept area S of the rotor blades and mass density ρ of the air.

$$\frac{d\dot{E}}{d\left(\frac{v_2}{v_1}\right)} = \frac{1}{4}\rho A v_1^3 \left(1 - 2\left(\frac{v_2}{v_1}\right) - 3\left(\frac{v_2}{v_1}\right)^2\right) \tag{A.8}$$

The derivative of equation A.8 is set equal to zero to determine the maximum value for the ratio between v_1 and v_2. The result is the equation A.9, which can be easily computed and solved with the help of the abc-formula.

$$0 = 1 - 2\left(\frac{v_2}{v_1}\right) - 3\left(\frac{v_2}{v_1}\right)^2 \tag{A.9}$$

The highest ratio between v_1 and v_2 for achieving the theoretical maximum power coefficient out of the wind is equal to the following value:

$$\frac{v_2}{v_1} = \frac{-2 \pm \sqrt{(-2)^2 - (4 \cdot 1 \cdot (-3))}}{2 \cdot 1} = \frac{1}{3} \tag{A.10}$$

The theoretical maximum performance coefficient factor can be calculated with the answer of equation A.10. This answer must be substituted inside equation A.8. The resulting and final equation is equal to:

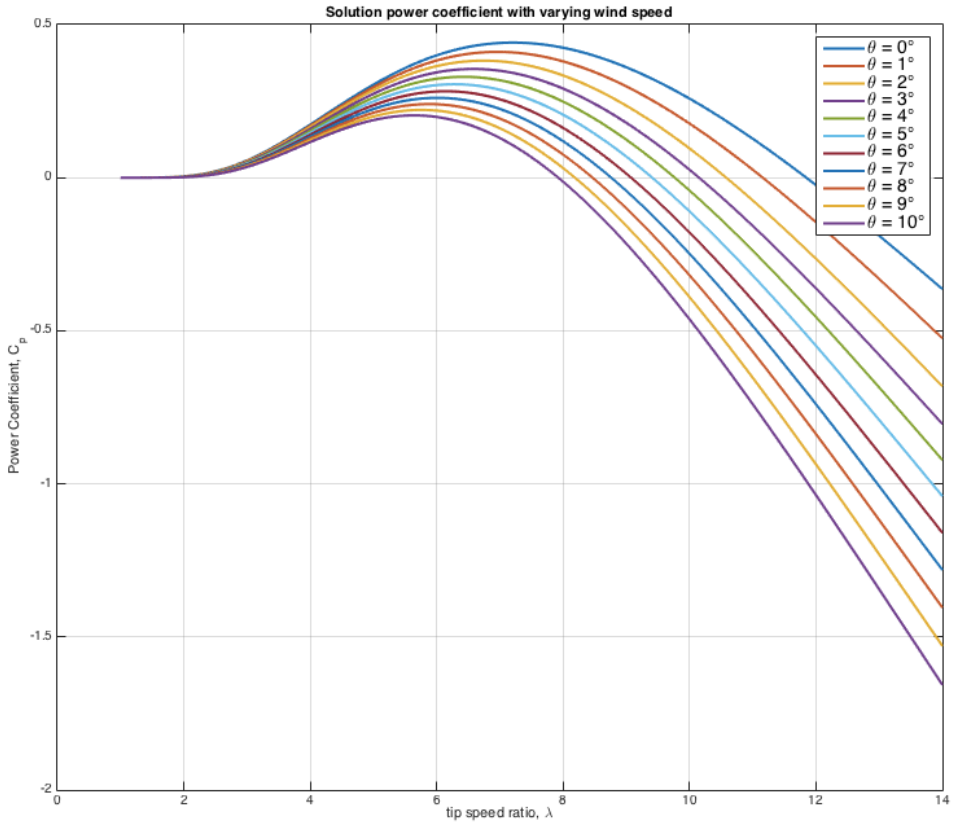

Figure A.1: Performance coefficient as function of tip speed ratio, with varying pitch angle

$$P_{max} = \frac{16}{27} \cdot \frac{1}{2} \cdot \rho \cdot A \cdot v_1^3 = \frac{1}{2} \cdot C_p \cdot \rho \cdot \pi \cdot r^2 \cdot v_1^3 \tag{A.11}$$

- C_p = theoretical maximum power coefficient: 0.5926,
- ρ = air density: 1.2041 kg/m3 at temperature of 25 ◦ C
- r = length of the rotor blades: in m,
- v = wind speed, in m/s.

The ratio $\frac{16}{27}$, better know as C_p or theoretical maximum performance coefficient, is the maximum theoretical efficiency (Betz limit) a wind turbine can achieve. The current types of wind turbines are able to realize a high percentage of this theoretical maximum performance, where this percentage is a function of the applied techniques (stall and pitch control) inside a wind turbine.

A.1.1. Performance coefficient

From the previous section, it is clear that the theoretical maximum performance coefficient (C_p) a wind turbine can achieve is equal to 0.5926. In practice, modern wind turbines are not able to get the same value for C_p as the theoretical maximum performance coefficient. The maximum power a wind turbine can subtract from the wind is a function of the applied techiques inside the wind turbine, see equation A.12. These techniques are a varying tip speed ratio(λ) and a changing pitch angle (θ) of attack for the rotor blades.

$$P_{tur} = \frac{1}{2} \cdot C_p(\lambda, \theta) \cdot \rho \cdot \pi \cdot r^2 \cdot v_1^3 \tag{A.12}$$

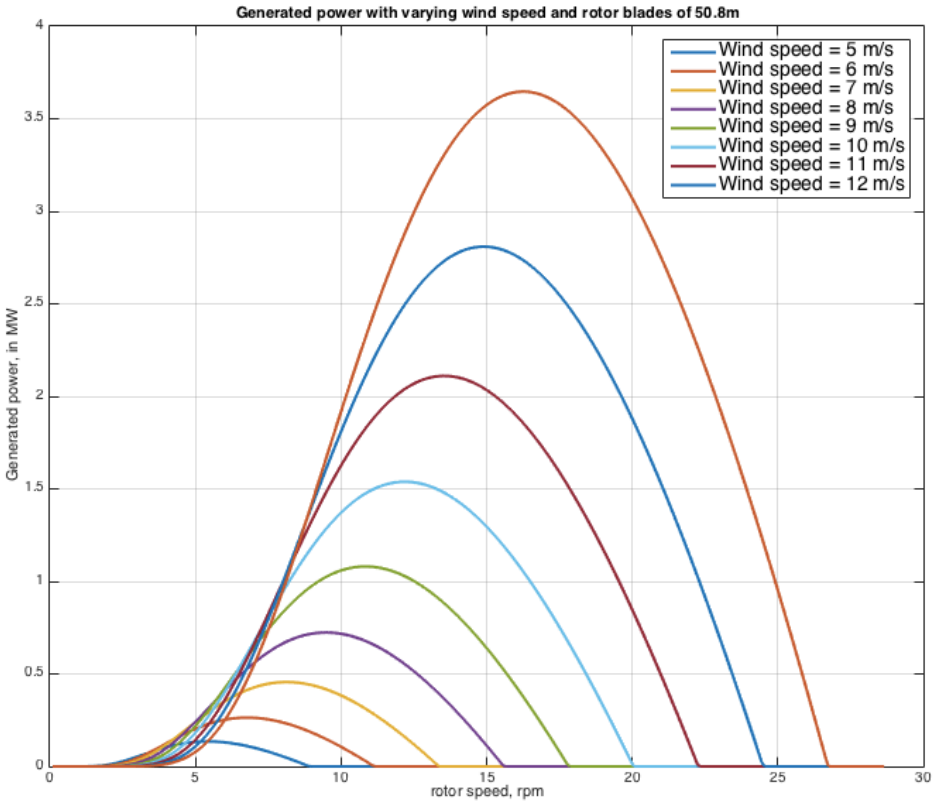

Figure A.2: Generated energy with varying wind speeds

The following equation is an approximation for determining $C_p(\lambda,\theta)$ and is better known as the simplified aerodynamic model of a wind turbine [24]. Equation A.13 is only applicable for variable wind speed turbines (DFIG and direct drive wind turbines) because of their variable pitch angle and tip speed ratio.

$$C_p(\lambda,\theta) = 0.73\left(\frac{151}{\lambda_i} - 0.58\cdot\theta - 0.004\cdot\theta^{2.14} - 13.2\right)e^{-\left(\frac{18.4}{\lambda_i}\right)} \tag{A.13}$$

Where λ_i is a function of the tip speed ratio (λ) and the pitch angle (θ) of the rotor blades. λ is determined by the tip speed of the blades (angular speed (ω) multiplied with the radius of the rotor blades (r)) and the actual wind speed (v) given in m/s, see equation A.14 and A.15.

$$\lambda_i = \frac{1}{\frac{1}{\lambda-0.02\cdot\theta} + \frac{0.003}{\theta^3+1}} \tag{A.14}$$

$$\lambda = \frac{\omega r}{v} \tag{A.15}$$

Figure A.1 shows the performance coefficient as function of the tip speed ratio, with a varying pitch angle (from 0° to 10°). An important observation from this figure is that the maximum achievable C_p decays with an increasing pitch angle (θ). The pitch angle can be utilized for decreasing or increasing the produced active power to improve power system stability. This pitch angle also can be used during very high wind speeds. This pitch angle will decrease the amount of energy extracted from the wind.

The maximum energy a turbine can extract from the wind is dependent on wind speed, and the length of the rotor blades. From figure A.2 it can be seen that the ideal radial frequency for the rotor blades to produce the maximum power increases with increasing wind speed. A maximum power tracking system is implemented to monitor the wind speed and active power to produce a signal for the speed controller. This speed controller controls the rotational speed of the rotor blades.

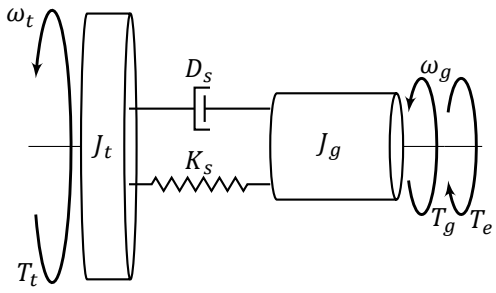

Figure A.3: Two mass mechanical system of a shaft

A.1.2. Shaft

Power can be obtained from the wind, due to the application of a wind turbine. The amount of energy a turbine can extract from the wind is a function of speed and pitch angle and is given by the aerodynamic equation A.12. This turbine is indirectly connected to the generator with the help of a shaft which transforms the power from the turbine to the generator. This mechanical system has to be modeled for stability analysis which must be at least a two-mass model, where one mass represents the turbine inertia (J_t) and the other mass represents the generator inertia (J_g), see figure A.3. The two masses are connected to the same shaft, where this shaft can be represented by the corresponding stiffness (K_s) and damping (D_s) factor. The inertia constants of the gear-box and the shaft are very small in comparison with the other inertia constants, and thereby are usually neglected in the equation of the shaft. The speed of the shaft is normalized with the base radial frequency (ω_0) and multiplied with the difference between the turbine speed (ω_t) and the generator speed (ω_g).

$$\frac{d\theta_s}{dt} = \omega_0(\omega_t - \omega_g) \tag{A.16}$$

$$J_t \frac{d\omega_t}{dt} = T_t - K_s\theta_s - D_s(\omega_t - \omega_g) \tag{A.17}$$

$$J_g \frac{d\omega_g}{dt} = K_s\theta_s + D_s(\omega_t - \omega_g) - T_e \tag{A.18}$$

It is also possible to neglect the stiffness and damping factors of the shaft by applying a one mass system. A one-mass system combines the inertia of the turbine and generator in one big inertia constant (J_m).

$$J_m \frac{d\omega_m}{dt} = T_m - T_e \tag{A.19}$$

A.1.3. DFIG wind turbine

A DFIG wind turbine is one of the two variable wind speed turbines. A variable wind speed turbine applies two types of controllers during normal operational mode. The first controller is a pitch angle controller that controls the pitch angle of the rotor blades corresponding with the current rotor speed. The speed of the rotor will accelerate during a fault inside the connected network, due to the loss of load. This acceleration is controlled by applying a different pitch angle to the rotor blades. The second controller controls the active and reactive power generated by the wind turbine. The setpoint for the active power is determined by the rotor speed, and the setpoint for the generated reactive power is determined by the voltage on the terminals of the wind turbine.

A DFIG wind turbine supplies an induction generator with a wound rotor, better known as a doubly-fed induction generator (DFIG), see figure A.4. A back-to-back PWM (pulse width modulation) converter (usually 30% of the rated power of the generator) is placed between the rotor and the grid for providing an electrical rotor frequency. This converter decouples the mechanical an electrical rotor frequency. The stator frequency of a DFIG is equal to the frequency of the connected network, which doesn't change despite changes in the torque that the rotor is subjected to fluctuating wind speeds. The frequency that the back-to-back converter provides to the rotor has to change constantly to maintain a

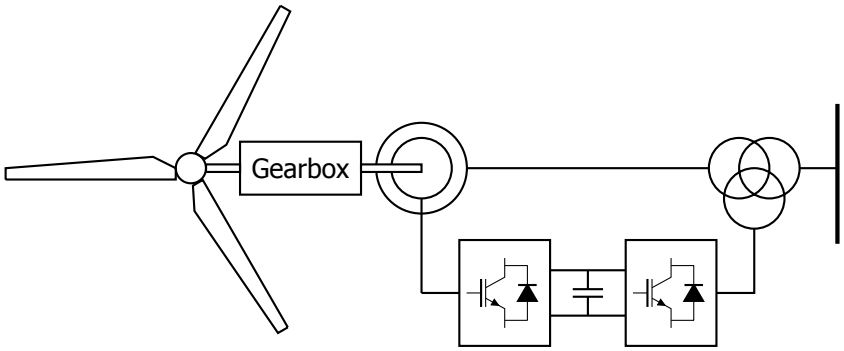

Figure A.4: DFIG wind turbine

constant frequency during these fluctuations in torque. The frequency of the rotor should be consistent with the following equation [25]:

$$f_s = \frac{N_r \cdot p}{120} + f_r \tag{A.20}$$

- N_r: rotational speed of the rotor in rpm,
- p: number of poles,
- f_s: frequency of the stator, equal to the frequency of the connected network
- f_r: frequency provided to the rotor by the back-to-back converter

The polarity of f_s determines the rotation direction for the voltage applied to the rotor windings. The voltage produced by the stator windings needs to be equal to the voltage of the connected network. This voltage is adjusted accordingly by maintaining a constant magnetic flux value for the stator windings. This constant voltage is achieved by applying a voltage to the rotor windings which is proportional to the frequency of the voltages applied to the rotor windings. This principle allows the stator and rotor frequency to be matched, independent of the mechanical rotor speed. A significant advantage of a DFIG is the control of the power factor for a large range of speed. The slip varies between 40% at sub-synchronous speed (rotor speed under synchronous speed) and -30% at super-synchronous speed (rotor speed over synchronous speed) [26].

The main difference between a doubly fed induction machine and a squirrel cage induction machine is that the rotor windings are not short circuited. These windings are attached to a back-to-back converter which controls the frequency and amplitude of the current applied to these windings. This means that the rotor voltage is not equal to zero, like in a usual squirrel cage induction machine. The stator equations for a DFIG are as follows [27]-[28]:

$$e_{ds} = \dot{\psi_{ds}} - \omega_s \psi_{qs} - R_s i_{ds} \tag{A.21a}$$
$$e_{qs} = \dot{\psi_{qs}} + \omega_s \psi_{ds} - R_s i_{qs} \tag{A.21b}$$

With the flux linkages for the stator equal to:

$$\psi_{ds} = -(L_s + L_m) i_{ds} - L_m i_{dr} \tag{A.22a}$$
$$\psi_{qs} = -(L_s + L_m) i_{qs} - L_m i_{qr} \tag{A.22b}$$

The voltages for the rotor are given as follows:

$$e_{dr} = \dot{\psi_{dr}} - s\omega_s \psi_{qr} - R_r i_{dr} \tag{A.23a}$$
$$e_{qr} = \dot{\psi_{qr}} + s\omega_s \psi_{dr} - R_r i_{qr} \tag{A.23b}$$

The variable s is defined as the slip between the rotating rotor and the rotating magnetic field of the stator.

$$s = \frac{\omega_s - \omega_m}{\omega_s} \tag{A.24}$$

With the flux linkages for the rotor equal to:

$$\psi_{dr} = -(L_r + L_m)i_{dr} - L_m i_{ds} \tag{A.25a}$$
$$\psi_{qr} = -(L_r + L_m)i_{qr} - L_m i_{ds} \tag{A.25b}$$

The generated active power and the generated/consumed reactive power of this type of induction machine is now not only a function of the stator voltage but also a function of the rotor voltage, due to the back-to-back converter provided between the rotor and the grid. These equations are given by:

$$P = e_{ds}i_{ds} + e_{qs}i_{qs} + e_{dr}i_{dr} + e_{qr}i_{qr} \tag{A.26a}$$
$$Q = e_{qs}i_{ds} - e_{ds}i_{qs} + e_{qr}i_{dr} - e_{dr}i_{qr} \tag{A.26b}$$

It has to be noted that the stator transients during simulations are neglected. This is common practice during dynamic power system modelling, and is also done when a synchronous machine is simulated [24].

B

Model for Digsilent PowerFactory

During this research the software package DIgSilent PowerFactory, further referred to as PowerFactory, will be used to model the applied DG units and the distribution system. This software package is widely used in the industry for modelling of generation units, transmission-, distribution- and industrial system. This software package is capable of computing a lot of different calculation like voltage stability, load flow, small signal stability etc. Further more this software package is able to calculate electromagnetic and electromechanical transients in the time domain, by applying a RMS-simulation or a EMT-simulation respectively, where these simulations apply different assumptions towards the applied models. This function can be compared with Matlab Simulink which also is able to compute calculation in the time domain.

B.1. Models

One of the big advantages of PowerFactory is the use of dynamic simulation function in the time domain during different events inside the distribution system which is being studied. PowerFactory applies a hierarchical system modelling approach for applying the models in the time domain. This hierarchical system model make use of the following building blocks:

- DSL block definitions: These blocks are created with the DIgSilent Simulation Language (DSL) and are the basic building blocks which can represent a transfer function, a differential equation or another type of equation.
- Common model: This model combines block definitions with a specific set of parameters values which can be altered by the user. This common model can be for example a set of several interconnected DSL block definitions to form a model of a IEEE defined excitation system or a shaft model. Each of these common models have their own inputs and outputs which will be used to interconnect other common models with each other to form a total model of a system.
- Composite model: This model applies a composite frame to interconnect the inputs and outputs of the created common models. Such a composite frame can represent a total mechanical and electrical system of a wind turbine, solar farm or a CHP unit. See figure B.1 for a composite frame model of a DFIG wind turbine

The composite model is running in the background of the single-line diagram during dynamic simulations. During this simulation the inputs and outputs of the common models inside the composite frame can be presented with the help of a virtual instrument page. For a load flow calculation different models are applied where the induction machine model is usually simplified for fast computation. The software package PowerFactory provides the user with already build-in models of a DFIG and direct drive wind turbine, solar farm and frequency controlled battery package which will be modified and used during this research.

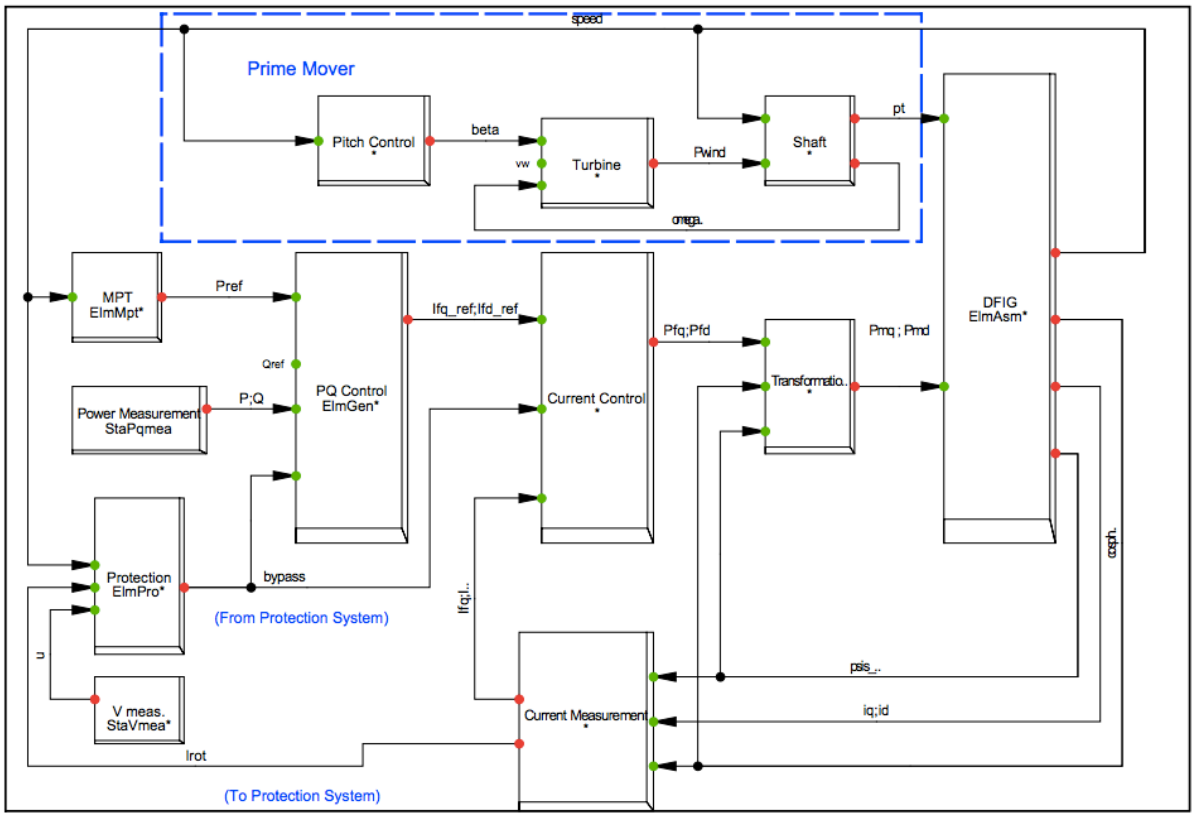

Figure B.1: Composite frame of a DFIG wind turbine

B.2. RMS vs. EMT simulation

A induction machine can be represented via a set of differential equations, which corresponds to the mathematical model of the induction machine. For example, a asynchronous induction machine with a wound rotor (DFIG wind turbine) can be represented by a set of five fist order differential equation, better known as a 5th order model. This 5th order model is defined by the following set of differential equations:

$$\frac{d\psi_{ds}}{dt} = e_{ds} + \omega_s \psi_{qs} + R_s i_{ds} \tag{B.1a}$$

$$\frac{d\psi_{qs}}{dt} = e_{qs} - \omega_s \psi_{ds} + R_s i_{qs} \tag{B.1b}$$

$$\frac{d\psi_{dr}}{dt} = e_{dr} + s\omega_s \psi_{qr} + R_r i_{dr} \tag{B.1c}$$

$$\frac{d\psi_{qr}}{dt} = e_{qr} - s\omega_s \psi_{dr} + R_r i_{qr} \tag{B.1d}$$

$$\frac{d\omega_m}{dt} = \frac{T_m - T_e}{J_m} \tag{B.1e}$$

The asynchronous induction machine is represented by the 5 state variables on the left side of the equations given in B.1 (ψ_{ds}, ψ_{qs}, ψ_{dr}, ψ_{qr}, ω_m). The EMT-simulation (electromagnetic transients simulation) computes the full order model of each induction machine in the power system that is being studied. The EMT-simulation takes a longer time to compute compared with the RMS-simulation (root mean square simulation), because of the use of the full order model of each applied induction machine. This is not a problem for a small system, but can be a issue when an power system is being studied with multiple induction machines, and moreover when the events in the power system are occurring over a long period of time (larger than 10 seconds). Not only the stator transients are considered

during an EMT-simulation but also the transient behaviour of transformers and lines will be considered, the models applied for this components can be examined in [29].

The RMS-simulation in PowerFactory neglects the stator transients (ψ_{ds} and ψ_{qs}) during simulations in the time domain, and is because of this able to compute the solution in a fast time period. These stator transients are usually present for a very short time period which is not of interest during transients stability studies, and that is why it is common practice to neglect these transients during system studies. In [30] the effect of neglecting the stator transients of a DFIG wind turbine are studied and concludes that the results are very similar from transient stability point of view and furthermore that the rotor speeds are close to identical during transients. By neglecting the stator transients the 5th order model of the DFIG given in equation B.1 is reduced to a 3th order model.

B.3. Evenst

PowerFactory is able to introduce events inside the power system that is being studied, during the simulations in the time domain for both the RMS- and EMT-simulation. Events inside the power system can be for example an: (un)symmetrical fault, variation in load, operation of a switch, parameter change, tap change, power plan shut down and an synchronous machine event. These are one of the many events that can be applied inside the model during simulations in the time domain. This research will mainly apply (un)symmetrical fault events to show the behavior of the DG units during these fault events and how they interact with the protection scheme.

This research will look at the dynamic behavior and protection of medium voltage networks, where software tools are employed for providing the correct calculations. These software tools make use of dynamic models of the electrical components for providing the answer to the magnitude of the voltage, current, active and reactive power and power angles of the machines and voltages during steady-state and transient behavior. The main research question of this thesis will be answered by providing a case-study of a distribution network with several types of DGs. Each of these DGs makes use of different models.

C

MatLab scripts

C.1. Short circuit transient

```
close all
clear all

%% Initial values

U_line      = 13; %% in kV
Sk_grid     = 300;n %% in MVA
RX_grid     = 0.341; %% R/X factor grid
Z_grid_abs  = (U_line^2)/Sk_grid; %% Calculate Z component external grid
R           = Z_grid_abs/sqrt(1+(1/RX_grid)^2); %% Calculate R component
    external grid
X           = Z_grid_abs/sqrt(1+RX_grid^2); %% Calculate X component
    external grid
alfa        = 0; %% alfa 0 and pi*2 amplitude max
t           = 0: 1/100000: 0.1; %% time from 0 to 0.2sec

%% Calculations
L = X/(2*pi*50); %% inductance
U_rms = U_line/sqrt(3); %% U_line ---> U_rms
U_top = U_rms*sqrt(2); %% U_rms  ---> U_top
Z = sqrt(R^2 + (2*pi*50*L)^2); %% equivalent impedance

Itop = U_line/(sqrt(3)*Z); %% top short circuit current steady state
Ith  = 2*sqrt(2)*(Itop/sqrt(2)); %% I stoot

theta = atan((2*pi*50*L)/(R)); %% Theta calculation
idc  = exp(-t*(R/L))*(-Itop * sin (alfa - theta)); %% DC  component
isin = Itop * sin ( 2*pi*50*t + alfa - theta); %% SIN component

i = idc + isin; %% Short-circuit current contribution

idctop    = idc - Itop; %% hulplijn 1
idcbottom = idc + Itop; %% hulplijn 2

%% Plot

fig1 = figure (1);
set(fig1,'position', [200, 200, 1000, 500]);
```

```
37
38 set(gcf, 'Color', [1,1,1]);
39 h = plot(t,i,t,idc,t,idctop,'--',t,idcbottom,'--');
40 set(h,'linewidth',2);
41
42 grid minor;
43 title('Short-circuit current RL series circuit');
44
45 h_legend = legend('Solution','DC-component');
46 set(h_legend,'FontSize',12);
47
48 xlabel('time (s)');
49 ylabel('current (kA)');
50 set(gca,'xtick',[0:1/100:3])
51 set(gca,'ytick',[-20:5:40])
```

C.2. False Tripping

```
close all
clear all

%                BUS
%   ______        | R1              |
%  |\ \ \ |       |-X---cable1------|dg-unit
%  | \ \ \|       |                 |
%  |\grid |-------|
%  | \ \ \|       | R2              |
%  |\_\_\_|       |-X---cable2------|short-circuit
%                 |                 |
%

step = 0.001; %% per km

%% Max short-circuit contribution of the grid
U_line      = 13; %% in kV
Sk_grid     = 320; %% in MVA
RX_grid     = 0.35; %% R/X factor grid
Z_grid_abs  = (U_line^2)/Sk_grid; %% Calculate Z component external grid
R_grid      = Z_grid_abs/sqrt(1+(1/RX_grid)^2); %% Calculate R component
    external grid
X_grid      = Z_grid_abs/sqrt(1+RX_grid^2); %% Calculate X component
    external grid
Z_grid      = complex(R_grid,X_grid)

%% Fault location impedance
R_fault = 0.0;
X_fault = 0.0;
Z_fault = complex(R_fault,X_fault);

%% How many parallel DG units and information about DG unit!!!
DG_units    = 7; %% Parallel DG units
MVA_DG      = 2.7*1000000; %% Power DG in MVA
U_DG        = 13*1000; %% Voltage DG in kV
I_DG_nom    = (DG_units*MVA_DG)/(sqrt(3)*U_DG);

X_DG        = 0.168; %% Subtransient reactance per DG in p.u
R_DG        = 0.0504; %% Stator resistance per DG in p.u

Xd_DG       = X_DG*(U_DG^2)/MVA_DG;
rg_DG       = R_DG *(U_DG^2)/MVA_DG;
Z_DG        = complex(rg_DG,Xd_DG);

%% Information about the cable/line, neglecting the capacitance

length_cable1 = 2; %% in km  3*1*150 AL XLPE 12/20 trefoil
I_nom_type_cable1 = 290; %% Nominal current of one feeder
Parallel_cable1 = ceil(I_DG_nom/I_nom_type_cable1); %% How man cable
    parallel, standard 1
R_cable1 = 0.205/Parallel_cable1; %% R cable in ohm/km
X_cable1 = 0.125/Parallel_cable1; %% X cable in ohm/km

length_cable2 = 4; %% in km  3*1*150 AL XLPE 12/20 trefoil
```

```
52 Parallel_cable2 = 1; %% How man cable parallel, standard 1
53 R_cable2 = 0.205/Parallel_cable2; %% R cable in ohm/km
54 X_cable2 = 0.125/Parallel_cable2; %% X cable in ohm/km
55 PickupCurrentRelay = 3000;
56
57 %% The calculation for calculating short-circuit contribution with NO DG
58 for i = 1 : (length_cable2*1000)
59
60 j = 1;
61 cable2(i,j) = step*i; %% each step + 10m
62
63 % Total impedance seen by fault
64 X_cable2_tot = X_cable2*cable2(i,j);
65 R_cable2_tot = R_cable2*cable2(i,j);
66 Z_cable2_tot = complex(R_cable2_tot,X_cable2_tot);
67 Z_faultlocation(i,j) = Z_grid + Z_cable2_tot + Z_fault;
68
69 % Calculate 3phase short-circuit current, no correctionfactor (Storing
       Sequentieel in Vision)
70 Z_th(i,j) = abs(Z_faultlocation(i,j));
71 I_f(i,j)  = (U_line)/(sqrt(3)*Z_th(i,j));
72
73 % Index the calculated variables
74 I_grid(i,j) = I_f(i,j);
75 I_tot(i,j)  = I_f(i,j);
76
77 end
78
79 %% The calculation for calculating short-circuit contribution with DG
80 for j = 2 : DG_units+1
81
82 DG_parallel = -1 + j;
83
84 Z_DG_tot = Z_DG/DG_parallel;
85
86 % Calculate impedance of cable 1
87 X_cable1_tot = X_cable1*length_cable1;
88 R_cable1_tot = R_cable1*length_cable1;
89 Z_cable1_tot = complex(R_cable1_tot,X_cable1_tot);
90
91 for i = 1 : (length_cable2*1000)
92
93 cable2(i,j) = step*i; %% each step + 10m
94
95 % Calculate impedance of cable 2
96 X_cable2_tot = X_cable2*cable2(i,j);
97 R_cable2_tot = R_cable2*cable2(i,j);
98 Z_cable2_tot = complex(R_cable2_tot,X_cable2_tot);
99
100 % Calculate equivalent impedance
101 Z_faultlocation(i,j) = (((Z_cable1_tot + Z_DG_tot)*Z_grid)/(Z_cable1_tot +
       Z_DG_tot + Z_grid)) + Z_cable2_tot + Z_fault;
102
103 % Calculate 3phase short-circuit current, no correctionfactor (Storing
       Sequentieel in Vision)
104 Z_th(i,j) = abs(Z_faultlocation(i,j));
```

```
105
106 % Calculate 3phase short-circuit current, no correctionfactor (Storing
        Sequentieel in Vision)
107 I_f(i,j)  = (U_line)/(sqrt(3)*Z_th(i,j));
108
109 % Calculate the short-circuit contribution of DG and the Grid
110 I_grid(i,j)   = I_f(i,j)*abs(((Z_cable1_tot + Z_DG_tot)/(Z_cable1_tot +
        Z_DG_tot + Z_grid)));
111 I_dg(i,j+1)     = I_f(i,j)*abs(Z_grid/(Z_cable1_tot + Z_DG_tot + Z_grid));
112 I_fault(i,j)  = I_f(i,j);
113
114 end
115 end
116
117
118 cabledg = cable2;
119 cabledg(:,j+1) = cable2(:,j);
120 I_dg(:,1) = PickupCurrentRelay/1000;
121
122 %% Plot variables
123 fig1 = figure (1);
124 set(fig1,'position', [200, 200, 1000, 500]);
125 h = plot(cable2,I_f);
126 set(h,'linewidth',2);
127 hold on
128
129 set(gcf, 'Color', [1,1,1]);
130 legend('No DG','DG units = 1','DG units = 2','DG units = 3','DG units = 4'
        ,'DG units = 5','DG units = 6','DG units = 7');
131
132 grid minor;
133 title('Sub-transient short-circuit current seen by feeder 2');
134 xlabel('Length feeder 2 (km)');
135 ylabel('Short-circuit current (kA)');
136 set(gca,'xtick',[0:1/2:20])
137 set(gca,'ytick',[0:1:30])
138
139 fig2 = figure (2);
140 set(fig2,'position', [200, 200, 1000, 500]);
141 g = plot(cable2,I_grid);
142 set(g,'linewidth',2);
143 hold on
144
145 set(gcf, 'Color', [1,1,1]);
146 legend('No DG','DG units = 1','DG units = 2','DG units = 3','DG units = 4'
        ,'DG units = 5','DG units = 6','DG units = 7');
147
148 grid minor;
149 title('Sub-transient short-circuit contribution grid');
150 xlabel('Length feeder 2 (km)');
151 ylabel('Short-circuit current (kA)');
152 set(gca,'xtick',[0:1/2:20])
153 set(gca,'ytick',[0:1:20])
154
155 fig3 = figure (3);
156 set(fig3,'position', [200, 200, 1000, 500]);
```

```
157 f = plot(cabledg,I_dg);
158 set(f,'linewidth',2);
159 hold on
160
161 set(gcf, 'Color', [1,1,1]);
162 legend('Pick-up current R1','No DG','DG units = 1','DG units = 2','DG
        units = 3','DG units = 4','DG units = 5','DG units = 6','DG units = 7')
        ;
163
164 grid minor;
165 title('Sub-transient short-circuit contribution DG units');
166 xlabel('Length feeder 2 (km)');
167 ylabel('Short-circuit current (kA)');
168 set(gca,'xtick',[0:1/2:20])
169 set(gca,'ytick',[0:1:10])
```

C.3. Protection Blinding

```
close all
clear all

%                                   |                     |
%                                   |-X--cable2-----------|dg-unit
%   ______          bus             |                     |
%  |\ \ \ |          |               |
%  | \ \ \|          |               |                     |
%  |\grid |---------|-X--cable1------|-X--cable3-----------|short-circuit
%  | \ \ \|          |               |                     |
%  |\_\_\_|          |               |
%

step = 0.001;                                   %% per km

%% Max short-circuit contribution of the grid
U_line      = 13; %% in kV
Sk_grid     = 230; %% in MVA
RX_grid     = 0.4737; %% R/X factor grid
Z_grid_abs  = (U_line^2)/Sk_grid; %% Calculate Z component external grid
R_grid      = Z_grid_abs/sqrt(1+(1/RX_grid)^2); %% Calculate R component
    external grid
X_grid      = Z_grid_abs/sqrt(1+RX_grid^2); %% Calculate X component
    external grid
Z_grid      = complex(R_grid,X_grid);

%% Fault location impedance
R_fault = 0.0;
X_fault = 0.0;
Z_fault = complex(R_fault,X_fault);

%% How many parallel DG units and information about DG unit!!!
DG_units    = 7; %% Parallel DG units
MVA_DG      = 2.7*1000000; %% Power DG in MVA
U_DG        = 13*1000; %% Voltage DG in kV
I_DG_nom    = (DG_units*MVA_DG)/(sqrt(3)*U_DG);

X_DG        = 0.168; %% Subtransient reactance per DG in p.u
R_DG        = 0.0504; %% Stator resistance per DG in p.u

Xd_DG       = X_DG*(U_DG^2)/MVA_DG;
rg_DG       = R_DG *(U_DG^2)/MVA_DG;
Z_DG        = complex(rg_DG,Xd_DG);

%% Information about the cable/line, neglecting the capacitance

length_cable1 = 14; %% in km  3*1*150 AL XLPE 12/20 trefoil
I_nom_type_cable1 = 290; %% Nominal current of one feeder
Parallel_cable1 = ceil(I_DG_nom/I_nom_type_cable1); %% How man cable
    parallel, standard 1
I_nom_cable1 = I_nom_type_cable1*Parallel_cable1; %% Nom current parallel
    feeders
R_cable1 = 0.205/Parallel_cable1; %% R cable in ohm/km
X_cable1 = 0.125/Parallel_cable1; %% X cable in ohm/km
```

```
51 PickupCurrentRelay = 1.2; %% Pick up current * Inom cable1
52
53 length_cable3 = 0.05; %% in km  3*1*150 AL XLPE 12/20 trefoil
54 Parallel_cable3 = Parallel_cable1; %% How man cable parallel, standard 1
55 R_cable3 = 0.205/Parallel_cable3; %% R cable in ohm/km
56 X_cable3 = 0.125/Parallel_cable3; %% X cable in ohm/km
57
58 length_cable2 = 14; %% in km  3*1*150 AL XLPE 12/20 trefoil
59 Parallel_cable2 = 1; %% How man cable parallel, standard 1
60 R_cable2 = 0.205/Parallel_cable2; %% R cable in ohm/km
61 X_cable2 = 0.125/Parallel_cable2; %% X cable in ohm/km
62
63 %% The calculation for calculating short-circuit contribution with NO DG
64 for i = 1 : (length_cable2*1000)
65
66 j = 1;
67 cable2(i,j) = step*i; %% each step + 10m
68
69 % Calculate impedance of cable 1
70 X_cable1_tot = X_cable1*length_cable1;
71 R_cable1_tot = R_cable1*length_cable1;
72 Z_cable1_tot = complex(R_cable1_tot,X_cable1_tot);
73
74 % Total impedance seen by fault
75 X_cable2_tot = X_cable2*cable2(i,j);
76 R_cable2_tot = R_cable2*cable2(i,j);
77 Z_cable2_tot = complex(R_cable2_tot,X_cable2_tot);
78 Z_faultlocation(i,j) = Z_grid + Z_cable1_tot + Z_cable2_tot + Z_fault;
79
80 % Calculate 3phase short-circuit current, no correctionfactor (Storing
     Sequentieel in Vision)
81 Z_th(i,j) = abs(Z_faultlocation(i,j));
82 I_f(i,j)  = (U_line)/(sqrt(3)*Z_th(i,j));
83
84 % Index the calculated variables
85 I_grid(i,j+1) = I_f(i,j);
86 I_tot(i,j)  = I_f(i,j);
87
88 end
89
90 %% The calculation for calculating short-circuit contribution with DG
91 for j = 2 : DG_units+1
92
93 DG_parallel = -1 + j;
94
95 Z_DG_tot = Z_DG/DG_parallel;
96
97 % Calculate impedance of cable 1
98 X_cable1_tot = X_cable1*length_cable1;
99 R_cable1_tot = R_cable1*length_cable1;
100 Z_cable1_tot = complex(R_cable1_tot,X_cable1_tot);
101
102 X_cable3_tot = X_cable3*length_cable3;
103 R_cable3_tot = R_cable3*length_cable3;
104 Z_cable3_tot = complex(R_cable3_tot,X_cable3_tot);
105
```

```
106 for i = 1 : (length_cable2*1000)
107
108 cable2(i,j) = step*i;                          %% each step + 10m
109
110 % Calculate impedance of cable 2
111 X_cable2_tot = X_cable2*cable2(i,j);
112 R_cable2_tot = R_cable2*cable2(i,j);
113 Z_cable2_tot = complex(R_cable2_tot,X_cable2_tot);
114
115 % Calculate equivalent impedance
116 Z_faultlocation(i,j) = (((Z_cable3_tot + Z_DG_tot)*(Z_cable1_tot + Z_grid)
    )/(Z_cable1_tot + Z_cable3_tot + Z_DG_tot + Z_grid)) + Z_cable2_tot +
    Z_fault;
117
118 % Calculate 3phase short-circuit current, no correctionfactor (Storing
    Sequentieel in Vision)
119 Z_th(i,j) = abs(Z_faultlocation(i,j));
120
121 % Calculate 3phase short-circuit current, no correctionfactor (Storing
    Sequentieel in Vision)
122 I_f(i,j)  = (U_line)/(sqrt(3)*Z_th(i,j));
123
124 % Calculate the short-circuit contribution of DG and the Grid
125 I_grid(i,j+1) = I_f(i,j)*abs(((Z_DG_tot + Z_cable3_tot)/(Z_cable1_tot +
    Z_DG_tot + Z_grid + Z_cable3_tot)));
126 I_dg(i,j)     = I_f(i,j)*abs((Z_cable1_tot + Z_grid)/(Z_cable1_tot +
    Z_DG_tot + Z_grid + Z_cable3_tot));
127 I_fault(i,j)  = I_f(i,j);
128
129 end
130 end
131
132 cablegrid = cable2;
133 cablegrid(:,j+1) = cable2(:,j);
134 I_grid(:,1) = PickupCurrentRelay*(I_nom_cable1/1000);
135
136
137 %% Plot variables
138 fig1 = figure (1);
139 set(fig1,'position', [200, 200, 1000, 500]);
140 h = plot(cable2,I_f);
141 set(h,'linewidth',2);
142 hold on
143
144 set(gcf, 'Color', [1,1,1]);
145 legend('No DG','DG units = 1','DG units = 2','DG units = 3','DG units = 4'
    ,'DG units = 5','DG units = 6','DG units = 7');
146
147 grid minor;
148 title('Sub-transient short-circuit current seen by feeder 2');
149 xlabel('Length feeder 2 (km)');
150 ylabel('Short-circuit current (kA)');
151 set(gca,'xtick',[0:2:length_cable2])
152 set(gca,'ytick',[0:1:20])
153
154 fig2 = figure (2);
```

```
155 set(fig2,'position', [200, 200, 1000, 500]);
156 g = plot(cablegrid,I_grid);
157 set(g,'linewidth',2);
158 hold on
159
160 set(gcf, 'Color', [1,1,1]);
161 legend('Pick-up current R1','No DG','DG units = 1','DG units = 2','DG
        units = 3','DG units = 4','DG units = 5','DG units = 6','DG units = 7')
        ;
162
163 grid minor;
164 title('Sub-transient short-circuit contribution grid');
165 xlabel('Length feeder 2 (km)');
166 ylabel('Short-circuit current (kA)');
167 set(gca,'xtick',[0:2:length_cable2])
168 set(gca,'ytick',[0:1/4:20])
169
170 fig3 = figure (3);
171 set(fig3,'position', [200, 200, 1000, 500]);
172 f = plot(cable2,I_dg);
173 set(f,'linewidth',2);
174 hold on
175
176 set(gcf, 'Color', [1,1,1]);
177 legend('No DG','DG units = 1','DG units = 2','DG units = 3','DG units = 4'
        ,'DG units = 5','DG units = 6','DG units = 7');
178
179 grid minor;
180 title('Sub-transient short-circuit contribution DG units');
181 xlabel('Length feeder 2 (km)');
182 ylabel('Short-circuit current (kA)');
183 set(gca,'xtick',[0:2:length_cable2])
184 set(gca,'ytick',[0:1:20])
```

C.4. Instantaneous current protection

```
close all
clear all

%
%                              B
%   _ _ _                      |-X--dg-units
%  |\ \ \ |     A              |              C              D
%  | \ \ \|     |              |              |              |           |
%  |\grid |-----|-X--cable1--|-X--cable2--|-X--cable3--|-X--cable4-|
%  | \ \ \|     |              |              |              |           |
%  |\_\_\_|
%

step = 0.001;                                  %% per km

%% Max short-circuit contribution of the grid
U_line      = 13; %% in kV
Sk_grid     = 320; %% in MVA
RX_grid     = 0.35; %% R/X factor grid
Z_grid_abs  = (U_line^2)/Sk_grid; %% Calculate Z component external grid
R_grid      = Z_grid_abs/sqrt(1+(1/RX_grid)^2); %% Calculate R component
    external grid
X_grid      = Z_grid_abs/sqrt(1+RX_grid^2); %% Calculate X component
    external grid
Z_grid      = complex(R_grid,X_grid);

%% Fault location impedance
R_fault = 0.0;
X_fault = 0.0;
Z_fault = complex(R_fault,X_fault);

%% How many parallel DG units and information about DG unit!!!
DG_units    = 7; %% Parallel DG units
MVA_DG      = 2.7*1000000; %% Power DG in MVA
U_DG        = 13*1000; %% Voltage DG in kV
I_DG_nom    = (DG_units*MVA_DG)/(sqrt(3)*U_DG);

X_DG        = 0.168; %% Subtransient reactance per DG in p.u
R_DG        = 0.0504; %% Stator resistance per DG in p.u

Xd_DG       = X_DG*(U_DG^2)/MVA_DG;
rg_DG       = R_DG *(U_DG^2)/MVA_DG;
Z_DG        = complex(rg_DG,Xd_DG);

%% Information about the cable/line, neglecting the capacitance

length_cable1 = 2.5; %% in km  3*1*150 AL XLPE 12/20 trefoil
I_nom_type_cable1 = 290; %% Nominal current of one feeder
Parallel_cable1 = ceil(I_DG_nom/I_nom_type_cable1); %% How man cable
    parallel, standard 1
%Parallel_cable1 = 1;
I_nom_cable1 = I_nom_type_cable1*Parallel_cable1; %% Nom current parallel
    feeders
R_cable1 = 0.205/Parallel_cable1; %% R cable in ohm/km
```

```
51 X_cable1 = 0.125/Parallel_cable1; %% X cable in ohm/km
52 Z_cable1 = complex(R_cable1,X_cable1);
53
54 length_cable2 = 5.0; %% in km  3*1*150 AL XLPE 12/20 trefoil
55 Parallel_cable2 = 1; %% How man cable parallel, standard 1
56 R_cable2 = 0.205/Parallel_cable2; %% R cable in ohm/km
57 X_cable2 = 0.125/Parallel_cable2; %% X cable in ohm/km
58 Z_cable2 = complex(R_cable2,X_cable2);
59
60 length_cable3 = 7.5; %% in km  3*1*150 AL XLPE 12/20 trefoil
61 Parallel_cable3 = 1; %% How man cable parallel, standard 1
62 R_cable3 = 0.205/Parallel_cable3; %% R cable in ohm/km
63 X_cable3 = 0.125/Parallel_cable3; %% X cable in ohm/km
64 Z_cable3 = complex(R_cable3,X_cable3);
65
66 length_cable4 = 10.0; %% in km  3*1*150 AL XLPE 12/20 trefoil
67 Parallel_cable4 = 1; %% How man cable parallel, standard 1
68 R_cable4 = 0.205/Parallel_cable4; %% R cable in ohm/km
69 X_cable4 = 0.125/Parallel_cable4; %% X cable in ohm/km
70 Z_cable4 = complex(R_cable4,X_cable4);
71
72 %% The calculation for calculating short-circuit contribution with NO DG
73 for i = 1 : (length_cable1*1000)
74
75 j = 1;
76 cable(i,j) = step*i; %% each step + 10m
77
78 % Total impedance seen by fault
79 X_cable1_tot = X_cable1*cable(i,j);
80 R_cable1_tot = R_cable1*cable(i,j);
81 Z_cable1_tot = complex(R_cable1_tot,X_cable1_tot);
82
83 % Calculate equivalent impedance
84 Z_faultlocation(i,j) = Z_grid + Z_cable1_tot + Z_fault;
85
86 % Calculate 3phase short-circuit current, no correctionfactor (Storing
    Sequentieel in Vision)
87 Z_th(i,j) = abs(Z_faultlocation(i,j));
88 I_f(i,j)  = (U_line)/(sqrt(3)*Z_th(i,j));
89
90 % Index the calculated variables
91 I_grid(i,j) = I_f(i,j);
92 I_tot(i,j)  = I_f(i,j);
93
94 end
95
96 for i = ((length_cable1*1000)+1) : length_cable2*1000
97
98 j = 1;
99 cable(i,j) = step*i; %% each step + 10m
100
101 % Calculate impedance of cable 1
102 X_cable1_tot = X_cable1*length_cable1;
103 R_cable1_tot = R_cable1*length_cable1;
104 Z_cable1_tot = complex(R_cable1_tot,X_cable1_tot);
105
```

```
106 % Total impedance seen by fault
107 X_cable2_tot = X_cable2*(cable(i,j)-length_cable1);
108 R_cable2_tot = R_cable2*(cable(i,j)-length_cable1);
109 Z_cable2_tot = complex(R_cable2_tot,X_cable2_tot);
110
111 % Calculate equivalent impedance
112 Z_faultlocation(i,j) = Z_grid + Z_cable1_tot + Z_cable2_tot + Z_fault;
113
114 % Calculate 3phase short-circuit current, no correctionfactor (Storing
        Sequentieel in Vision)
115 Z_th(i,j) = abs(Z_faultlocation(i,j));
116 I_f(i,j)  = (U_line)/(sqrt(3)*Z_th(i,j));
117
118 % Index the calculated variables
119 I_grid(i,j) = I_f(i,j);
120 I_tot(i,j)  = I_f(i,j);
121
122 end
123
124 for i = ((length_cable2*1000)+1) : length_cable3*1000
125
126 j = 1;
127 cable(i,j) = step*i; %% each step + 10m
128
129 % Calculate impedance of cable 1
130 X_cable1_tot = X_cable1*length_cable1;
131 R_cable1_tot = R_cable1*length_cable1;
132 Z_cable1_tot = complex(R_cable1_tot,X_cable1_tot);
133
134 % Calculate impedance of cable 2
135 X_cable2_tot = X_cable2*length_cable2;
136 R_cable2_tot = R_cable2*length_cable2;
137 Z_cable2_tot = complex(R_cable2_tot,X_cable2_tot);
138
139 % Total impedance seen by fault
140 X_cable3_tot = X_cable3*(cable(i,j)-length_cable1-length_cable2);
141 R_cable3_tot = R_cable3*(cable(i,j)-length_cable1-length_cable2);
142 Z_cable3_tot = complex(R_cable3_tot,X_cable3_tot);
143
144 % Calculate equivalent impedance
145 Z_faultlocation(i,j) = Z_grid + Z_cable1_tot + Z_cable2_tot + Z_cable3_tot
        + Z_fault;
146
147 % Calculate 3phase short-circuit current, no correctionfactor (Storing
        Sequentieel in Vision)
148 Z_th(i,j) = abs(Z_faultlocation(i,j));
149 I_f(i,j)  = (U_line)/(sqrt(3)*Z_th(i,j));
150
151 % Index the calculated variables
152 I_grid(i,j) = I_f(i,j);
153 I_tot(i,j)  = I_f(i,j);
154
155 end
156
157 for i = ((length_cable3*1000)+1) : length_cable4*1000
158
```

```
159 j = 1;
160 cable(i,j) = step*i; %% each step + 10m
161
162 % Calculate impedance of cable 1
163 X_cable1_tot = X_cable1*length_cable1;
164 R_cable1_tot = R_cable1*length_cable1;
165 Z_cable1_tot = complex(R_cable1_tot,X_cable1_tot);
166
167 % Calculate impedance of cable 2
168 X_cable2_tot = X_cable2*length_cable2;
169 R_cable2_tot = R_cable2*length_cable2;
170 Z_cable2_tot = complex(R_cable2_tot,X_cable2_tot);
171
172 % Calculate impedance of cable 3
173 X_cable3_tot = X_cable3*length_cable3;
174 R_cable3_tot = R_cable3*length_cable3;
175 Z_cable3_tot = complex(R_cable3_tot,X_cable3_tot);
176
177 % Total impedance seen by fault
178 X_cable4_tot = X_cable4*(cable(i,j)-length_cable1-length_cable2-
       length_cable3);
179 R_cable4_tot = R_cable4*(cable(i,j)-length_cable1-length_cable2-
       length_cable3);
180 Z_cable4_tot = complex(R_cable4_tot,X_cable4_tot);
181
182 % Calculate equivalent impedance
183 Z_faultlocation(i,j) = Z_grid + Z_cable1_tot + Z_cable2_tot + Z_cable3_tot
        + Z_cable4_tot + Z_fault;
184
185 % Calculate 3phase short-circuit current, no correctionfactor (Storing
       Sequentieel in Vision)
186 Z_th(i,j) = abs(Z_faultlocation(i,j));
187 I_f(i,j)  = (U_line)/(sqrt(3)*Z_th(i,j));
188
189 % Index the calculated variables
190 I_grid(i,j) = I_f(i,j);
191 I_tot(i,j)  = I_f(i,j);
192
193 end
194
195 %% The calculation for calculating short-circuit contribution with DG
196 for j = 2 : DG_units+1
197
198 DG_parallel =  j-1;
199 Z_DG_eq = Z_DG/DG_parallel;
200
201 for i = 1 : (length_cable1*1000)
202 cable(i,j) = step*i;                          %% each step + 10m
203
204 % Calculate impedance of cable 1
205 X_cable1_tot = X_cable1*cable(i,j);
206 R_cable1_tot = R_cable1*cable(i,j);
207 Z_cable1_tot = complex(R_cable1_tot,X_cable1_tot);
208
209 Z_DG_tot = Z_DG_eq + (Z_cable1*(length_cable1-cable(i,j)));
210
```

```
211 % Calculate equivalent impedance
212 Z_faultlocation(i,j) = (Z_DG_tot*(Z_cable1_tot+Z_grid))/(Z_DG_tot+
        Z_cable1_tot+Z_grid) + Z_fault;
213
214 % Calculate 3phase short-circuit current, no correctionfactor (Storing
        Sequentieel in Vision)
215 Z_th(i,j) = abs(Z_faultlocation(i,j));
216
217 % Calculate 3phase short-circuit current, no correctionfactor (Storing
        Sequentieel in Vision)
218 I_f(i,j)  = (U_line)/(sqrt(3)*Z_th(i,j));
219
220 % Calculate the short-circuit contribution of DG and the Grid
221 I_grid(i,j) = I_f(i,j)*abs((Z_DG_tot)/(Z_DG_tot+Z_cable1_tot+Z_grid));
222 I_dg(i,j)     = I_f(i,j)*abs((Z_cable1_tot + Z_grid)/(Z_DG_tot+
        Z_cable1_tot+Z_grid));
223 I_fault(i,j)  = I_f(i,j);
224 end
225
226 for i = ((length_cable1*1000)+1) : length_cable2*1000
227 cable(i,j) = step*i;                        %% each step + 10m
228
229 % Calculate impedance of cable 1
230 X_cable1_tot = X_cable1*length_cable1;
231 R_cable1_tot = R_cable1*length_cable1;
232 Z_cable1_tot = complex(R_cable1_tot,X_cable1_tot);
233
234 % Total impedance seen by fault
235 X_cable2_tot = X_cable2*(cable(i,j)-length_cable1);
236 R_cable2_tot = R_cable2*(cable(i,j)-length_cable1);
237 Z_cable2_tot = complex(R_cable2_tot,X_cable2_tot);
238
239 % Calculate equivalent impedance
240 Z_faultlocation(i,j) = (Z_DG_eq*(Z_cable1_tot+Z_grid))/(Z_DG_eq+
        Z_cable1_tot+Z_grid) + Z_cable2_tot + Z_fault;
241
242 % Calculate 3phase short-circuit current, no correctionfactor (Storing
        Sequentieel in Vision)
243 Z_th(i,j) = abs(Z_faultlocation(i,j));
244 %
245 % Calculate 3phase short-circuit current, no correctionfactor (Storing
        Sequentieel in Vision)
246 I_f(i,j)  = (U_line)/(sqrt(3)*Z_th(i,j));
247
248 % Calculate the short-circuit contribution of DG and the Grid
249 I_grid(i,j) = I_f(i,j)*abs((Z_DG_eq)/(Z_DG_eq+Z_cable1_tot+Z_grid));
250 I_dg(i,j)     = I_f(i,j)*abs((Z_cable1_tot + Z_grid)/(Z_DG_eq+Z_cable1_tot
        +Z_grid));
251 I_fault(i,j)  = I_f(i,j);
252 end
253
254 for i = ((length_cable2*1000)+1) : length_cable3*1000
255 cable(i,j) = step*i;                        %% each step + 10m
256
257 % Calculate impedance of cable 1
258 X_cable1_tot = X_cable1*length_cable1;
```

```
259 R_cable1_tot = R_cable1*length_cable1;
260 Z_cable1_tot = complex(R_cable1_tot,X_cable1_tot);
261
262 % Calculate impedance of cable 2
263 X_cable2_tot = X_cable2*length_cable2;
264 R_cable2_tot = R_cable2*length_cable2;
265 Z_cable2_tot = complex(R_cable2_tot,X_cable2_tot);
266
267 % Total impedance seen by fault
268 X_cable3_tot = X_cable3*(cable(i,j)-length_cable1-length_cable2);
269 R_cable3_tot = R_cable3*(cable(i,j)-length_cable1-length_cable2);
270 Z_cable3_tot = complex(R_cable3_tot,X_cable3_tot);
271
272 % Calculate equivalent impedance
273 Z_faultlocation(i,j) = (Z_DG_eq*(Z_cable1_tot+Z_grid))/(Z_DG_eq+
      Z_cable1_tot+Z_grid) + Z_cable2_tot + Z_cable3_tot + Z_fault;
274
275 % Calculate 3phase short-circuit current, no correctionfactor (Storing
      Sequentieel in Vision)
276 Z_th(i,j) = abs(Z_faultlocation(i,j));
277 %
278 % Calculate 3phase short-circuit current, no correctionfactor (Storing
      Sequentieel in Vision)
279 I_f(i,j)  = (U_line)/(sqrt(3)*Z_th(i,j));
280
281 % Calculate the short-circuit contribution of DG and the Grid
282 I_grid(i,j) = I_f(i,j)*abs((Z_DG_eq)/(Z_DG_eq+Z_cable1_tot+Z_grid));
283 I_dg(i,j)     = I_f(i,j)*abs((Z_cable1_tot + Z_grid)/(Z_DG_eq+Z_cable1_tot
      +Z_grid));
284 I_fault(i,j)  = I_f(i,j);
285 end
286
287 for i = ((length_cable3*1000)+1) : length_cable4*1000
288 cable(i,j) = step*i;                          %% each step + 10m
289
290 % Calculate impedance of cable 1
291 X_cable1_tot = X_cable1*length_cable1;
292 R_cable1_tot = R_cable1*length_cable1;
293 Z_cable1_tot = complex(R_cable1_tot,X_cable1_tot);
294
295 % Calculate impedance of cable 2
296 X_cable2_tot = X_cable2*length_cable2;
297 R_cable2_tot = R_cable2*length_cable2;
298 Z_cable2_tot = complex(R_cable2_tot,X_cable2_tot);
299
300 % Calculate impedance of cable 3
301 X_cable3_tot = X_cable3*length_cable3;
302 R_cable3_tot = R_cable3*length_cable3;
303 Z_cable3_tot = complex(R_cable3_tot,X_cable3_tot);
304
305 % Total impedance seen by fault
306 X_cable4_tot = X_cable4*(cable(i,j)-length_cable1-length_cable2-
      length_cable3);
307 R_cable4_tot = R_cable4*(cable(i,j)-length_cable1-length_cable2-
      length_cable3);
308 Z_cable4_tot = complex(R_cable4_tot,X_cable4_tot);
```

```
309
310
311 % Calculate equivalent impedance
312 Z_faultlocation(i,j) = (Z_DG_eq*(Z_cable1_tot+Z_grid))/(Z_DG_eq+
        Z_cable1_tot+Z_grid) + Z_cable2_tot + Z_cable3_tot + Z_cable4_tot +
        Z_fault;
313
314 % Calculate 3phase short-circuit current, no correctionfactor (Storing
        Sequentieel in Vision)
315 Z_th(i,j) = abs(Z_faultlocation(i,j));
316 %
317 % Calculate 3phase short-circuit current, no correctionfactor (Storing
        Sequentieel in Vision)
318 I_f(i,j)  = (U_line)/(sqrt(3)*Z_th(i,j));
319
320 % Calculate the short-circuit contribution of DG and the Grid
321 I_grid(i,j)   = I_f(i,j)*abs((Z_DG_eq)/(Z_DG_eq+Z_cable1_tot+Z_grid));
322 I_dg(i,j)     = I_f(i,j)*abs((Z_cable1_tot + Z_grid)/(Z_DG_eq+Z_cable1_tot
        +Z_grid));
323 I_fault(i,j)  = I_f(i,j);
324 end
325
326 end
327
328 cablegrid = cable;
329 %cablegrid(:,j+1) = cablegrid(:,j);
330
331 %% Plot variables
332 fig1 = figure (1);
333 set(fig1,'position', [200, 200, 1000, 500]);
334 x=[0:0.1:10];
335 h = plot(cable,I_f);
336 set(h,'linewidth',2);
337 hold on
338 x1=length_cable1;
339 x2=length_cable2;
340 x3=length_cable3;
341 y1=2;
342 y2=20;
343 text(0.1,  19 , 'Bus A', 'Color', 'k');
344 text(length_cable1+0.1,  19 , 'Bus B', 'Color', 'k');
345 text(length_cable2+0.1,  19 , 'Bus C', 'Color', 'k');
346 text(length_cable3+0.1,  19 , 'Bus D', 'Color', 'k');
347 text(0.8*length_cable1-0.365,  3 , '80% no DG', 'Color', 'k');
348 text((0.8*(length_cable2-length_cable1))+length_cable1-0.365,  3 , '80% no
        DG', 'Color', 'k');
349 text((0.8*(length_cable3-length_cable2))+length_cable2-0.365,  3 , '80% no
        DG', 'Color', 'k');
350 h = plot([x1 x1],[y1 y2],[x2 x2],[y1 y2],[x3 x3],[y1 y2]);
351 set(h,'LineStyle','-','linewidth',2);
352 hold on
353 x4=0.8*length_cable1;
354 x5=(0.8*(length_cable2-length_cable1))+length_cable1;
355 x6=(0.8*(length_cable3-length_cable2))+length_cable2;
356 h = plot([x4 x4],[y1 y2],[x5 x5],[y1 y2],[x6 x6],[y1 y2]);
357 set(h,'LineStyle','--','linewidth',2);
```

```
358 hold on
359
360 set(gcf, 'Color', [1,1,1]);
361 legend('No DG','DG units = 1','DG units = 2','DG units = 3','DG units = 4'
    ,'DG units = 5','DG units = 6','DG units = 7');
362
363 grid minor;
364 title('Sub-transient short-circuit current seen by the feeder');
365 xlabel('Length feeder (km)');
366 ylabel('Short-circuit current (kA)');
367 set(gca,'xtick',[0:0.5:length_cable4])
368 set(gca,'ytick',[0:1:20])
369
370 fig2 = figure (2);
371 set(fig2,'position', [200, 200, 1000, 500]);
372 g = plot(cablegrid,I_grid);
373 set(g,'linewidth',2);
374 hold on
375 x1=length_cable1;
376 x2=length_cable2;
377 x3=length_cable3;
378 y1=get(gca,'ylim');
379 text(0.1,  15 , 'Bus A', 'Color', 'k');
380 text(length_cable1+0.1,  15 , 'Bus B', 'Color', 'k');
381 text(length_cable2+0.1,  15 , 'Bus C', 'Color', 'k');
382 text(length_cable3+0.1,  15 , 'Bus D', 'Color', 'k');
383 text(0.8*length_cable1-0.365,  3 , '80% no DG', 'Color', 'k');
384 text((0.8*(length_cable2-length_cable1))+length_cable1-0.365,  3 , '80% no
    DG', 'Color', 'k');
385 text((0.8*(length_cable3-length_cable2))+length_cable2-0.365,  3 , '80% no
    DG', 'Color', 'k');
386 h = plot([x1 x1],y1,[x2 x2],y1,[x3 x3],y1);
387 set(h,'LineStyle','-','linewidth',2);
388 hold on
389 x4=0.8*length_cable1;
390 x5=(0.8*(length_cable2-length_cable1))+length_cable1;
391 x6=(0.8*(length_cable3-length_cable2))+length_cable2;
392 y1=get(gca,'ylim');
393 h = plot([x4 x4],y1,[x5 x5],y1,[x6 x6],y1);
394 set(h,'LineStyle','--','linewidth',2);
395 hold on
396
397 set(gcf, 'Color', [1,1,1]);
398 legend('No DG','DG units = 1','DG units = 2','DG units = 3','DG units = 4'
    ,'DG units = 5','DG units = 6','DG units = 7');
399
400 grid minor;
401 title('Sub-transient short-circuit contribution grid');
402 xlabel('Length feeder(km)');
403 ylabel('Short-circuit current (kA)');
404 set(gca,'xtick',[0:0.5:length_cable4])
405 set(gca,'ytick',[0:1:20])
406
407 fig3 = figure (3);
408 set(fig3,'position', [200, 200, 1000, 500]);
409 f = plot(cable,I_dg);
```

```
410 set(f,'linewidth',2);
411 hold on
412 x1=length_cable1;
413 x2=length_cable2;
414 x3=length_cable3;
415 y1=get(gca,'ylim');
416 text(0.1,  4.5 , 'Bus A', 'Color', 'k');
417 text(length_cable1+0.1,  4.5 , 'Bus B', 'Color', 'k');
418 text(length_cable2+0.1,  4.5 , 'Bus C', 'Color', 'k');
419 text(length_cable3+0.1,  4.5 , 'Bus D', 'Color', 'k');
420 text(0.8*length_cable1-0.365,  3 , '80% no DG', 'Color', 'k');
421 text((0.8*(length_cable2-length_cable1))+length_cable1-0.365,  3 , '80% no
        DG', 'Color', 'k');
422 text((0.8*(length_cable3-length_cable2))+length_cable2-0.365,  3 , '80% no
        DG', 'Color', 'k');
423 h = plot([x1 x1],y1,[x2 x2],y1,[x3 x3],y1);
424 set(h,'LineStyle','-','linewidth',2);
425 hold on
426 x4=0.8*length_cable1;
427 x5=(0.8*(length_cable2-length_cable1))+length_cable1;
428 x6=(0.8*(length_cable3-length_cable2))+length_cable2;
429 y1=get(gca,'ylim');
430 h = plot([x4 x4],y1,[x5 x5],y1,[x6 x6],y1);
431 set(h,'LineStyle','--','linewidth',2);
432 hold on
433
434 set(gcf, 'Color', [1,1,1]);
435 legend('No DG','DG units = 1','DG units = 2','DG units = 3','DG units = 4'
       ,'DG units = 5','DG units = 6','DG units = 7');
436
437 grid minor;
438 title('Sub-transient short-circuit contribution DG units');
439 xlabel('Length feeder (km)');
440 ylabel('Short-circuit current (kA)');
441 set(gca,'xtick',[0:0.5:length_cable4])
442 set(gca,'ytick',[0:1:20])
```